2025-12

Mathematical Model and Analysis of Fasciola Hepatica Disease Transmission Dynamics with Optimal Control

Dagnaw, Tantie

BAHIR DAR UNIVERSITY

COLLEGE OF SCIENCE

DEPARTMENT OF MATHEMATICS

Mathematical Model and Analysis of *Fasciola Hepatica* Disease Transmission Dynamics with Optimal Control

By

Dagnaw Tantie Yihunie

December 24, 2025

Bahir Dar, Ethiopia

BAHIR DAR UNIVERSITY

COLLEGE OF SCIENCE

DEPARTMENT OF MATHEMATICS

Mathematical Model and Analysis of *Fasciola Hepatica* Transmission Dynamics with Optimal Control

By

Dagnaw Tantie Yihunie

A Dissertation Submitted in Partial Fulfillment of the Requirements for the Degree of Doctor of Philosophy in Mathematics.

Supervisor: Joseph Y.T Mugisha (Professor)
Makerere University, Uganda

Co-supervisor: Dawit Melese Gebru (Associate Professor)
Bahir Dar University, Bahir Dar
Haileyesus Tessema (Associate Professor)
University of Gondar, Gondar

December 24, 2025
Bahir Dar, Ethiopia

Declaration

I certify that this dissertation, "Mathematical model and analysis of *Fasciola hepatica* disease transmission dynamics with optimal control", submitted in partial fulfillment of the requirements for the Doctorate of Philosophy in Mathematics at Bahir Dar University, Department of Mathematics, is my original work and has not been submitted elsewhere for any degree or certificate. All assistance received is acknowledged.

Dagnaw Tantie Yihunie	_____	_____
Name of the candidate	Signature	Date

BAHIR DAR UNIVERSITY

COLLEGE OF SCIENCE

DEPARTMENT OF MATHEMATICS

Approval of Dissertation for Defense

I certify that I have supervised and evaluated the dissertation "Mathematical model and analysis of *Fasciola hepatica* disease transmission dynamics with optimal control" by Dagnaw Tantie Yihunie and recommend its submission for oral defense.

Joseph Mugisha (Professor)		January 1, 2026
Supervisor's name	Signature	Date
Dawit melese (Associate Professor)	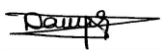	January 1, 2026
Co-supervisor's name	Signature	Date
Haileyesus Tessema (Associate Professor)		January 2, 2026
Co-supervisor's name	Signature	Date
Postgraduate Head	Signature	Date

BAHIR DAR UNIVERSITY

COLLEGE OF SCIENCE

DEPARTMENT OF MATHEMATICS

Approval of Dissertation for Defense

We the undersigned members of the dissertation examination board, have examined the dissertation titled "**Mathematical model and analysis of *Fasciola hepatica* disease transmission dynamics with optimal control**" submitted by Dagnaw Tantie Yihunie. We certify that this dissertation meets the academic standards and requirements for the award of the degree Doctor of Philosophy in Applied Mathematics (Mathematical Modeling) and has been approved upon defense.

Board of examiners:

Peter Joseph Witbooi (Professor)	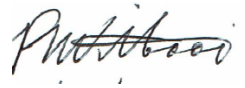	January 5, 2026
External examiner name I	Signature	Date
Mohammed Yiha (Associate Professor)	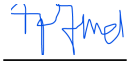	January 5, 2026
External examiner name II	Signature	Date
Getachew Teshome (Associate Professor)		January 5, 2026
Internal examiner name	Signature	Date
Hunegnaw Dessie (Associate Professor)		January 6, 2026
Chairperson's name	Signature	Date

Dedication

To my family, mentors and friends: this work is dedicated to you. Your unwavering support, wisdom and love have shaped me, making this achievement as much yours as mine. Thank you for walking with me.

List of Publications

This dissertation includes research papers published in accredited journals or submitted for publication and currently under review.

(1) Dagnaw Tantie Yihunie, Joseph Y.T. Mugisha, Dawit Melese Gebru, Haileyesus Tessema Alemneh (2024). 'Modeling and analysis of *Fasciola hepatica* disease transmission'. Abstract and Applied Analysis, vol. 2024, no. 1, p. 8843680. Wiley. https://doi.org/10.1155/2024/8843680

(2) Dagnaw Tantie Yihunie, Joseph Y.T. Mugisha, Dawit Melese Gebru, Haileyesus Tessema Alemneh (2024). 'Optimal control and cost-effectiveness analysis of the *Fasciola hepatica* model'. Heliyon, vol. 2024, no. 10, p.e38540, Elsevier. https://doi.org/10.1016/j.heliyon.2024.e38540

(3) Dagnaw Tantie Yihunie, Joseph Y.T. Mugisha, Dawit Melese Gebru, Haileyesus Tessema Alemneh. 'The Impact of Early Diagnosis and Treatment in a *Fasciola Hepatica* Model'. Journal of Applied Mathematics, Wiley. Under review.

(4) Dagnaw Tantie Yihunie, Joseph Y.T. Mugisha, Dawit Melese Gebru, Haileyesus Tessema Alemneh. 'Analyzing Human-Cattle Dynamics for Effective *Fasciola Hepatica* Management'. Neglected Tropical Diseases, PLoS. Under review.

Conference and Seminar Presentation

Conference Presentation:

- Addis Ababa University (2025). "Optimal control and cost-effectiveness analysis of a *Fasciola hepatica* model" at the Ethio-Italy Colloquium on Applied Mathematics on theme "Classical and new approaches for modeling life science problems".
- Arba Minch University (2025). "Modeling human-cattle dynamics for effective *Fasciola hepatica* management" at the 11th National Symposium on "Science for sustainable development."
- Debre Berhan University (2025). "Modeling human-cattle dynamics for effective *Fasciola hepatica* management" at the 4th Annual National Research Conference on "Investing in science for innovation and development of sustainable technology."

Seminar Presentation:

- Bahir Dar University (2022). "Mathematical model and analysis of *Fasciola hepatica* transmission dynamics with optimal control."

List of Abbreviations

Abbreviation	Meaning
ACER	Average Cost Effectiveness Ratio
CDC	Center for Disease Control and Prevention
CEA	Cost Effective Analysis
DFE	Disease-Free Equilibrium
EE	Endemic Equilibrium
Eq.	Equation
F. Hepatica	*Fasciola Hepatica*
Fig.	Figure
IAR	Infected Averted Ratio
ICER	Incremental Cost Effective Ratio
LPD	Locally Positive Definite
MSD	Merck Sharp & Dohme
NTD	Neglected Tropical Disease
ODE	Ordinary Differential Equation
PAHO	Pan American Health Organization
PMP	Pontryagin Minimum Principle
WHO	World Health Organization

Acknowledgment

I thank Almighty God for enabling the completion of this dissertation. I am profoundly grateful to my supervisor, Professor Joseph Y.T. Mugisha, for his invaluable guidance and unwavering support throughout the research work. My heartfelt thanks also go to my co-supervisors Dr. Dawit Melese and Dr. Haileyesus Tessema for their insightful guidance and constructive criticism, which played a crucial role in shaping this dissertation.

I extend my sincere gratitude to Yibekal Walle and Dr. Dagnachew Mengstie for their tremendous support and encouragement. I am also very grateful to my entire family, particularly my wife, Meseret Fentaye and my daughter, Hilina Dagnaw, for their patience and unwavering support throughout this journey.

I am deeply grateful for the invaluable resources and assistance provided by both Bahir Dar University and Debre Tabor University.

I would like to extend my heartfelt gratitude to my friends and the staff of the mathematics department at Debre Tabor University and Bahir Dar University for their unwavering encouragement and support throughout the completion of my dissertation.

Abstract

Fascioliasis, a snail-borne zoonotic disease recognized by the World Health Organization as a neglected tropical disease, significantly impacted human and livestock health and economies, affecting over 700 million animals and 180 million humans are at risk of infection. This dissertation addressed the limited understanding of *Fasciola hepatica* transmission dynamics by developing a mathematical model exploring various scenarios, including stability analysis, bifurcation, sensitivity, optimal control, and cost-effectiveness. Model analysis revealed that snail mortality rate as a key factor in disease spread, with optimal control strategies, derived via the Pontryagin maximum principle, indicating that combined pasture management, cattle treatment, and molluscicide use effectively reduce transmission. Cost-effectiveness analysis identified pasture management with molluscicides as the most efficient strategy, further enhanced by integrating molluscicide use with cattle treatment. The study concluded that integrated control strategies, incorporating public health education, treatment, and molluscicide application, offer the most substantial and immediate reduction in *fascioliasis* in both cattle and human populations, providing a basis for effective global interventions.

Contents

List of Tables

List of Figures

Chapter 1

1 General Introduction

1.1 Background to the Study

1.1.1 Epidemiology of *Fascioliasis*

Fasciololasis is a zoonotic disease caused by two parasitic flatworms or trematodes called *Fasciola hepatica* and *Fasciola gigantica* (Bridle 2021, Logue et al. 2017, Mas-Coma et al. 2014, Kamaruddin et al. 2021). These highly pathogenic liver flukes primarily affect the liver in both humans and livestock (Bargues et al. 2021). It is a neglected tropical disease prioritized by the World Health Organization (WHO), which is a food-borne trematode disease (Kamaruddin et al. 2021, Lalor et al. 2021, Bargues et al. 2021, WHO 2023). *Fasciola hepatica*, in particular, is a widespread parasite affecting domestic animals like cattle, sheep, and goats, and occasionally humans (Diaby et al. 2019). Animal *fascioliasis* poses a significant veterinary problem globally, impacting livestock productivity and causing substantial economic losses due to morbidity and mortality (Ashrafi et al. 2015, Zewde et al. 2019, Logue et al. 2017, Lan et al. 2024).

Human *fascioliasis* is emerging or re-emerging globally, with increasing prevalence, intensity and geographic range (Mas-Coma 2005, Beesley et al. 2018). The differences in geographical distribution are mainly related to minimum larval development temperature thresholds: 10°C for *Fasciola hepatica* and 16°C for *Fasciola gigantica*, although cercaria shedding in the latter has been observed at 13-18°C (Bargues et al. 2021). Freshwater snails of the Lymnaeidae family are the world's intermediate hosts for the liver fluke *Fasciola* (Kaset et al. 2010, Vázquez et al. 2019). The snail, as an intermediate host of *Fasciola*, is a critical factor in the transmission of *fasciolosis*. The ecology of the snail determines the epidemiology of *fascioliasis*.

Snail surveillance informs the prevention of targeted *fasciolosis* in humans and ruminants (Pan et al. 2022).

Infection typically occurs through ingestion of metacercariae encysted in water and food (Logue et al. 2017), often through contaminated vegetation. Human cases often result from eating raw watercress or other water plants harboring the parasite (CDC 2019). The liver flukes *Fasciola hepatica* and *Fasciola gigantica* are leaf-shaped flatworms. *Fasciola hepatica* grows to 30 mm by 15 mm, while *F. gigantica* reaches 75 mm by 15 mm (CDC 2019, Waikagul et al. 2015).

1.1.2 Mode of Transmission and Life Cycle of *Fasciola Hepatica*

Fasciola parasite is transmitted to humans and animals by eating contaminated water or aquatic plants with metacercariae (Caravedo & Cabada 2020). It has a complicated life cycle that includes intermediate snails as well as definitive mammal hosts such as sheep, cattle, goats and humans (CDC 2020, Lan et al. 2024). This pattern could be explained by a cycle of transmission from animal to snail to plant to animal. The life cycle of *Fasciola gicantica* is similar to that of *Fasciola hepatica*, except that most of the parasitic phases are longer, the prepatent period is 10–16 weeks and the intermediate host species of snails are different (Alemu 2019). The life cycle of *F. hepatica* is indirect (Caravedo & Cabada 2020). It has a number of larval stages in its life. It passes through five stages of life: egg, miracidium, cercaria, metacercaria and adult fluke.

The life cycle of *F. hepatica* (can be seen in Fig. 1.1) begins when a female lays eggs in the liver of ruminants (their main definite host). Juvenile eggs are excreted in the feces after being discharged from the biliary ducts. When the eggs are immersed in water, they become embryonated and hatch into miracidia larvae. The miracidium swims, invades an amphibian snail (the parasite's intermediate host), and develops into a sporocyst. This then transforms into redia, facilitating the temperature-dependent production of cercariae (Diaby et al. 2019). A single miracidium can clonally expand, producing 10 to 700 cercariae, with an infected snail releasing hundreds over time. This large number of cercariae increases the likelihood of the parasite's

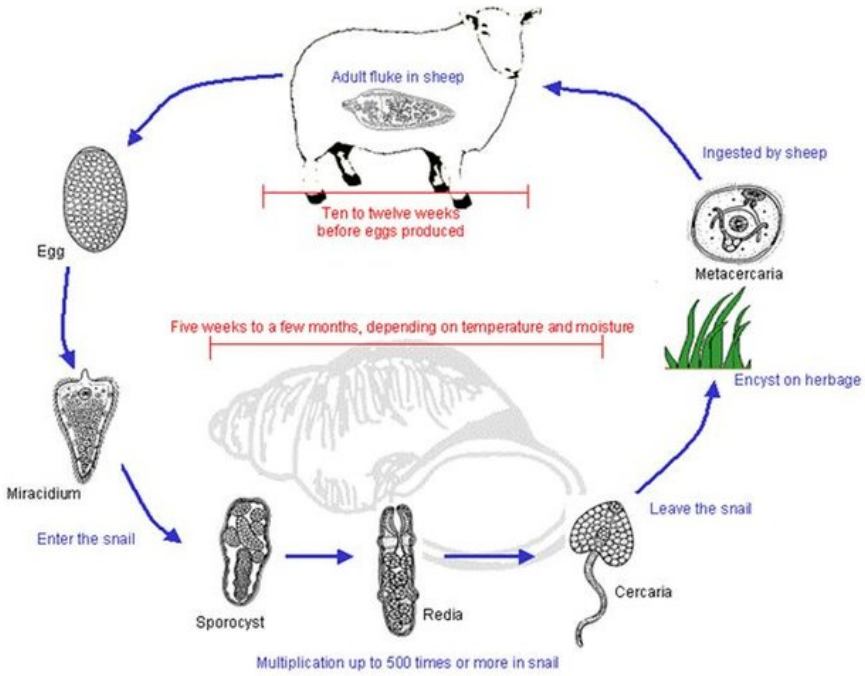

Figure 1.1: Life cycle of *F. hepatica*.

Source: Abdisa & Jilo (2017)

life cycle continuing (Lalor et al. 2021). The cercariae are released and leave the snail to attach to the vegetation. Cercariae form infective metacercariae as they encircle vegetation. A definite host consumes the freshwater plant that contains the cyst. The young worms pass through the intestinal wall, the abdominal cavity and the liver tissue to reach the bile ducts, where they mature into adult flukes that produce eggs (CDC 2020).

1.1.3 Global Distribution of *Fascioliasis*

Human *fascioliasis*, a food-borne trematode infection, is increasing globally in correlation with high infection rates in ruminants. The prevalence is highest among farming and herding communities in low-income countries due to a close association with livestock (Nyindo & Lukambagire 2015). Human infection has been reported in parts of Africa, Asia, the Caribbean, Europe, Latin America (e.g. Bolivia and Peru), Middle East, Oceania and, on rare occasions, Australia (CDC 2019, Nyindo & Lukambagire 2015, Atalabi & Lawal 2020). *Fasciola gigantica* is found mostly in the

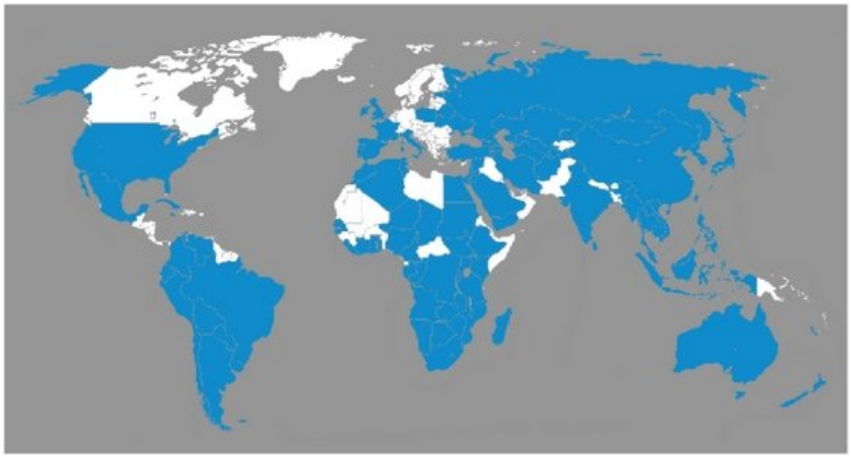

Figure 1.2: Global distribution of *fascioliasis*.
Source: http://www.bvgh.org/Current-Programs/Neglected-Disease-Product-Pipelines/Global-Health-Primer/Diseases/cid/ViewDetails/ItemID/23.aspx

tropics and subtropics.

Bovine *fascioliasis* is a worldwide zoonotic disease, it occurs in more than 70 countries (Diaz-Quevedo et al. 2021), especially where cattle and sheep are reared. *Fasciola hepatica* is a trematode parasite with a worldwide distribution that causes significant disease and production losses in a variety of food-producing species. With the exception of Antarctica, *fascioliasis* is endemic on all continents (Atalabi & Lawal 2020, Alba et al. 2018). *Fasciola hepatica* is distributed throughout the world, but is most common in temperate regions, whereas *F. gigantica* is restricted to specific regions of Africa and Asia (Mas-Coma et al. 2014, Waikagul et al. 2015). It is one of the most important domestic ruminant flukes in the world. Fig 1.2 shows the global distribution of *fascioliasis* in 2015, with blue shading indicating countries reporting cases (Nyindo & Lukambagire 2015). This figure shows that *fascioliasis* is distributed in more than 90% of the world.

1.1.4 Risk Factors for *Fascioliasis*

Fascioliasis has infected 700 million animals and 180 million people worldwide are at risk of infection (Pan et al. 2022). The WHO 2007 report estimates that 2.4 to 17

million people worldwide have active *fascioliasis* and more than 180 million live in high-risk areas (Lan et al. 2024). *Fascioliasis* is emerging in new geographic regions due to the combined effects of climate change, anthropogenic activities and globalization (Sabourin et al. 2018). Warmer temperatures and altered rainfall patterns may expand the geographic distribution of *fascioliasis*, while international trade and travel could further its spread. As a zoonotic disease, *fascioliasis* highlights the need for integrated approaches that address both animal and human health (Cuervo et al. 2024). The main risk factors include:

- Humans are primarily infected by consuming raw or undercooked watercress and other aquatic plants.
- People involved in agriculture or animal husbandry are exposed to greater danger.
- Animals ingestion of encysted metacercariae on vegetables or aquatic plants.
- Lack of access to clean water, sanitation and limited education contribute to the spread of *fascioliasis*.

1.1.5 Economic Burden of *Fascioliasis*

Fascioliasis is an economically important parasitic snail-borne disease of ruminant animals such as cattle, sheep and goats that has implications for public health due to the risk of transmission of infection to humans. Infected animals suffer from growth retardation, decreased milk and meat production and liver damage (Opio et al. 2021).

Economically, global losses in animal productivity due to *fasciolosis* have been conservatively estimated to be more than $3.2 billion dollars per year (Ardo & Aliyara 2014) and have a negative impact on both milk production (20% – 80%) and meat production (8% – 50%) (García-López et al. 2018). The actual number of human and animal infections, and associated economic losses, are likely underestimated due to a lack of comprehensive investigations, poor coordination, and limited diagnostic tools in some developing countries (Fontenla et al. 2022).

Fasciolosis, which is caused by Fasciola of the liver fluke, can result in significant economic losses in African livestock (Howell et al. 2015). These economic losses are divided into two categories: direct losses (drug costs, labor and liver condemnation in abattoirs) and indirect losses (reduced production, poor growth rate, increased costs for replacement stock, reduced milk production and, quality and lower feed conversion rates in cattle)(Opio et al. 2021).

1.1.6 Diagnosis, Symptoms, Prevention, Treatment and Control of *Fasioliasis*

Accurately modeling *fasioliasis* requires incorporating its diagnosis, symptoms, prevention, treatment, and control. This integration enables simulations to evaluate interventions, optimize resource allocation, and predict outcomes, informing evidence-based policy and targeted control programs for this zoonotic disease.

a. Diagnosis

The diagnosis of *Fasciola hepatica* or liver fluke, in humans and cattle involves a combination of direct and indirect methods. Bovine *fasciolosis* is diagnosed based on clinical signs, grazing history, seasonal occurrence, fecal examination (stool) under a microscope, laboratory tests on faces, post-mortem examination and the presence of immature and mature flukes in the liver (Seid & Melese 2018, Alemu 2019, Diyana et al. 2019).

b. Symptoms

After ingestion of larvae through contaminated food or water, a symptomless incubation period begins that can last from a few days to a few months. The clinical manifestations of chronic *fasioliasis* vary according to the number of metacercariae consumed (Alemu 2019). Inflammation and obstruction of the bile duct can cause symptoms. Immature worms begin to penetrate the intestine wall during the acute phase, causing symptoms such as vomiting, intermittent fever, skin rash, itching, nausea, malaise, swollen liver, extreme abdominal pain, weight loss, diarrhea, and

anemia (Logue et al. 2017, MSD 2022). *Fascioliasis* manifests in asymptomatic, acute, and chronic forms, with clinical presentations associated with short- and long-term health impacts in both humans and animals (Logue et al. 2017, MSD 2022). The complex pathophysiology of *Fasciola* infection in definite hosts may pose challenges for the diagnosis and management of the disease (Caravedo & Cabada 2020).

c. Prevention

To prevent *Fascioliasis* infection, avoid eating raw watercress and other water plants, particularly from grazing areas where *Fasciola* is common. Thoroughly cooking these plants kills the parasite. A "One Health" strategy, integrating hygiene, targeted chemotherapy, and environmental management to disrupt the parasite's life cycle, is essential for protecting both animals and humans from fasciolosis (Wesolowska et al. 2018, CDC 2020).

For humans, protective measures include:

- Avoid eating raw aquatic plants (e.g., watercress) from livestock grazing areas.
- Drink boiled or treated/bottled water, especially in areas with poor sanitation.
- Establish proper sewage systems to prevent water source contamination.
- Implement public health education campaigns to raise awareness about transmission and prevention.
- Administer preventive chemotherapy in highly endemic areas as recommended by health authorities (e.g., triclabendazole by the WHO).

For animals, protective measures include:

- Strategic anthelmintic treatment using effective flukicides (e.g., triclabendazole, where effective) eliminates flukes and reduces pasture contamination.
- Grazing management should avoid high-risk, wet pastures where snails thrive, especially during peak seasons.

- Snail habitat can be controlled by draining swampy areas, improving irrigation maintenance, and fencing off water sources.

d. Treatment

Livestock is treated with medications including albendazole, closantel, clorsulon and triclabendazole. Bithionol was the only treatment available until the introduction of single-dose triclabendazole and was severely limited in terms of cost and duration of treatment (Tolan Jr 2011). Triclabendazole is the most commonly used and preferred flukicide (Nyindo & Lukambagire 2015). Effective *fascioliasis* control involves treating infected ruminants with an oral narrow-spectrum anthelmintic such as triclabendazole and reducing the intermediate host population (Alemu 2019). The only medicine recommended by the WHO for the treatment of human *fascioliasis* is triclabendazole (PAHO 2016). The drug of choice for treating *fascioliasis* is triclabendazole, a benzimidazole compound that is active against immature and adult *Fasciola* parasites (CDC 2020).

e. Control

Controlling bovine *fasciolosis* requires reducing the population of the intermediate host or using an anthelmintic (Admassu et al. 2015, Seid & Melese 2018). Fluke control should aim to reduce infection levels in both snails and cattle. Pasture drainage is another option, but in most cases it is impractical, prohibitively expensive and discouraged for environmental reasons (Howell et al. 2015). The emergence of drug-resistant strains of liver flukes has necessitated the development of a vaccine. Despite the enormous efforts of researchers in this area, no commercial vaccine is currently available (Atalabi & Lawal 2020). The current strategy to control *Fasciola hepatica* is mainly through the use of anthelmintic drugs that kill the parasite. It will not prevent infection, but it will reduce burden and egg production. The vaccine works to prevent transmission in three ways. It has the potential to reduce fluke fecundity, lengthen the average fluke maturation time and increase the mortality rate of immature fluke (Turner et al. 2016).

1.2 Mathematical Model of *Fasciolasis*

Mathematical models are valuable for understanding and predicting the spread of infectious diseases and evaluating control measures (Li & Zhao 2019). Although models exist for *fascioliasis* transmission, mathematical modeling of the disease remains limited. Existing models, often systems of non-linear ODEs, capture the dynamics of cattle and sheep (main hosts), snails (intermediate hosts), and *Fasciola* larval stages (egg, miracidia, metacercariae) to inform control strategies. (Turner et al. 2016, Diaby et al. 2019, Ogunmiloro 2021, 2022, Avazzadeh et al. 2023) have been developed to study *Fasciola* transmission and control. For example, Turner et al. (2016) developed a model to evaluate the effectiveness of limited protection vaccinations, finding that while vaccination can reduce burden and egg production, it does not prevent infections. It may also reduce fluke fertility, increase maturation time and increase juvenile mortality. Diaby et al. (2019) suggests that quarantine combined with medical therapy can effectively prevent *Fasciola hepatica*.

Optimal Control of *Fasciolasis*

Mathematical models can optimize *fascioliasis* control strategies. Controlling this disease is challenging due to the complex interplay of host factors (animal movement, immunity, human behavior), snail ecology, environmental conditions (temperature, moisture, water bodies) and agricultural practices (Dube et al. 2023). Mathematical modeling, particularly optimal control theory, has emerged as a powerful tool to design cost-effective, time-dependent intervention strategies by mathematically balancing disease burden reduction against intervention costs (Gaff & Schaefer 2009). Controlling disease effectively requires integrating medication, environmental management, snail control and community involvement to significantly improve human and animal health (Mesfin et al. 2024). Ogunmiloro (2022) used optimal control analysis to model the time-dependent effects of preventive measures, hygiene practices, and environmental sanitation. Their results showed that combining these strategies significantly reduced disease prevalence in domestic animals, emphasizing the

importance of integrated application.

1.3 Statement of the Problem

Zoonotic trematode infections, neglected tropical diseases, pose a significant global health burden (Nyindo & Lukambagire 2015). *F. hepatica*, a major veterinary and economic concern, reduces cattle productivity, increases costs and restricts trade. Limited understanding of its dynamics in cattle hampers effective control. Livestock is vital for protein, agriculture, transport and economic stability, providing livelihoods through meat, milk and income (Mekuriaw & Harris-Coble 2021, Bahiru & Assefa 2020). However, *F hepatica* diseases threaten the health and productivity of livestock, increasing maintenance costs. Eradication remains challenging due to high prevalence and inadequate control, especially in resource-poor settings. *Fasciolosis* significantly impacts productivity, veterinary costs, trade, public health and environmental sustainability.

Mathematical models are valuable tools for the analysis and control of infectious diseases, helping to design effective control strategies (Yusuf & Benyah 2012). Although some models address *Fasciola* transmission, research on optimal control strategies remains limited. This work develops a mathematical model of the transmission dynamics of *F. hepatica* with optimal control.

This study aims to develop a comprehensive disease model in cattle and humans for *F. hepatica* to understand transmission, identify optimal control measures and evaluate intervention strategies.

1.4 Objectives of the Study

1.4.1 General Objective

The general objective of this research is to develop deterministic models for the dynamics of *Fasciola hepatica* in the presence of optimal control strategies in order to combat the disease.

1.4.2 Specific Objectives

The specific objectives of this research are:

- To formulate a mathematical model for *Fasciola hepatica* in cattle and snails.
- To analyze cost-effective control strategies for *Fasciola hepatica* model in cattle.
- To formulate a mathematical model of *Fasciola hepatica* with early diagnosis and treatment effect.
- To investigate an optimal control model for *Fasciola hepatica* transmission in humans and cattle.

1.5 Significance of the Study

Fasciola hepatica is a re-emerging zoonotic parasite disease that has important health and economic impacts in many parts of the world. However, the emphasis on treatment, application of molluscicides, pasture management, education and awareness programs to improve sanitation is insufficient to combat this endemic disease. The development of the *Fasciola hepatica* model is very important in the full understanding of disease behavior, the investigation of transmission mechanisms and the design of control strategies that mitigate the disease. The study has the following main contributions:

- The findings provide critical information on the temporal dynamics of *Fasciola hepatica* infection in cattle and human populations.
- The study improves evidence based control of *Fasciola hepatica* in livestock and humans.
- The study investigates the responsiveness of optimal control inputs to determine the best approach to combating the disease.
- The findings help stakeholders to apply the most effective policies for preventing and monitoring disease.

- The study serves as a foundation for future studies on the dynamics of *Fasciola hepatica* disease and other related diseases.

1.6 Scope and Limitations of the Study

This research develops continuous deterministic models to describe the transmission dynamics of *Fasciola hepatica*. It does not consider geographical, seasonal, spatial, or stochastic factors. Optimal control strategies are limited to fundamental techniques governing the disease dynamics. The main limitation of the study is the generalization of the findings because the distribution of *fascioliasis* differs by region according to the climatic and geographical conditions. There are also problems with the accessibility of some data and the general lack of earlier studies on mathematical modeling of *fascioliasis*, which relied on estimating the value of some parameters within a plausible range. In addition, these findings have not been reviewed or commented on by key stakeholders in this area of practice, such as health professionals, governmental organizations and policymakers, which may affect the broader generalizability and validity of the findings.

1.7 Organization of the Dissertation

The dissertation is structured as follows. Chapter 2 reviews the relevant literature; Chapter 3 models and analyzes *Fasciola hepatica* disease transmission; Chapter 4 presents a mathematical model of *Fasciola hepatica* incorporating early diagnosis and treatment; Chapter 5 explores optimal control and cost-effectiveness analysis of the model; Chapter 6 analyzes human-cattle dynamics for effective *Fasciola hepatica* management; and Chapter 7 summarizes the findings, conclusions, recommendations and future work.

Chapter 2

2 Literature Review

2.1 Epidemiological Studies on *Fascioliasis*

Several researchers reported the prevalence, risk factors for association and economic loss of bovine *fasciolosis* in various parts of the world. Among many parasitic problems of farm animals, *fasciolosis* is a major disease that imposes an economic impact on livestock production, particularly cattle and sheep and has an important public health role, as it has zoonotic value (Feyisa 2021). This re-emerging zoonotic disease poses a major veterinary and public health concern, particularly in the developing world (Caravedo & Cabada 2020). It reduces milk and meat production, causes economic losses from liver infestation and mortality in young animals, and incurs treatment costs. International livestock production losses due to *fascioliasis* were estimated at over $3.2 billion USD annually in 1999 (Opio et al. 2021). Despite numerous epidemiological studies, *fascioliasis* remains a prevalent and uncontrolled public health and veterinary problem.

2.2 Mathematical Approaches in Infectious Disease Epidemiology

The first model for mathematical transmission of infectious diseases is the work of Daniel Bernoulli (1700-1782) on smallpox Dietz & Heesterbeek (2002), Bishop et al. (2010). Kermack and McKendrick's three papers (1927, 1932, 1933) introduced the basic compartmental models in mathematical epidemiology. Their work laid the foundation for understanding how infectious diseases spread through populations by categorizing individuals into compartments like susceptible, infected and recovered (Brauer 2017). Modern mathematical epidemiology uses compartmental models and

statistical analysis to understand and predict outbreaks, considering biological, host and environmental factors, contact patterns and public health interventions that influence disease transmission (Opio et al. 2021).

Mathematical modeling is increasingly used to study the transmission and control of *fascioliasis*. Early studies adapted classical SIR models to describe livestock infection dynamics, incorporating snail intermediate hosts. Modeling diseases in domestic animal populations is crucial for understanding pathogen-host interactions and developing effective disease control strategies. A One Health approach facilitates understanding the dynamics of disease risk, informs prevention and control strategies, examines threats and opportunities and improves our capacity for proactive solutions Osterhaus et al. (2020).

2.3 Mathematical Models of *Fasciolasis*

The interest in mathematical models for trematode infections in domestic ruminants originated from early generic stochastic and deterministic models, although these were not always directly foundational for later parasite-specific models. Early models analyzed the structure of the parasite age within hosts and the influence of weather on parasite survival and transmission, building on approaches such as (Ross 1970) work on sheep parasites and the "Stormont Wet Day" forecasting system. This system, used in Scotland and Ireland, used weather data from specific months to predict the risk of *fascioliasis*. This approach helped to forecast outbreaks and inform control measures. Despite a unified modeling framework that eventually emerged, most early models were developed ad hoc for specific control scenarios (Smith 2011).

Turner et al. (2016) developed a model to evaluate the efficacy of liver fluke vaccines under simulated field conditions. The model incorporates fluke development within a group of animals, considering host susceptibility, seasonal exposure to metacercariae and temperature-dependent metacercarial survival. The results suggest that potential vaccine candidates could reduce the total fluke burden and egg production by up to 43% and 99%, respectively. Furthermore, the study indicates that a vaccine must protect at least 90% of animals throughout the entire season to

be effective.

A more recent study Diaby et al. (2019) developed a nine-dimensional ODE model incorporating treatment and quarantine to analyze *Fasciola* epidemics. This work develops a multi-scale model that links disease transmission within a mammalian host population to the parasite's life cycle in the environment and its intermediate snail host. The model accounts for the various stages of the parasite's development, including the parasitic forms in the vertebrate host, the larval stages in the snail and the environmental cysts. The study investigates the parasite's presence in susceptible, infected and quarantined cattle, as well as fluke eggs on pasture, snail eggs, juvenile and mature snails, infected snails and metacercariae on pasture. This model analyzes disease dynamics, the impact of interventions and the role of intermediate hosts. The analysis highlights the importance of parasite-snail-host interaction parameters for understanding disease spread and intervention effectiveness. The result suggests that combining treatment and quarantine is more effective than either measure alone, demonstrating a synergistic effect that significantly reduces disease prevalence.

Ogunmiloro (2021) study *fascioliasis* transmission model using a fractional-order Caputo model to analyze interactions between humans, domestic animals and the environment. Both human and domestic animal populations are divided into three groups: those at risk of *fascioliasis*, those currently infected and those who have recovered. Environmental factors significantly affect transmission. The research establishes the existence and uniqueness of solutions, determines the basic reproduction number and examines the stability of disease-free and endemic equilibrium points. Focusing on mathematical analysis and approximate solutions, the study aimed to understand *fascioliasis* dynamics and inform control strategies. Simulations using the modified Euler method validated the efficiency and convergence of the model. Fractional-order modeling can stabilize systems and control disease spread, offering insights for public health interventions against *fascioliasis*. These findings highlight the potential of this modeling approach to inform public health strategies, like transmission rate reduction, for minimizing disease prevalence.

Ogunmiloro (2022) studied on an optimal control analysis of the transmission dynamics of *fascioliasis* disease. The study provides a detailed analysis of *fascioliasis* transmission in domestic ruminants using a non-linear optimal control model. The study examines the effects of three preventive strategies: treating infected animals, hygiene compliance and environmental sanitation. The results reveal that while each strategy individually reduces infection rates, their combined implementation is significantly more effective in controlling the disease's prevalence. The study also finds that maintaining these control measures for several months before gradually reducing them is crucial to optimal disease management. This research underscores the importance of integrated control strategies in effectively mitigating *fascioliasis* in domestic ruminant populations.

Avazzadeh et al. (2023) presented and optimized a fractional-order mathematical model for *fascioliasis* using generalized Fibonacci polynomials. The fractional *fascioliasis* model uses seven compartments: susceptible, infected and recovered human and domestic animal populations, plus an environmental source. This model examined the interactions between humans, domestic animals and the environment. Simulations demonstrated that fractional derivatives enhance modeling details for understanding real-world dynamics. The decrease in infected humans may be attributed to treatment or asymptomatic infections. The optimization technique effectively solved the model, offering a novel method to analyze and potentially control the disease, using generalized Fibonacci polynomials as basis functions and innovative operational matrices.

Understanding the specific impacts of various factors on parasite-snail-cattle-human interactions remains a key research gap. Furthermore, the application of advanced mathematical techniques like optimal control models is still nascent and requires further study to improve model accuracy and inform effective control strategies for both bovine and human *fascioliasis*. The study examines diagnostics, treatment, and snail control strategies to lessen the impact of *F. hepatica* on livestock and humans. This study employs cost-effectiveness analysis to determine the most efficient disease control approach in endemic areas with limited resources. Applying

optimal control theory to deterministic compartmental models can inform resource allocation strategies for managing infectious disease outbreaks. Therefore, we developed a mathematical model of *F. hepatica* in cattle and humans, using optimal control and cost-effectiveness analyses to determine effective and efficient control strategies, thus addressing this research gap.

Chapter 3

3 Modeling and Analysis of *Fasciola Hepatica* Disease Transmission

3.1 Introduction

This chapter presents a deterministic mathematical model of *Fasciola hepatica* transmission in cattle. The model incorporates various transmission pathways and parasite life stages, including interactions with cattle, snail populations and environmental factors. The mathematical model in Diaby et al. (2021) uniquely incorporates interactions between parasite development stages and intermediate hosts, as well as a quarantine strategy. The model explicitly accounts for egg and metacercariae stages. It tracks the parasite lifecycle across multiple stages and locations, including: susceptible cattle, infected cattle, quarantined cattle, fluke eggs on pasture, snail eggs, juvenile snails, mature snails, infected snails, and metacercariae on pasture. Our study modified previous models by including treatment at a compartment and the two key environmental stages of *Fasciola hepatica*, miracidia and metacercariae. In a *Fasciola* transmission model, miracidia and metacercariae production rates are key coupling parameters between host and environment. Their sensitivity to climate and control measures makes them primary drivers for understanding and managing the system. The model's well-posedness, positivity, invariant set and boundedness have been confirmed. The local and global stability, forward bifurcation and sensitivity of the model are analyzed. Sensitivity analysis identifies key parameters influencing disease prevalence, offering insights for targeted interventions.

3.2 Model Formulation

We develop a model describing the transmission dynamics of *Fasciola hepatica*. It considers various life stages of the parasite, the free-living larval stage and intermediate snail host, together with epidemiological conditions in cattle. It provides an overview of the different phases in the life cycle of the disease. First, we considered the cattle population to consist of three subpopulations: susceptible, infected, and treated, denoted by $S_C(t)$, $I_C(t)$, and $T_C(t)$, respectively. Also, there are two classes of snail populations: susceptible snails, denoted by $S_S(t)$, and infected snails, denoted by $I_S(t)$. Similarly, the *Fasciola* larvae population is categorized as miracidium and metacercariae, $M(t)$ and $P(t)$, respectively.

The model formulation is based on the following assumptions:

(i) There is no direct transmission of the disease between the cattle and snail populations.

(ii) Climate change does not impact the transmission of the disease.

(iii) Treatment leads to recovery, but does not provide immunity against reinfection.

(iv) The population dynamics of the hosts are not affected by the number of miracidia or metacercariae entering them.

(v) Metacercariae are uniformly distributed throughout the pasture.

Cattle transition between health classes as the disease progresses. Susceptible cattle become infected by ingesting metacercariae from vegetation or water. Susceptible cattle are those that have not yet contacted the disease but are still able to contract it. Infected cattle have consumed metacercariae. Treated cattle have received treatment for the disease. More details on the disease's progression:

(i) Susceptible to infected transition: Susceptible cattle progress to the infected state at a rate of γ_c. This transition occurs when the susceptible cattle consume metacercariae, which is the infectious stage of the parasite found on the pasture.

(ii) Treatment and recovery: Infected cattle undergo treatment at a rate of δ_c. The treatment aims to combat the infection. Treated cattle then recover from the disease at a rate of λ, indicating their transition back to a susceptible state.

(iii) Recruitment rates: New cattle and snails are added to the populations through birth rates, Λ_c and Λ_c, respectively.

(iv) Natural death rate: All cattle compartments: susceptible, infected, and treated cattle experience a natural death rate denoted by μ_c. This accounts for the regular mortality within the cattle population.

(v) Miracidia release and snail penetration: Infected cattle release miracidia at a rate of γ_m , representing the shedding rate per infected cattle. The term $\gamma_m I_C(t)$ represents the rate at which infected cattle (I_C) produce and release miracidia into the environment (compartment M). A portion of the miracidia population penetrates snails at a rate of γ_s, initiating the next stage of the parasite's life cycle.

(vi) Metacercariae production: Infected snail release miracidia at a rate of γ_p , representing the shedding/generation rate per infected snail. The term $\gamma_p I_S(t)$ represents the rate at which infected snail (I_S) produce and release eetacercariae into the environment (compartment P).

Figure 3.1 illustrates the disease's spread and interaction with cattle. Table 3.1 summarizes system parameters.

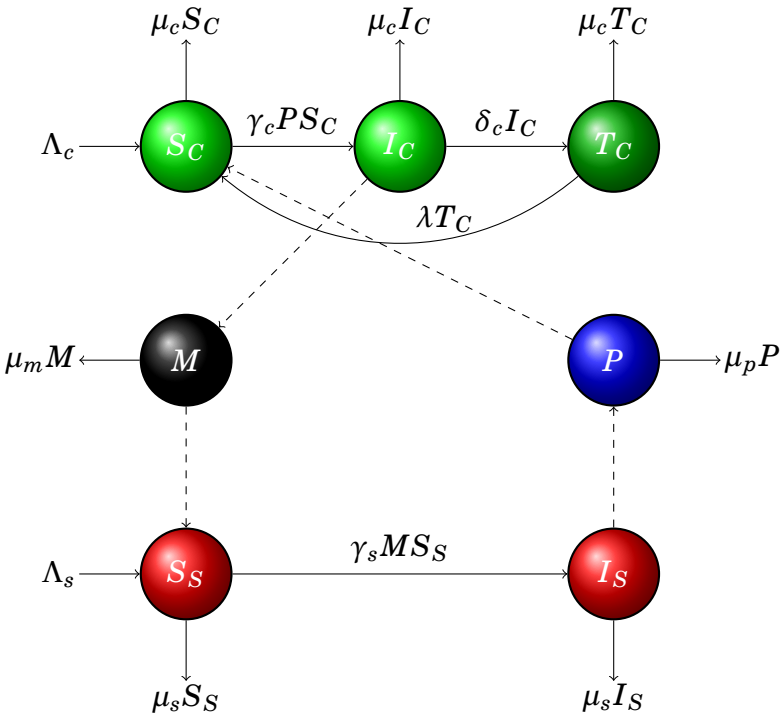

Figure 3.1: Flow diagram of the *Fasciola hepatica* disease transfer for model (3.1).

The model is presented using the ODE systems as follows:

$$\begin{aligned}
\frac{dS_C(t)}{dt} &= \Lambda_c - \gamma_c S_C(t)P(t) - \mu_c S_C(t) + \lambda T_C(t),\\
\frac{dI_C(t)}{dt} &= \gamma_c S_C(t)P(t) - (\delta_c + \mu_c)I_C(t),\\
\frac{dT_C(t)}{dt} &= \delta_c I_C(t) - (\lambda + \mu_c)T_C(t),\\
\frac{dM(t)}{dt} &= \gamma_m I_C(t) - \mu_m M(t),\\
\frac{dS_S(t)}{dt} &= \Lambda_s - \gamma_s S_S(t)M(t) - \mu_s S_S(t),\\
\frac{dI_S(t)}{dt} &= \gamma_s S_S(t)M(t) - \mu_s I_S(t),\\
\frac{dP(t)}{dt} &= \gamma_p I_S(t) - \mu_p P(t),
\end{aligned} \tag{3.1}$$

with nonnegative initial conditions: $S_C(0) \geq 0$, $I_C(0) \geq 0$, $T_C(0) \geq 0$, $M(0) \geq 0$, $P(0) \geq 0$, $S_S(0) \geq 0$ and $I_S(0) \geq 0$. Table 3.1 presents the values and biological relevance of each parameter of the system.

Table 3.1: Values and descriptions of the model (3.1) parameters.

Parameter	Epidemiological Description	Value	Source
Λ_c	Cattle recruitment rate	67/day	(Diaby et al. 2019)
Λ_s	Snail recruitment rate	3000/day	(Kanyi et al. 2021)
μ_c	Cattle natural death rate	0.0185/day	(Diaby et al. 2019)
μ_s	Snails natural death rate	0.001644/day	(Diaby et al. 2019)
μ_m	Natural death rate for miracidia larvae	0.9/day	(Kanyi et al. 2021, Chiyaka & Garira 2009)
μ_p	Natural death rate for metacercariae larvae	0.6452/day	(Diaby et al. 2019)
γ_m	Production rate of miracidia from infected cattle	6.96 /day	(Kanyi et al. 2021)
γ_p	Production rate of metacercariae from infected snail	2.6 /day	(Kanyi et al. 2021)
γ_c	Per capita infection rate of cattle	0.0000005 /day	(Diaby et al. 2019)
γ_s	Per capita infection rate of snails	0.00000004 /day	Assumed
δ_c	Treatment rate of infected cattle	0.65/day	Assumed
λ	Treatment efficiency of the infected cattle	0.9567/day	(Diaby et al. 2019)

3.3 Model Analysis

We aim to ensure the biological relevance and accurate presentation of the model (3.1) by rigorously verifying that all fundamental state components start with and maintain positive values throughout the region.

3.3.1 Well-posedness

Rewrite the system (3.1) as $\frac{dx}{dt} = f(x)$, where $x = (S_C, I_C, T_C, M, S_S, I_S, P) \in \mathbb{R}^7_+$. The right hand side is smooth (continuously differentiable in the state variable), thus

locally Lipschitz continuous on $\mathbb{R}^7_+$. Therefore, by the Cauchy–Lipschitz theorem, for any initial condition in $\mathbb{R}^7_+$, there exists a unique maximal solution defined on $[0,\ T]$.

3.3.2 Positive Invariant Region

Proposition 3.1. *If all initial values $S_C(0)$, $I_C(0)$, $T_C(0)$, $M(0)$, $S_S(0)$, $I_S(0)$ and $P(0)$ are non-negative, then the solutions to the model (3.1) will remain non-negative for all $t \geq 0$.*

Proof. Let $\Gamma = \{(S_C, I_C, T_C, M, S_S, I_S, P)\ | S_C, I_C, T_C, M, S_S, I_S, P \geq 0\}$. By the Cauchy-Lipschitz theorem, for any $x(0) \in \Gamma$, there is a unique solution $x(t)$ on a maximal interval $[0, T]$. Now, examine the vector field along the boundaries of Γ:

- When $S_C = 0$, $\frac{dS_C}{dt} = \Lambda_c + \lambda T_C \geq 0$, since $T_C \geq 0$.
- When $I_C = 0$, $\frac{dI_C}{dt} = \gamma_c S_C P - (\delta_c + \mu_c) I_C = \gamma_c S_C P \geq 0$.
- When $T_C = 0$, $\frac{dT_C(t)}{dt} = \delta_c I_C \geq 0$, since $I_C \geq 0$.
- When $M = 0$, $\frac{dM(t)}{dt} = \gamma_m I_C \geq 0$.
- When $S_S = 0$, $\frac{dS_S}{dt} = \Lambda_s \geq 0$.
- When $I_S = 0$, $\frac{dI_S}{dt} = \gamma_s S_S M \geq 0$.
- When $P = 0$, $\frac{dP}{dt} = \gamma_p I_S \geq 0$.

Since the vector field is directed inward along the boundaries of Γ, it is invariant, ensuring non-negative solutions. Consequently, for any $x(0) \in \Gamma$, the solution is unique and invariant within Γ due to Lipschitz continuity. Therefore, all state variables remain non-negative for all non-negative t. □

3.3.3 Boundedness of Solutions

Proposition 3.2. *All possible solutions to model (3.1) remain within a uniformly bounded region:*

$$\Omega = \left\{(S_C, I_C, T_C, M, S_S, I_S, P) \in \mathbb{R}^7 : N_C \leq \frac{\Lambda_c}{\mu_c}, N_S \leq \frac{\Lambda_s}{\mu_s}, M \leq \frac{\gamma_m \Lambda_c}{\mu_c \mu_m}, P \leq \frac{\gamma_p \Lambda_s}{\mu_s \mu_p}\right\}, \quad (3.2)$$

where, $N_C(t) = S_C(t) + I_C(t) + T_C(t)$ *and* $N_S(t) = S_S(t) + I_S(t)$ *are the total cattle and snail population at time t.*

Proof. Consider the total population of cattle in the model (3.1),

$$\frac{dN_C}{dt} = \Lambda_c - \mu_c N_C. \tag{3.3}$$

Solving the differential equation (3.3) leads to the solution

$$N_C(t) = \frac{\Lambda_c}{\mu_c} - \left(\frac{\Lambda_c - \mu_c N_C(0)}{\mu_c}\right) e^{-\mu_c t}.$$

As $t \to \infty$, $N_C(t)$ converges to $\frac{\Lambda_c}{\mu_c}$. If $0 \leq N_C(0) \leq \frac{\Lambda_c}{\mu_c}$, then

$$0 \leq N_C(t) \leq \frac{\Lambda_c}{\mu_c}. \tag{3.4}$$

Adding the equations for the snail subclass yields the overall dynamics of the snail population.

$$\frac{dN_S}{dt} = \Lambda_s - \mu_s N_S \tag{3.5}$$

Obtaining the solution to the differential equation (3.5) for $N_S(t)$ provides

$$N_S(t) = \frac{\Lambda_s}{\mu_s} - (\frac{\Lambda_s - \mu_s N_S(0)}{\mu_s}) e^{-\mu_s t} \tag{3.6}$$

As time approaches infinity ($t \to \infty$), then $N_S(t)$ approaches to the value of $\frac{\Lambda_s}{\mu_s}$. Hence, we can conclude that

$$0 \leq N_s(t) \leq \frac{\Lambda_s}{\mu_s} \tag{3.7}$$

Using the fourth equation (3.1) and equation (3.4), we have

$$\frac{dM}{dt} = \gamma_m I_C - \mu_m M \leq \gamma_m \frac{\Lambda_c}{\mu_c} - \mu_m M$$

Applying Chaplygin's Method Zwillinger & Dobrushkin (1998) to this differential inequality implies that

$$0 \leq M(t) \leq \frac{\gamma_m \Lambda_c}{\mu_c \mu_m}.$$

Combining equations (3.1) and (3.7), we obtain

$$\frac{dP}{dt} = \gamma_p I_S - \mu_p P \leq \gamma_p \frac{\Lambda_s}{\mu_s} - \mu_p P$$

This leads to the result that

$$0 \leq P \leq \frac{\gamma_p \Lambda_s}{\mu_s \mu_p}$$

.

Thus, we have $\limsup_{t\to\infty} N_C(t) \leq \frac{\Lambda_c}{\mu_c}$, $\limsup_{t\to\infty} N_S(t) \leq \frac{\Lambda_s}{\mu_s}$, $\limsup_{t\to\infty} M \leq \frac{\Lambda_c \gamma_m}{\mu_c \mu_m}$ and $\limsup_{t\to\infty} P \leq \frac{\Lambda_s \gamma_p}{\mu_s \mu_p}$. Since, f satisfies local Lipschitz conditions and the solutions are bounded in Γ, they cannot tend toward infinity within finite time. Therefore, the maximal interval $[0,T]$ can be extended to $[0,\infty)$. This completes the proof, confirming that Ω in (3.2) defines the feasible region of the system. □

Therefore, the model is suitable for an epidemiological study.

3.3.4 Disease-Free Equilibrium (DFE)

The disease-free equilibrium of *Fasciola hepatica* is a state without infection. This equilibrium point is found by setting the derivatives of the model (3.1) to zero and the disease class states equals zero ($I_C = 0$, $I_S = 0$, $M = 0$ and $P = 0$) and :

$$\begin{aligned}
\frac{dS_C}{dt} &= \Lambda_c - \mu_c S_C + \lambda T_C = 0, \\
\frac{dI_C}{dt} &= 0, \\
\frac{dT_C}{dt} &= -(\lambda + \mu_c) T_C = 0, \\
\frac{dM}{dt} &= 0, \\
\frac{dS_S}{dt} &= \Lambda_s - \mu_s S_S = 0, \\
\frac{dI_S}{dt} &= 0, \\
\frac{dP}{dt} &= 0.
\end{aligned} \tag{3.8}$$

Thus, $S_C = \frac{\Lambda_c}{\mu_c}$, $T_C = 0$ and $S_C = \frac{\Lambda_c}{\mu_c}$.

Therefore the disease-free equilibrium point is

$$E_0 = \left(S_C^0, I_C^0, T_C^0, M^0, S_S^0, I_S^0, P^0\right) = \left(\frac{\Lambda_c}{\mu_c}, 0, 0, 0, \frac{\Lambda_s}{\mu_s}, 0, 0\right). \tag{3.9}$$

3.3.5 Local Stability of the Disease-Free Equilibrium

In epidemiological studies, the next-generation matrix technique (van den Driessche & Watmough 2002) is used to quantify the basic reproduction number for the compartmental model of infectious disease. In model (3.1), the compartments I_C, M, I_S and P represent various stages or categories of individuals within the infected population. Therefore, the system of differential equations governing these disease compartments can be described as follows:

$$\begin{cases} I_C'(t) &= \gamma_c S_C(t) P(t) - (\delta_c + \mu_c) I_C(t), \\ M'(t) &= \gamma_m I_C(t) - \mu_m M(t), \\ I_S'(t) &= \gamma_s S_S(t) M(t) - \mu_s I_S(t), \\ P'(t) &= \gamma_p I_S(t) - \mu_p P(t). \end{cases} \tag{3.10}$$

We can express equation (3.10) as:

$$\frac{d\mathscr{Y}}{dy} = f(\mathscr{Y}) - v(\mathscr{Y}),$$

where $f(\mathscr{Y})$ represents the incidence rate of new incidents appearing in the disease compartments and $v(\mathscr{Y})$ represents the rate at which individuals are moved into and out of the compartments. The variable $\mathscr{Y}$ represents the disease subclass of the system, $\mathscr{Y} = (I_C, M, I_S, P)$,

$$f = \begin{pmatrix} \gamma_c S_C P \\ 0 \\ \gamma_s S_s M \\ 0 \end{pmatrix} \text{ and } v = \begin{pmatrix} (\delta_c + \mu_c) I_C \\ -\gamma_m I_C + \mu_m M \\ \mu_s I_S \\ -\gamma_p I_S + \mu_p P \end{pmatrix}.$$

Evaluating the derivatives of f and v with respect to the disease variables at the disease-free equilibrium yields Jacobian matrices $\mathscr{F}$ and $\mathscr{V}$, representing the transfer and new infection terms, respectively.

$$\mathscr{F} = \begin{pmatrix} 0 & 0 & 0 & \frac{\gamma_c \Lambda_c}{\mu_c} \\ 0 & 0 & 0 & 0 \\ 0 & \frac{\gamma_s \Lambda_s}{\mu_s} & 0 & 0 \\ 0 & 0 & 0 & 0 \end{pmatrix},$$

$$\mathcal{V} = \begin{pmatrix} \delta_c + \mu_c & 0 & 0 & 0 \\ -\gamma_m & \mu_m & 0 & 0 \\ 0 & 0 & \mu_s & 0 \\ 0 & 0 & -\gamma_p & \mu_p \end{pmatrix} and$$

$$\mathcal{V}^{-1} = \begin{pmatrix} \frac{1}{\delta_c+\mu_c} & 0 & 0 & 0 \\ \frac{\gamma_m}{\mu_m(\delta_c+\mu_c)} & \frac{1}{\mu_m} & 0 & 0 \\ 0 & 0 & \frac{1}{\mu_s} & 0 \\ 0 & 0 & \frac{\gamma_p}{\mu_p\mu_s} & \frac{1}{\mu_p} \end{pmatrix}.$$

After some algebraic simplification, we get

$$\mathcal{F}\mathcal{V}^{-1} = \begin{pmatrix} 0 & 0 & \frac{\gamma_c\gamma_p\Lambda_c}{\mu_c\mu_s\mu_p} & \frac{\gamma_c\Lambda_c}{\mu_c\mu_p} \\ 0 & 0 & 0 & 0 \\ \frac{\Lambda_s\gamma_m\gamma_s}{\mu_m\mu_s(\delta_c+\mu_c)} & \frac{\Lambda_s\gamma_s}{\mu_s\mu_m} & 0 & 0 \\ 0 & 0 & 0 & 0 \end{pmatrix}.$$

Therefore, the effective reproduction number, which is the spectral radius of $\mathcal{F}\mathcal{V}^{-1}$, is

$$R_0 = \sqrt{\frac{\gamma_c\gamma_m\gamma_s\gamma_p\Lambda_c\Lambda_s}{\mu_c(\delta_c+\mu_c)\mu_m\mu_p\mu_s^2}}. \tag{3.11}$$

Rewrite the equation provides,

$$R_0 = \sqrt{\underbrace{\frac{\gamma_c\gamma_p\Lambda_c}{\mu_c\mu_p(\delta_c+\mu_c)}}_{\text{Cattle infection potential}} \times \underbrace{\frac{\gamma_m\gamma_s\Lambda_s}{\mu_m\mu_s^2}}_{\text{Snail infection potential}}}.$$

This R_0 is the effective reproduction number for the *Fasciola hepatica* model, representing the average number of new secondary infections produced by one infected individual in a completely susceptible population (Bakare et al. 2014). The square root appears because of the cycle involves two transition steps(cattle to snail and snail to cattle).

The basic reproduction number (when $\delta_c = 0$) is

$$R_b = \sqrt{\frac{\gamma_c\gamma_p\Lambda_c}{\mu_c^2\mu_p} \times \frac{\gamma_m\gamma_s\Lambda_s}{\mu_m\mu_s^2}}$$

Theorem 3.3. *The disease-free equilibrium point is locally asymptotically stable in* Ω *when* $R_0 < 1$.

Proof. Linearizing equation (3.1) at DFE, E_0 yields the Jacobian matrix $J(E_0)$.

$$J(E_0) = \begin{pmatrix} -\mu_c & 0 & \lambda & 0 & 0 & 0 & -\frac{\gamma_c \Lambda_c}{\mu_c} \\ 0 & -(\delta_c + \mu_c) & 0 & 0 & 0 & 0 & \frac{\gamma_c \Lambda_c}{\mu_c} \\ 0 & \delta_c & -(\lambda + \mu_c) & 0 & 0 & 0 & 0 \\ 0 & \gamma_m & 0 & -(\mu_m + \gamma_s) & 0 & 0 & 0 \\ 0 & 0 & 0 & -\frac{\gamma_s \Lambda_s}{\mu_s} & -\mu_s & 0 & 0 \\ 0 & 0 & 0 & \frac{\gamma_s \Lambda_s}{\mu_s} & 0 & -\mu_s & 0 \\ 0 & 0 & 0 & 0 & 0 & \gamma_p & -(\mu_p + \gamma_c) \end{pmatrix} \tag{3.12}$$

The eigenvalues of the Jacobian matrix are $-\mu_c$, $-\mu_s$, $-\lambda - \mu_c$ and roots of the following characteristic equation

$$P_4 X^4 + P_3 X^3 + P_2 X^2 + P_1 X + P_0 = 0 \tag{3.13}$$

Where,

$P_4 = \mu_c \mu_s$,

$P_3 = \mu_c \mu_s (\gamma_c + \gamma_s + \delta_c + \mu_c + \mu_m + \mu_p + \mu_s)$,

$p_2 = \mu_c \mu_s (\delta_c \mu_m + \mu_c \mu_m + \delta_c \mu_p + \mu_c \mu_p + \mu_m \mu_p + \delta_c \mu_s + \mu_c \mu_s + \mu_m \mu_s + \mu_p \mu_s + \gamma_c (\gamma_s + \delta_c + \mu_c + \mu_m + \mu_s) + \gamma_s (\delta_c + \mu_c + \mu_p + \mu_s))$,

$P_1 = \mu_c \mu_s (\delta_c \mu_m \mu_p + \mu_c \mu_m \mu_p + \delta_c \mu_m \mu_s + \mu_c \mu_m \mu_s + \delta_c \mu_p \mu_s + \mu_c \mu_p \mu_s + \mu_m \mu_p \mu_s + \gamma_c (\mu_c \mu_m + \mu_c \mu_s + \mu_m \mu_s + \gamma_s (\delta_c + \mu_c + \mu_s) + \delta_c (\mu_m + \mu_s)) + \gamma_s (\mu_p \mu_s + \delta_c (\mu_p + \mu_s) + \mu_c (\mu_p + \mu_s)))$,

$P_0 = \mu_c (\delta_c + \mu_c)(\gamma_s + \mu_m)(\mu_c + \gamma_p) \mu_s^2)(1 - R_0^2)$

By Routh-Hurwitz conditions for 4th degree polynomial, all roots have negative real parts if and only if

(i) $P_i > 0$, for all $i = 0, 1, 2, 3, 4$ and

(ii) $P_1 P_2 P_3 > P_1^2 P_4 + P_0 P_3^2$.

Clearly, P_4, P_3, P_2, P_1 and P_0 are positive, for $R_0 < 1$.

Condition (ii) can be expressed as:

$$P_1 P_2 P_3 - P_1^2 P_4 - P_0 P_3^2 > 0. \tag{3.14}$$

Let us rewrite the coefficients in compact form:

$$P_4 = \mu_c \mu_s,$$
$$P_3 = \mu_c \mu_s a_3,$$
$$P_2 = \mu_c \mu_s a_2,$$
$$P_1 = \mu_c \mu_s a_1,$$

where:

$$\begin{aligned}
a_3 &= \gamma_c + \gamma_s + \delta_c + \mu_c + \mu_m + \mu_p + \mu_s, \\
a_2 &= \delta_c\mu_m + \mu_c\mu_m + \delta_c\mu_p + \mu_c\mu_p + \mu_m\mu_p + \delta_c\mu_s + \mu_c\mu_s + \mu_m\mu_s + \mu_p\mu_s \\
&\quad + \gamma_c(\gamma_s + \delta_c + \mu_c + \mu_m + \mu_s) + \gamma_s(\delta_c + \mu_c + \mu_p + \mu_s), \\
a_1 &= \delta_c\mu_m\mu_p + \mu_c\mu_m\mu_p + \delta_c\mu_m\mu_s + \mu_c\mu_m\mu_s + \delta_c\mu_p\mu_s + \mu_c\mu_p\mu_s + \mu_m\mu_p\mu_s \\
&\quad + \gamma_c\big(\mu_c\mu_m + \mu_c\mu_s + \mu_m\mu_s + \gamma_s(\delta_c + \mu_c + \mu_s) + \delta_c(\mu_m + \mu_s)\big) \\
&\quad + \gamma_s\big(\mu_p\mu_s + \delta_c(\mu_p + \mu_s) + \mu_c(\mu_p + \mu_s)\big).
\end{aligned}$$

Now substitute into (3.14):

$$\begin{aligned}
P_1P_2P_3 &= (\mu_c\mu_s a_1)(\mu_c\mu_s a_2)(\mu_c\mu_s a_3) = (\mu_c\mu_s)^3 a_1a_2a_3, \\
P_1^2P_4 &= (\mu_c\mu_s a_1)^2(\mu_c\mu_s) = (\mu_c\mu_s)^3 a_1^2, \\
P_0P_3^2 &= \left[\mu_c(\delta_c + \mu_c)(\gamma_s + \mu_m)(\mu_c + \gamma_p)\mu_s^2(1 - R_0^2)\right] \cdot (\mu_c\mu_s a_3)^2 \\
&= \mu_c(\delta_c + \mu_c)(\gamma_s + \mu_m)(\mu_c + \gamma_p)\mu_s^2(1 - R_0^2) \cdot \mu_c^2\mu_s^2 a_3^2 \\
&= \mu_c^3(\delta_c + \mu_c)(\gamma_s + \mu_m)(\mu_c + \gamma_p)\mu_s^4(1 - R_0^2)a_3^2.
\end{aligned}$$

Thus condition (3.14) becomes:

$$(\mu_c\mu_s)^3 a_1a_2a_3 - (\mu_c\mu_s)^3 a_1^2 - \mu_c^3(\delta_c + \mu_c)(\gamma_s + \mu_m)(\mu_c + \gamma_p)\mu_s^4(1 - R_0^2)a_3^2 > 0. \tag{3.15}$$

Factor out $\mu_c^3\mu_s^3 > 0$:

$$\mu_c^3\mu_s^3\left[a_1a_2a_3 - a_1^2\right] - \mu_c^3(\delta_c + \mu_c)(\gamma_s + \mu_m)(\mu_c + \gamma_p)\mu_s^4(1 - R_0^2)a_3^2 > 0. \tag{3.16}$$

Divide both sides by $\mu_c^3\mu_s^3 > 0$:

$$a_1a_2a_3 - a_1^2 - (\delta_c + \mu_c)(\gamma_s + \mu_m)(\mu_c + \gamma_p)\mu_s(1 - R_0^2)a_3^2 > 0. \tag{3.17}$$

Define:

$$K = (\delta_c + \mu_c)(\gamma_s + \mu_m)(\mu_c + \gamma_p)\mu_s > 0.$$

Then we obtain the final form:

$$\boxed{a_1 a_2 a_3 - a_1^2 - K(1 - R_0^2)a_3^2 > 0} \tag{3.18}$$

Condition (3.18) represents a nontrivial constraint involving all model parameters.

Therefore, the disease-free equilibrium is locally asymptotically stable if $R_0 < 1$, by Routh-Hurwitz criterion. □

3.3.6 Global Stability of Disease-Free Equilibrium

Castillo-Chavez et al. (2002) proposed a method to determine the global steady state of the DFE within $\Omega \in R_+^7$. The model (3.1) is expressed as follows:

$$\begin{aligned} \frac{dU}{dt} &= R(U,V), \\ \frac{dV}{dt} &= Q(U,V),\ Q(U,0) = 0, \end{aligned} \tag{3.19}$$

where, $U = (S_C, T_C, S_S)$ consists of the disease-free subgroups and $V = (I_C, M, I_S, P)$ consists of infectious subgroups.

If the requirements $(C1)$ and $(C2)$ stated below are satisfied, then E_0 will be globally stable whenever $R_0 < 1$.

$C1$: When $\frac{dU}{dt} = R(U,0)$, U^* is globally stable.

$C2$: $Q(U,V) = BV - \hat{Q}(U,V)$, $\hat{Q}(U,V) \geq 0$ for $(U,V) \in \Omega$,

with $B = D_V Q(U^*, 0)$ is Metzler-matrix (off-diagonal entries of B are nonnegative) and Ω is the set at which the system becomes feasible.

Theorem 3.4. *The disease-free equilibrium, E_0, is globally asymptotically stable if $R_0 < 1$ and unstable otherwise.*

Proof. From model (3.1) and equation (3.19), we have

$$R(U,0) = \begin{pmatrix} \Lambda_c - \mu_c S_C \\ 0 \\ \Lambda_s - \mu_s S_S \end{pmatrix}. \tag{3.20}$$

$$Q(U,V) = \begin{pmatrix} \gamma_c S_C P - (\delta_c + \mu_c) I_C \\ \gamma_m I_C - \mu_m M \\ \gamma_s S_S M - \mu_s I_S \\ \gamma_p I_S - \mu_p P \end{pmatrix}, \tag{3.21}$$

such that,

$$Q(U,V) = BV - \hat{Q}(U,V), \tag{3.22}$$

where,

$$B = \begin{pmatrix} -(\delta_c + \mu_c) & 0 & 0 & \frac{\gamma_c \Lambda_c}{\mu_c} \\ \gamma_m & -\mu_m & 0 & 0 \\ 0 & \frac{\gamma_s \Lambda_s}{\mu_s} & -\mu_s & 0 \\ 0 & 0 & \gamma_s & -\mu_p \end{pmatrix}, \tag{3.23}$$

$$\hat{Q}(U,V) = \begin{pmatrix} -\gamma_c S_C P + \frac{\gamma_c \Lambda_c}{\mu_c} P \\ 0 \\ -\gamma_s S_s M + \frac{\gamma_s \Lambda_s}{\mu_s} M \\ 0 \end{pmatrix} = \begin{pmatrix} P\gamma_c (\frac{\Lambda_c}{\mu_c} - S_C) \\ 0 \\ M\gamma_s (\frac{\Lambda_s}{\mu_s} - S_S) \\ 0 \end{pmatrix}. \tag{3.24}$$

Clearly, $U^* = (\frac{\Lambda_c}{\mu_c}, 0, \frac{\Lambda_s}{\mu_s})$ is the global asymptote of equation (3.20) and hence condition *C1* is satisfied. Also, from equation (3.24), $\hat{Q}(U,V) \geq 0$ for $S_C \leq \frac{\Lambda_c}{\mu_c}$ and $S_S \leq \frac{\Lambda_s}{\mu_s}$. Thus, $\hat{Q}(U,V) \geq 0,\ \forall (U,V) \in \Omega$ and condition *C2* hold. Since the non-diagonal entries are non-negative, A is an M-matrix. This shows that the DFE is globally stable whenever $R_0 < 1$. □

3.3.7 Existence of Endemic Equilibrium Point

Proposition 3.5. *The model (3.1) has a unique endemic equilibrium for* $R_0 > 1$.

The endemic equilibrium point E_e^* occurs when the *Fasciola hepatica* infection persists in cattle. It is given by

$$E_e^* = (S_C^*, I_C^*, T_C^*, M^*, S_S^*, I_S^*, P^*), \tag{3.25}$$

where

$$\left.\begin{aligned}
S_C^* &= \tfrac{(\delta_c+\mu_c)\mu_p\mu_s(\gamma_m\gamma_s\Lambda_c(\lambda+\mu_c)+\mu_c(\lambda+\delta_c+\mu_c)\mu_m\mu_s)}{\gamma_m\gamma_s\mu_c(\gamma_c\gamma_p\Lambda_s(\lambda+\delta_c+\mu_c)+(\lambda+\mu_c)(\delta_c+\mu_c)\mu_p\mu_s)},\\
I_C^* &= \tfrac{A(\lambda+\mu_c)(R_0^2-1)}{\gamma_m\gamma_s\mu_c(\gamma_c\gamma_p\Lambda_s(\lambda+\delta_c+\mu_c)+(\lambda+\mu_c)(\delta_c+\mu_c)\mu_p\mu_s)},\\
T_C^* &= \tfrac{\delta_c A(R_0^2-1)}{\gamma_m\gamma_s\mu_c(\gamma_c\gamma_p\Lambda_s(\lambda+\delta_c+\mu_c)+(\lambda+\mu_c)(\delta_c+\mu_c)\mu_p\mu_s)},\\
M^* &= \tfrac{A(\lambda+\mu_c)(R_0^2-1)}{\gamma_s\mu_c\mu_m(\gamma_c\gamma_p\Lambda_s(\lambda+\delta_c+\mu_c)+(\lambda+\mu_c)(\delta_c+\mu_c)\mu_p\mu_s)},\\
S_S^* &= \tfrac{\mu_c\mu_m(\gamma_c\gamma_p\Lambda_s(\lambda+\delta_c+\mu_c)+(\lambda+\mu_c)(\delta_c+\mu_c)\mu_p\mu_s)}{\gamma_c\gamma_p(\gamma_m\gamma_s\Lambda_c(\lambda+\mu_c)+\mu_c(\lambda+\delta_c+\mu_c)\mu_m\mu_s)},\\
I_S^* &= \tfrac{A(\lambda+\mu_c)(R_0^2-1)}{\gamma_c\gamma_p\mu_s(\gamma_m\gamma_s\Lambda_c(\lambda+\mu_c)+\mu_c(\lambda+\delta_c+\mu_c)\mu_m\mu_s)},\\
P^* &= \tfrac{A(\lambda+\mu_c)(R_0^2-1)}{\gamma_c\mu_p\mu_s(\gamma_m\gamma_s\Lambda_c(\lambda+\mu_c)+\mu_c(\lambda+\delta_c+\mu_c)\mu_m\mu_s)},
\end{aligned}\right\} \tag{3.26}$$

such that, $A = \mu_c(\delta_c+\mu_c)\mu_m\mu_p\mu_s^2$.

Thus, $S_C^* > 0$, $I_C^* > 0$, $T_C^* > 0$, $M^* > 0$, $S_S^* > 0$, $I_S^* > 0$ and $P^* > 0$ if $R_0 > 1$. This proves that the disease becomes endemic if $R_0 > 1$ □.

3.3.8 Local Stability of Endemic Equilibrium Point

Proposition 3.6. *The endemic equilibrium point, E_e^*, is locally asymptotically stable if $R_0 > 1$.*

Applying the theorem from Castillo-Chavez & Song (2004), the model demonstrates a forward bifurcation (see the proof of Theorem 3.7), indicating that the endemic equilibrium is locally asymptotically stable when $R_0 > 1$.

3.3.9 Forward Bifurcation Analysis

Bifurcation theory examines qualitative changes in system behavior, particularly stability or instability of fixed points and periodic orbits, as the parameters vary. It is a useful tool for analyzing qualitative changes in steady-state solutions (Sharma et al. 2015). The occurrence of a forward bifurcation indicates that the endemic equilibrium is locally stable if $R_0 > 1$ (Madubueze et al. 2022).

Theorem 3.7. *The model (3.1) has a forward bifurcation when $R_0 = 1$.*

Proof. We apply the Castillo-Chavez and Song theorem to prove this theorem. For simplicity, the following variable change is made for the model (3.1):

$S_C = y_1$, $I_C = y_2$, $T_C = y_3$, $M = y_4$, $S_S = y_5$, $I_S = y_6$ and $P = y_7$.

Thus, the model (3.1) transforms into:

$$\begin{aligned}
\frac{dy_1}{dt} &= \Lambda_c - \gamma_c y_1 y_7 - \mu_c y_1 + \lambda y_3 := r_1,\\
\frac{dy_2}{dt} &= \gamma_c y_1 y_7 - (\delta_c + \mu_c) y_2 := r_2,\\
\frac{dy_3}{dt} &= \delta_c y_2 - (\lambda + \mu_c) y_3 := r_3,\\
\frac{dy_4}{dt} &= \gamma_m y_2 - \mu_m y_4 := r_4,\\
\frac{dy_5}{dt} &= \Lambda_s - \gamma_s y_4 y_5 - \mu_s y_5 := r_5,\\
\frac{dy_6}{dt} &= \gamma_s y_4 y_5 - \mu_s y_6 := r_6,\\
\frac{dy_7}{dt} &= \gamma_p y_6 - \mu_p y_7 := r_7,
\end{aligned} \tag{3.27}$$

The disease-free equilibrium of (3.27) is $(y_1, y_2, y_3, y_4, y_5, y_6, y_7) = (\frac{\Lambda_c}{\mu_c}, 0, 0, 0, \frac{\Lambda_s}{\mu_s}, 0, 0)$. Assume $\phi = \gamma_c^*$ be the bifurcation parameter at $R_0 = 1$ and we obtained

$$\phi = \gamma_c^* = \frac{\mu_c(\delta_c + \mu_c)\mu_m \mu_p \mu_s^2)}{\gamma_m \gamma_p \gamma_s \Lambda_c \Lambda_s}. \tag{3.28}$$

When $\phi = \gamma_c^*$, the Jacobian matrix of equation (3.27) at disease-free equilibrium gives

$$J_\phi(E_0) = \begin{pmatrix}
-\mu_c & 0 & \lambda & 0 & 0 & 0 & -\frac{\phi\Lambda_c}{\mu_c}\\
0 & -(\mu_c + \delta_c) & 0 & 0 & 0 & 0 & \frac{\phi\Lambda_c}{\mu_c}\\
0 & \delta_c & -(\mu_c + \lambda) & 0 & 0 & 0 & 0\\
0 & \gamma_m & 0 & -\mu_m & 0 & 0 & 0\\
0 & 0 & 0 & -\frac{\gamma_s\Lambda_s}{\mu_s} & -\mu_s & 0 & 0\\
0 & 0 & 0 & \frac{\gamma_s\Lambda_s}{\mu_s} & 0 & -\mu_s & 0\\
0 & 0 & 0 & 0 & 0 & \gamma_p & -\mu_p
\end{pmatrix} \tag{3.29}$$

The eigenvalues of J_ϕ are $\lambda_1 = 0$, $\lambda_2 = -\mu_c$, $\lambda_3 = -\mu_s$, $\lambda_4 = -\lambda - \mu_c$ and other eigenvalues are given by,

$$m^3 + a_2 m^2 + a_1 m + a_0 = 0, \tag{3.30}$$

where,

$a_2 = \delta_c + \mu_c + \mu_m + \mu_p + \mu_s$,

$a_1 = \delta_c\mu_m + \mu_c\mu_m + \delta_c\mu_p + \mu_c\mu_p + \mu_m\mu_p + \delta_c\mu_s + \mu_c\mu_s + \mu_m\mu_s + \mu_p\mu_s$ and

$a_0 = \delta_c\mu_m\mu_p + \mu_c\mu_m\mu_p + \delta_c\ \mu_m\mu_s + \mu_c\mu_m\mu_s + \delta_c\mu_p\mu_s + \mu_c\mu_p\mu_s + \mu_m\mu_p\mu_s$.

Here a_2, a_1 and a_0 are positive. By direct calculation it can easily be shown that $a_2a_1 - a_0 > 0$. Thus, the Jacobian $J_\phi(E_0)$ has a simple zero eigenvalue, with all remaining eigenvalues having negative real components by the Routh-Hurwitz criterion. Therefore, the centre manifold theory can be used to examine the behavior of the model. Let $l = (l_1, l_2, l_3, l_4, l_5, l_6, l_7)$ and $h = (h_1, h_2, h_3, h_4, h_5, h_6, h_7)$ are left and right eigenvectors of $J(E_0)$.

The left eigenvectors are obtained by multiplying l by $J(E_0)$ and equating with 0. So after evaluating, the left eigenvector is

$$l = \left(0, l_2, 0, \frac{(\delta_c + \mu_c)l_2}{\gamma_m}, 0, \frac{(\delta_c + \mu_c)\mu_m\mu_s l_2}{\gamma_m\gamma_s\Lambda_s}, \frac{(\delta_c + \mu_c)\mu_m\mu_s^2 l_2}{\gamma_m\gamma_p\gamma_s\Lambda_s}\right).$$

Similarly, the right eigenvector is obtained by multiplying $J(E_0)$ by h and equating with 0. After computation, the right-eigenvector is

$$h = \left(\frac{-(\lambda + \delta_c + \mu_c)\mu_m\mu_p\mu_s^2\ h_7}{\gamma_m\gamma_p\gamma_s\Lambda_s(\lambda + \mu_c)}, \frac{\mu_m\mu_p\mu_s^2 h_7}{\gamma_m\gamma_p\gamma_s\Lambda_s}, \frac{\delta_c\mu_m\mu_p\mu_s^2 h_7}{\gamma_m\gamma_p\gamma_s\Lambda_s(\lambda + \mu_c)}, \frac{\mu_p\mu_s^2 h_7}{\gamma_p\gamma_s\Lambda_s}, \frac{-\mu_p h_7}{\gamma_p}, \frac{\mu_p h_7}{\gamma_p}, h_7\right).$$

The functions $r_1 = \Lambda_c - \gamma_c y_1 y_7 - \mu_c y_1 + \lambda y_3$, $r_2 = \gamma_c y_1 y_7 - (\delta_c + \mu_c)y_2$, $r_5 = \Lambda_s - \gamma_s y_4 y_5 - \mu_s y_5$ and $r_6 = \gamma_s y_4 y_5 - \mu_s y_6$ have the following non-zero second-order partial derivatives at DFE,

$\frac{\partial^2 r_1(E_0)}{\partial y_1 \partial y_7} = -\gamma_c$, $\frac{\partial^2 r_2(E_0)}{\partial y_1 \partial y_7} = \gamma_c$, $\frac{\partial^2 r_5(E_0)}{\partial y_4 \partial y_5} = -\gamma_s$, $\frac{\partial^2 r_6(E_0)}{\partial y_4 \partial y_5} = \gamma_s$, $\frac{\partial^2 r_1(E_0)}{\partial y_7 \partial \phi} = -\frac{\Lambda_c}{\mu_c}$ and $\frac{\partial^2 r_2(E_0)}{\partial y_7 \partial \phi} = \frac{\Lambda_c}{\mu_c}$.

The bifurcation coefficients are then derived using the Castillo-Chavez & Song

(2004) theorem as follows:

$$
\begin{aligned}
a &= \sum_{k,i,j=1}^{7} l_k h_i h_j \frac{\partial^2 r_k}{\partial y_i \partial y_j}(E_0) \\
&= l_1 h_1 h_7 \frac{\partial^2 r_1}{\partial y_1 \partial y_7}(E_0) + l_2 h_1 h_7 \frac{\partial^2 r_2}{\partial y_1 \partial y_7}(E_0) + l_5 h_4 h_5 \frac{\partial^2 r_5}{\partial y_4 \partial y_5}(E_0) + l_6 h_4 h_5 \frac{\partial^2 r_6}{\partial y_4 \partial y_5}(E_0) \\
&= (0) h_1 h_7 \frac{\partial^2 r_1}{\partial y_1 \partial y_7}(E_0) + l_2 h_1 h_7 \frac{\partial^2 r_2}{\partial y_1 \partial y_7}(E_0) + (0) h_4 h_5 \frac{\partial^2 r_5}{\partial y_4 \partial y_5}(E_0) + l_6 h_4 h_5 \frac{\partial^2 r_6}{\partial y_4 \partial y_5}(E_0) \\
&= (0) h_1 h_7 \frac{\partial^2 r_1}{\partial y_1 \partial y_7}(E_0) + l_2 h_1 h_7 \frac{\partial^2 r_2}{\partial y_1 \partial y_7}(E_0) + (0) h_4 h_5 \frac{\partial^2 r_5}{\partial y_4 \partial y_5}(E_0) + l_6 h_4 h_5 \frac{\partial^2 r_6}{\partial y_4 \partial y_5}(E_0) \\
&= l_2 h_1 h_7 \frac{\partial^2 r_2}{\partial y_1 \partial y_7}(E_0) + l_6 h_4 h_5 \frac{\partial^2 r_6}{\partial y_4 \partial y_5}(E_0) \\
&= l_2 h_7 \left(\frac{-(\lambda + \delta_c + \mu_c)\mu_m \mu_p \mu_s^2 \ h_7}{\gamma_m \gamma_p \gamma_s \Lambda_s (\lambda + \mu_c)} \right)(\gamma_c) + \left(\frac{(\delta_c + \mu_c)\mu_m \mu_s l_2}{\gamma_m \gamma_s \Lambda_s} \right) \left(\frac{\mu_p \mu_s^2 h_7}{\gamma_p \gamma_s \Lambda_s} \right)(\frac{-\mu_p h_7}{\gamma_p})(\gamma_s). \\
b &= \sum_{k,i=1}^{7} l_k h_i \frac{\partial^2 r_k}{\partial y_i \partial \phi}(E_0) \\
&= l_1 h_7 \frac{\partial^2 r_1}{\partial y_7 \partial \phi}(E_0) + l_2 h_7 \frac{\partial^2 r_2}{\partial y_7 \partial \phi}(E_0) \\
&= (0) h_7 \left(\frac{-\Lambda_c}{\mu_c} \right) + l_2 h_7 \left(\frac{\Lambda_c}{\mu_c} \right) \\
&= l_2 h_7 \left(\frac{\Lambda_c}{\mu_c} \right).
\end{aligned}
$$

Therefore, the bifurcation coefficients become:

$$
\begin{aligned}
a &= -l_2 h_7 \left(\frac{(\lambda + \delta_c + \mu_c)\mu_m \mu_p \mu_s^2 \ h_7 \gamma_c}{\gamma_m \gamma_p \gamma_s \Lambda_s (\lambda + \mu_c)} + \left(\frac{(\delta_c + \mu_c)\mu_m \mu_s}{\gamma_m \gamma_s \Lambda_s} \right) \left(\frac{\mu_p^2 \mu_s^2 h_7}{\gamma_p^2 \Lambda_s} \right) \right), \\
b &= l_2 h_7 \frac{\Lambda_c}{\mu_c}.
\end{aligned}
$$

Therefore, $a < 0$ and $b > 0$ for $h_7 > 0$ and $l_2 > 0$, the system exhibits a forward bifurcation at $R_0 = 1$ using the Theorem B.12 (see Figure 3.2). □

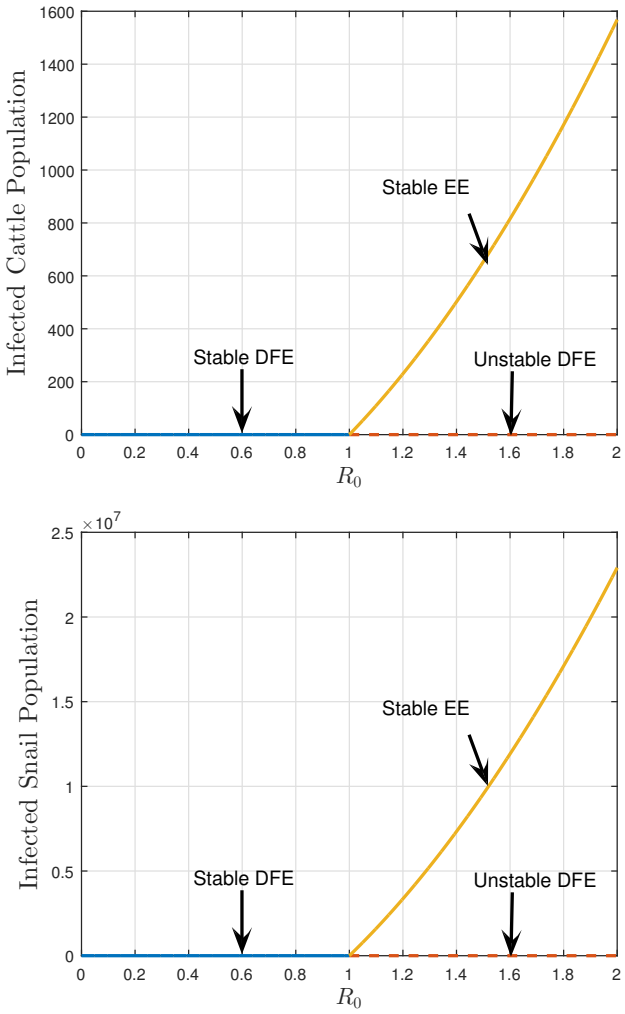

Figure 3.2: Forward bifurcation behavior of model (3.1).

3.3.10 Global Stability of Endemic Equilibrium

Theorem 3.8. *If $R_0 > 1$, then the endemic equilibrium point, E_e^*, is globally asymptotically stable.*

To prove the global stability of the endemic equilibrium, E_e^*, we employ the Lyapunov method with the Volterra-Lyapunov stable matrix (Chien & Shateyi 2021). We begin with a concise review of relevant definitions and theorems, and then construct the Lyapunov function.

Definition 3.9. A real square matrix A is (positive) stable iff there exists a positive definite matrix D such that $AD + DA^T$ is positive definite.

Definition 3.10. A real square matrix A is diagonally stable (or Lyapunov diagonally stable) if there exists a positive diagonal matrix D such that $AD + DA^T$ is positive definite.

Definition 3.11. A square $n \times n$ matrix A is said to be Volterra–Lyapunov stable if there exists a positive diagonal $n \times n$ matrix D such that $DA + A^T D$ is negative definite.

Lemma 3.12. *(Hershkowitz 1992) If A is a real square matrix with positive principal minors, then there exists a positive diagonal matrix D such that the matrix product DA has all positive eigenvalues.*

Lemma 3.13. *(Barker et al. 1978) A matrix A is Lyapunov diagonally stable if and only if there exists a positive diagonal matrix D such that $x^T DAx > 0$, for all non-zero vectors x.*

Define the Lyapunov function:

$$L = \frac{1}{2}[k_1(S_C - S_C^*)^2 + k_2(I_C - I_C^*)^2 + k_3(T_C - T_C^*)^2 + k_3(M - M^*)^2 + k_4(S_S - S_S^*)^2 + k_6(I_S - I_S^*)^2 + k_7(P - P^*)^2],$$

where k_i's are constants with positive values.

$$\frac{dL}{dt} = k_1(S_C - S_C^*)\frac{dS_C}{dt} + k_2(I_C - I_C^*)\frac{dI_C}{dt} + k_3(T_C - T_C^*)\frac{dT_C}{dt} + k_4(M - M^*)\frac{dM}{dt} + k_5(S_S - S_S^*)\frac{dS_S}{dt} + k_6(I_S - I_S^*)\frac{dI_S}{dt} + k_7(P - P^*)\frac{dP}{dt}. \quad (3.33)$$

Simplifying Equation (3.33) gives,

$$\frac{dL}{dt} = Y(WQ + Q^T W)Y^T,$$

where, $Y = (S_C - S_C^*, I_C - I_C^*, T_C - T_C^*, M - M^*, S_S - S_S^*, I_S - I_S^*, P - P^*)$, $W = diag(k_1, k_2, ..., k_7)$

and

$$Q = \begin{pmatrix} -P^*\gamma_c - \mu_c & 0 & \lambda & 0 & 0 & 0 & -S_C^*\gamma_c \\ P^*\gamma_c & -\delta_c - \mu_c & 0 & 0 & 0 & 0 & S_C^*\gamma_c \\ 0 & \delta_c & -\lambda - \mu_c & 0 & 0 & 0 & 0 \\ 0 & \gamma_m & 0 & -\mu_m & 0 & 0 & 0 \\ 0 & 0 & 0 & -S_S^*\gamma_s & -\mu_s - M^*\gamma_s & 0 & 0 \\ 0 & 0 & 0 & S_S^*\gamma_s & M^*\gamma_s & -\mu_s & 0 \\ 0 & 0 & 0 & 0 & 0 & \gamma_p & -\mu_p \end{pmatrix}. \quad (3.34)$$

Theorem 3.14. *The matrix Q stated in Equation (3.34) is Volterra–Lyapunov stable.*

Proof. We claim and demonstrate that , $C = -Q$ in equation (3.34) is diagonally stable, thus confirming the Volterra-Lyapunov stability of Q.

$$C = \begin{pmatrix} P^*\gamma_c + \mu_s & 0 & \lambda & 0 & 0 & 0 & S_C^*\gamma_c \\ -P^*\gamma_c & \delta_c + \mu_c & 0 & 0 & 0 & 0 & -S_C^*\gamma_c \\ 0 & -\delta_c & \lambda + \mu_c & 0 & 0 & 0 & 0 \\ 0 & -\gamma_m & 0 & \mu_m & 0 & 0 & 0 \\ 0 & 0 & 0 & S_S^*\gamma_s & \mu_s + M^*\gamma_s & 0 & 0 \\ 0 & 0 & 0 & -S_S^*\gamma_s & -M^*\gamma_s & \mu_s & 0 \\ 0 & 0 & 0 & 0 & 0 & -\gamma_p & \mu_p \end{pmatrix}. \quad (3.35)$$

Lemma 3.15. *The matrix C described in Equation (3.35) is diagonally stable.*

Proof. The principal minors of C are positive, implying by Lemma 3.12 the existence of a diagonal matrix W such that WC has positive eigenvalues. Thus, WC is positive definite, and there exists a nonzero vector x such that $x^T WCx > 0$. Therefore, by Lemma 3.13, C is Lyapunov diagonally stable.

A matrix C is diagonally stable (Definition 3.10), since there exists a positive diagonal matrix D such that $WC + C^T W > 0$. Consequently, if $C = -Q$, then $WQ + Q^T W < 0$, implying that Q is Volterra-Lyapunov stable (Definition 3.11).

Therefore, $\frac{dL}{dt} \leq 0$, satisfying the Lyapunov stability criterion. As a result, the singleton E_e^*, which represents the endemic equilibrium point, becomes the largest invariant set in Ω. Thus, based on Lasalle's invariance principle (LaSalle 1976), it can be concluded that E_e^* is globally asymptotically stable within Ω. □

3.4 Sensitivity Analysis

Sensitivity analysis is widely used in epidemiology to identify the most influential parameters of the model (Madubueze et al. 2022). The normalized sensitivity index that measures the percentage change of R_0 in relation to the parameter ω, denoted by $\Gamma_{\omega}^{R_0}$ and defined as (Zamir et al. 2016)

$$\Gamma_{\omega}^{R_0} = \frac{\partial R_0}{\partial \omega} . \frac{\omega}{R_0}. \tag{3.36}$$

Table 3.2 summarizes the sensitivity index results using the parameter values from Table 3.1. Figure 3.3 illustrates a graphical simulation of the sensitivity indices. The result of the sensitivity analysis shows that the recruitment rates, the production rates of miracidia and metacercariae and the transmission rates of cattle and snails are the most sensitive parameters with a direct influence on R_0. Biologically, the transmission rates for the snail and cattle populations, as well as the rates at which cattle produce miracidia and snails produce metacercariae, have contributed to the severity of *F. hepatica* in cattle. The positive index indicates that if the per capita infection rate of cattle (γ_c) is adjusted by 10%, the value of R_0 will increase or decrease similarly by approximately 5%.

The results also show that the mortality rates of the miracidia, metacercaria and snail populations, as well as the treatment rate of infected cattle, indirectly impact the effective reproduction number. The snail mortality rate is the most significant parameter that has an indirect effect on R_0. A 5% increase or decrease in the snail mortality rate (μ_s) will lead to an approximate 5% decrease or increase in the value of R_0, respectively. Therefore, to prevent the spread of *F. hepatica* infection in cattle, stakeholders should increase the treatment rates and mortality rates of the snail, miracidia and metacercaria populations.

3.5 Numerical Simulations and Discussion

This section presents simulations using the parameter values in Table 3.1 to investigate the dynamics of *F. hepatica* disease spread. Parameter values are sourced

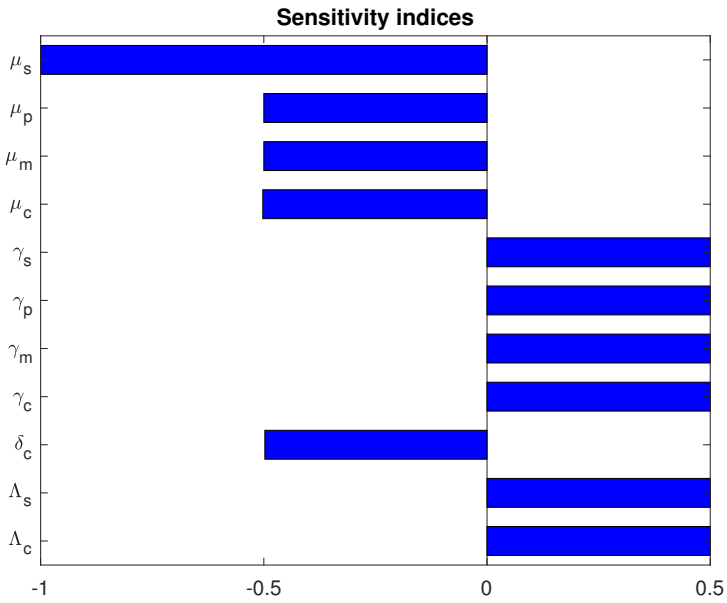

Figure 3.3: Sensitivity analysis of model (3.1) parameters.

Table 3.2: Normalized forward sensitivity indices for model (3.1).

Parameters	Sensitivity indices
μ_s	-1
μ_c	-0.5023
μ_m	-0.5
μ_p	-0.5
δ_c	-0.497698
Λ_c	+0.5
Λ_s	+0.5
γ_m	+0.5
γ_p	+0.5
γ_c	+0.5
γ_s	+0.5

from existing studies or proposed for simulation. Numerical simulations have been performed using the MATLAB ode45 code.

3.5.1 The Stability Behaviour of Endemic Equilibrium

Simulations are performed for the first 2000 days, with initial conditions set as $(S_C^*(0), I_C^*(0), T_C^*(0), M^*(0), S_S^*(0), I_S^*(0), P^*(0)) = (10^3, 800, 600, 6.5*10^3, 10^6, 3*10^5, 1.2*10^6)$. Using the values of the parameters Table 3.1 for model (3.1), we found the reproduction number, $R_0 = 1.93597 > 1$. In fact, using these parameter values in model (3.1), we obtain a unique endemic equilibrium point $E_e^* = (S_C^*, I_C^*, T_C^*, M^*, S_S^*, I_S^*, P*) = (1227.49, 1436.6, 957.535, 11109.7, 1.43651*10^6, 388303, 1.56477*10^6)$. Figure 3.4 shows

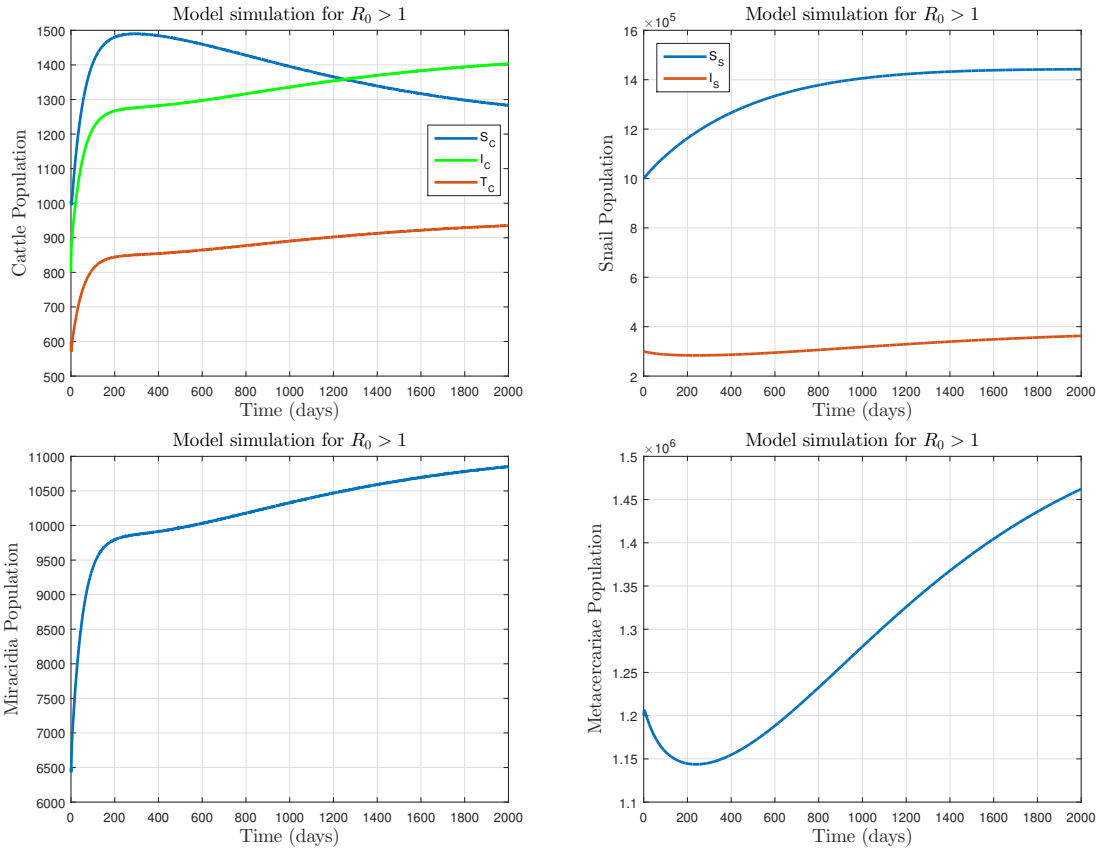

Figure 3.4: The population changes over time and the stability behavior of the endemic equilibrium for model (3.1).

that solution trajectories converge to the endemic equilibrium point E_e^*, which is locally stable when $R_0 > 1$. This indicates that *Fasciola hepatica* will continue to spread without intervention. Figure 3.5 shows that, regardless of the initial number of infected cattle with in the feasible region, the solution will always tend the

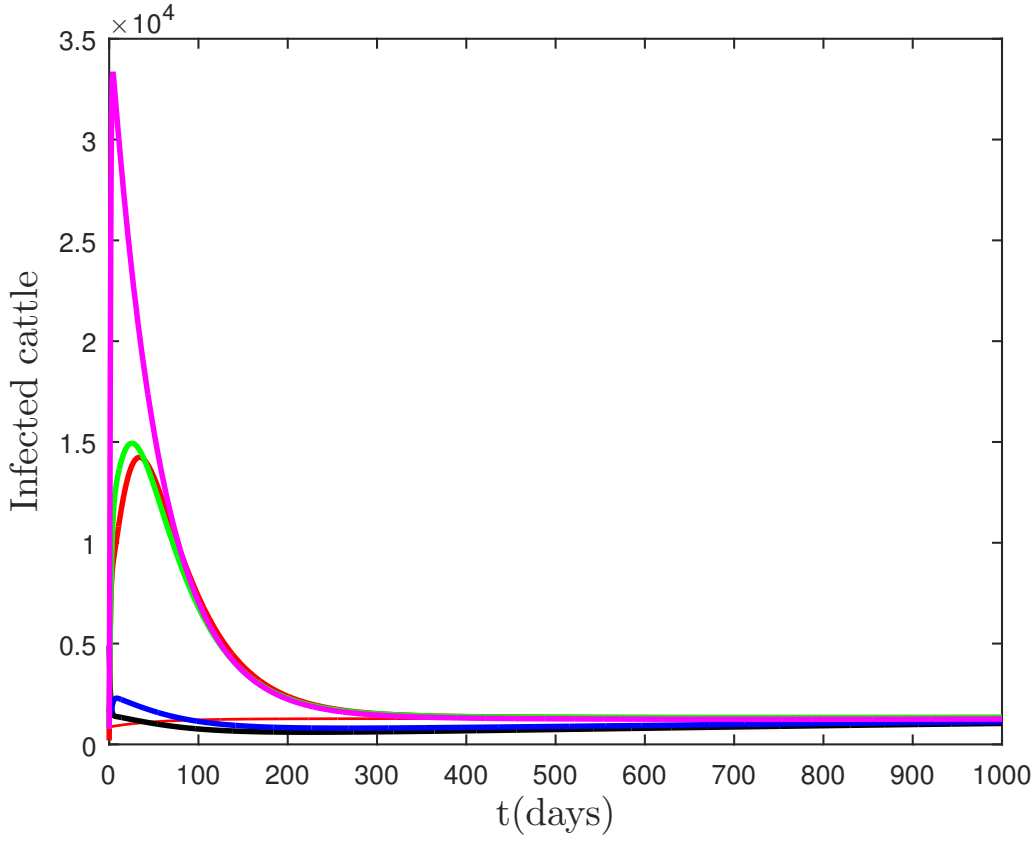

Figure 3.5: Global stability of the endemic equilibrium for infected cattle dynamics.

endemic equilibrium over time. This implies that *F. hepatica* will persist in cattle populations.

3.5.2 The Stability Behavior of Disease-Free Equilibrium

With transmission rates reduced to $\gamma_c = 0.0000003$ and $\gamma_s = 0.00000002$, a treatment rate of $\delta_c = 0.7$, and a snail mortality rate of 0.002, the reproduction number is $R_0 = 0.840751$, and the disease-free equilibrium is $E_0^* = (3621.62, 0, 0, 0, 1.5 * 10^6, 0, 0)$. Figure 3.6 illustrates that all the model solution trajectories converge to the disease-free equilibrium (DFE) over time, indicating its local stability. Furthermore, Figure 3.7 indicates that regardless of initial conditions, the number of infected cattle tends to zero over time. This further demonstrates that the disease would eventually be eliminated in the cattle population. In contrast, susceptible cattle and snail popula-

tions will reach their maximum values of $\frac{\Lambda_c}{\mu_c}$ and $\frac{\Lambda_s}{\mu_s}$, respectively. From a biological perspective, it can be concluded that *F. hepatica* disease in cattle can be eliminated when $R_0 < 1$. Stakeholders should aim to minimize the reproduction number as much as possible through interventions to accelerate the elimination of the disease.

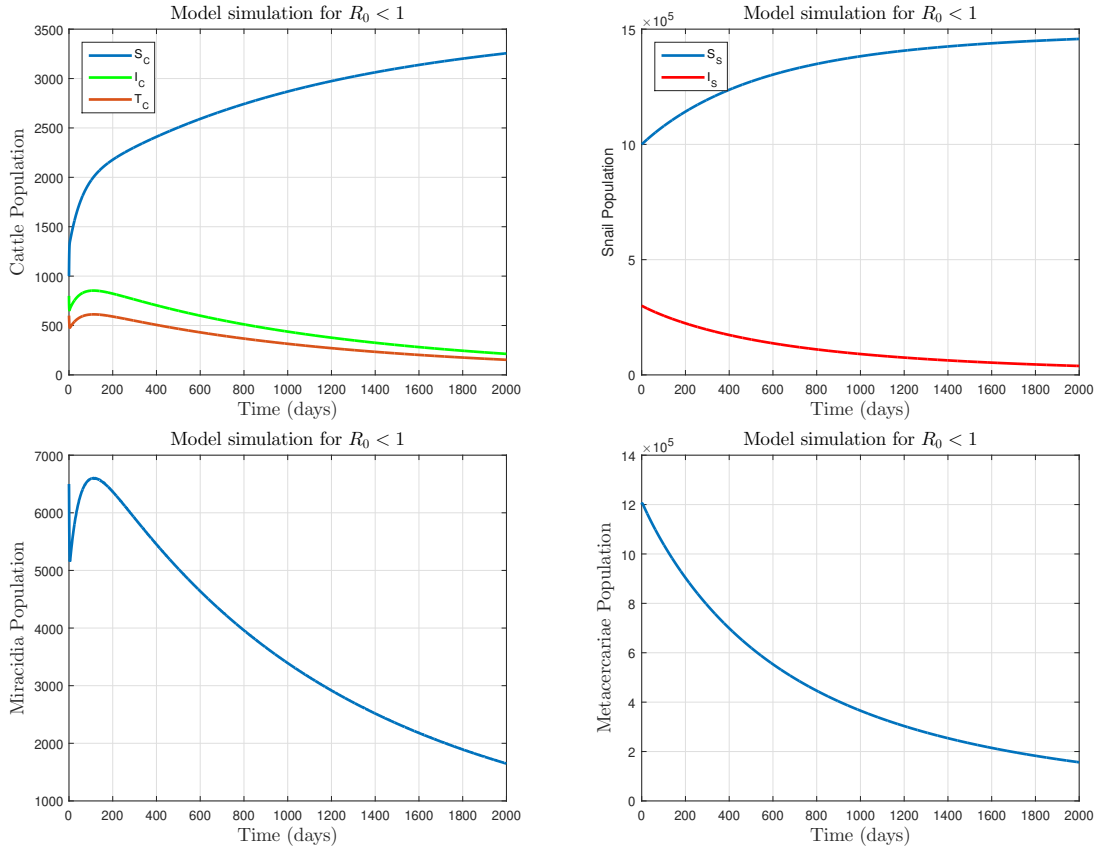

Figure 3.6: The changes in the number of cattle over time and stability behavior of disease-free equilibrium for model (3.1).

3.5.3 Contour and Surface Plots of R_0 for Combination of Parameters

Figure 3.8 (a-d) depicts how the reproduction number is affected by two control parameters, as demonstrated through the contour plots. Figure 3.8 (a) clearly illustrates the need to give utmost priority to the region below the yellow color when implementing snail control measures and proficiently managing the per capita infection rate of snails to achieve successful elimination of the disease. When the snail death rate is low, there is an inverse relationship, causing the reproduction number

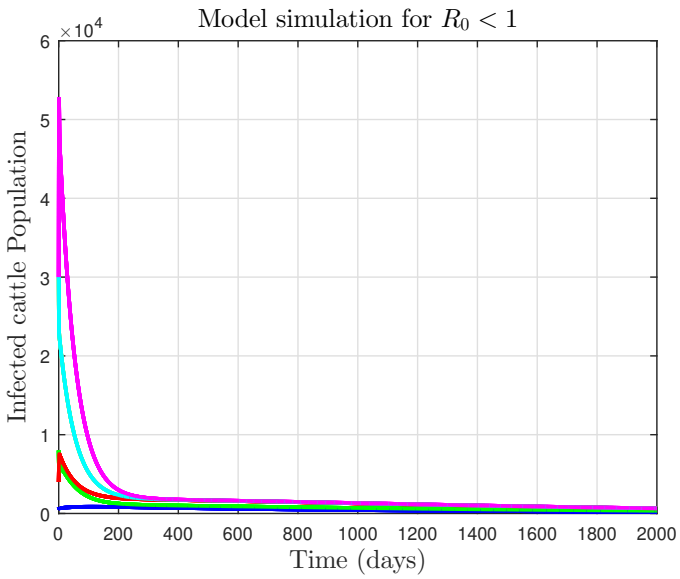

Figure 3.7: Global stability of the disease-free equilibrium for infected cattle dynamics (3.1).

to increase and the disease to persist. Figure 3.8 (b) emphasizes the crucial role of snail and cattle infection rates in the transmission and impact of *F. hepatica* disease in cattle. It highlights that higher snail infection rates lead to a larger reservoir of parasites in the environment, which subsequently increases the risk of cattle exposure to the parasite. To effectively control and potentially eliminate the disease, policymakers should aim to minimize these infection rates to a level where the reproduction number is less than 1.

Contour and surface plots (Figures 3.8(c) and 3.9) indicate that disease control strategies focused on improved treatment and reduced cattle infection rates can bring R_0 below one. This suggests that interventions targeting the treatment rate and the cattle infection rate can effectively reduce the spread of the disease and potentially lead to its eradication.

Policymakers and healthcare professionals can focus on establishing strategies to reduce treatment and cattle infection rates. These measures might include improving access to treatment options, implementing effective preventive measures for cattle and adopting bio-security protocols to minimize the risk of disease transmission.

Finally, Figure 3.8 (d) shows that simultaneously improving the combined treatment rate for infected cattle and snail mortality rate leads to a lower reproduction number. Without adequate adjustments to these rates, the reproduction number remains high, indicating the persistence of the disease.

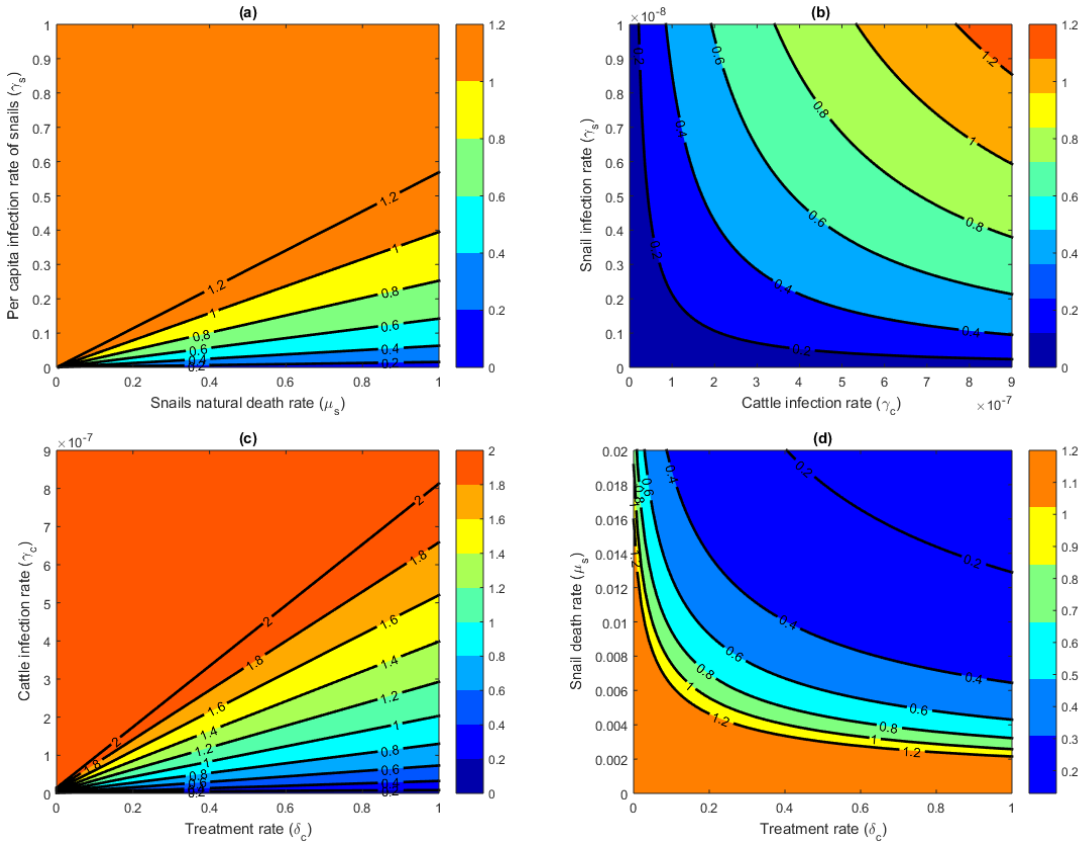

Figure 3.8: Contour plot of reproduction number for model (3.1). (a) R_0 as a function of μ_s and γ_s. (b) R_0 as a function of γ_c and γ_s. (c) Contour plot of R_0 as a function of δ_c and γ_c. (d) R_0 as a function of δ_c and μ_s.

3.5.4 Parameter Impact on the Disease Dynamics

Effect of Per Capita Infection Rates

Figure 3.10 illustrates a graphical representation of the reproductive number in terms of the disease transmission rates of cattle and snails based on parametric values in Table 3.1. It shows that as the values of γ_c and γ_s increase, R_0 also increases and becomes greater than one to the right of $\gamma_c^* = 1.4338 * 10^{-7}$ and $\gamma_s^* =$

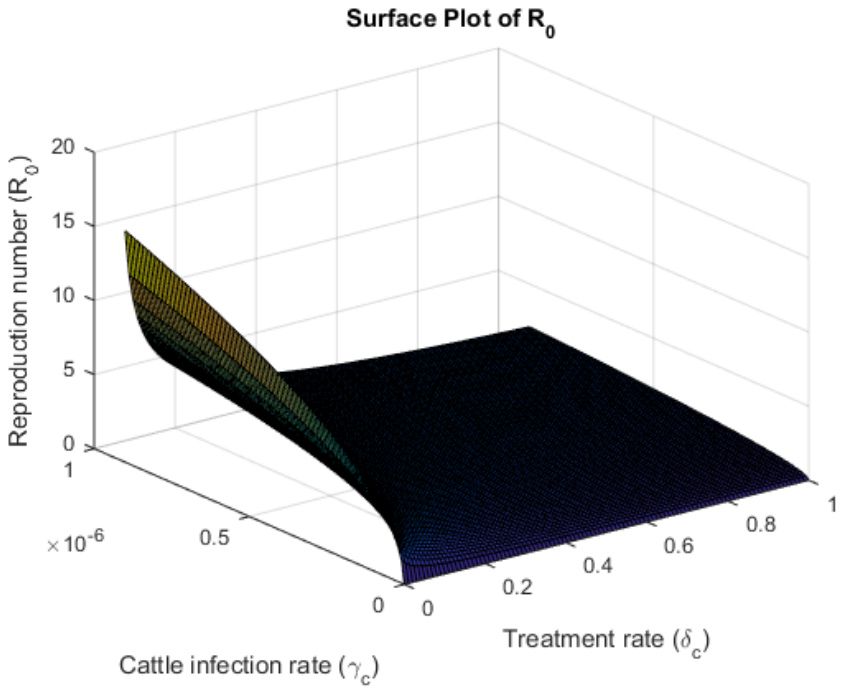

Figure 3.9: Surface plot of reproduction number (R_0) as a function of δ_c and γ_c, for model (3.1).

$1.1473 * 10^{-8}$. This shows that the transmission of the disease between cattle and snails contributes significantly to the endemic equlibrum of *F. hepatica*. Below the critical transmission rates γ_c^* and γ_s^*, the disease would die out. Figure 3.11 shows

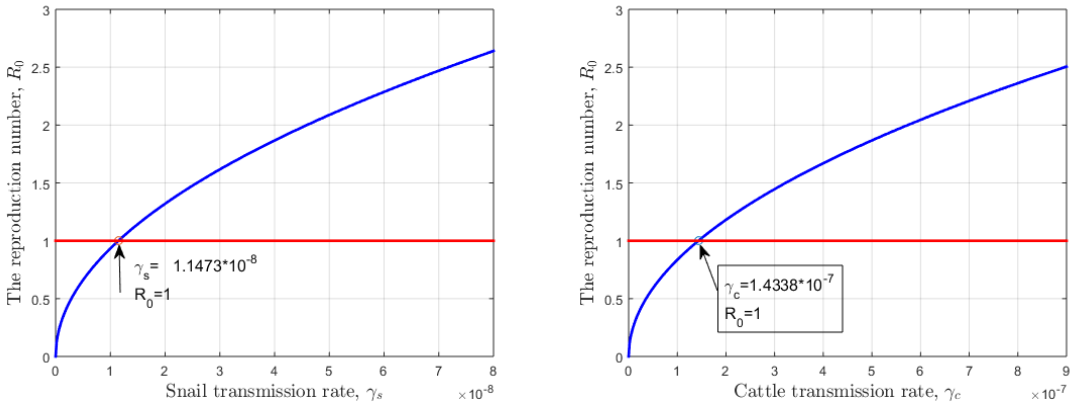

Figure 3.10: The effect of snail and cattle transmission rates on R_0 for model (3.1).

the effects of snail transmission rate on infected cattle using various values of $\gamma_s = 0.0000000147, 0.00000004, 0.00000005, 0.00000006$. In the same way, considering

different values of $\gamma_c = 0.0000001433, 0.0000005, 0.0000006, 0.0000007$, the impact of per capita infection rates on cattle has been investigated. Higher infection rates in both cattle and snails lead to an increase in infected cattle. Therefore, to control the spread of the disease in the cattle population, the transmission rates for cattle and snails should be reduced to below γ_c^* and γ_s^*, respectively.

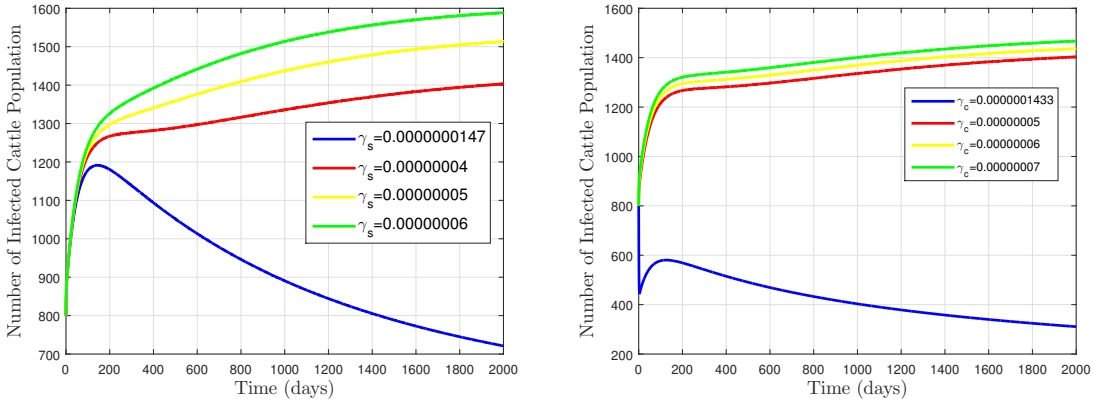

Figure 3.11: The effect of transmission rates on infected cattle for model (3.1).

Effect of the Cattle Treatment Rate

Figure 3.12 illustrates the impact of the treatment rate (δ_c) on R_0 and the epidemiology of the disease. It has been shown that as the intensity of treatment increases, both R_0 and the equilibrium number of infected cattle decrease. From an epidemiological perspective, improving treatment can reduce the number of infected cattle. For small values of the treatment rate, R_0 remains greater than 1. As a result, the solution graphs of the system will converge to the endemic equilibrium point, allowing the infection to persist. Increasing the rate of treatment and reducing disease transmission can help reduce the incidence of *F. hepatica* infection.

Effect of Snail Mortality Rate

Figures 3.13 and 3.14 illustrate the impacts of snail mortality rates (μ_s) on the reproduction number and the infected cattle population, respectively. Figure 3.14 shows that the number of infected cattle decreases correspondingly as the snail mortality rate increases (with values of μ_s = 0.001644, 0.0018, 0.002, 0.004). When the snail

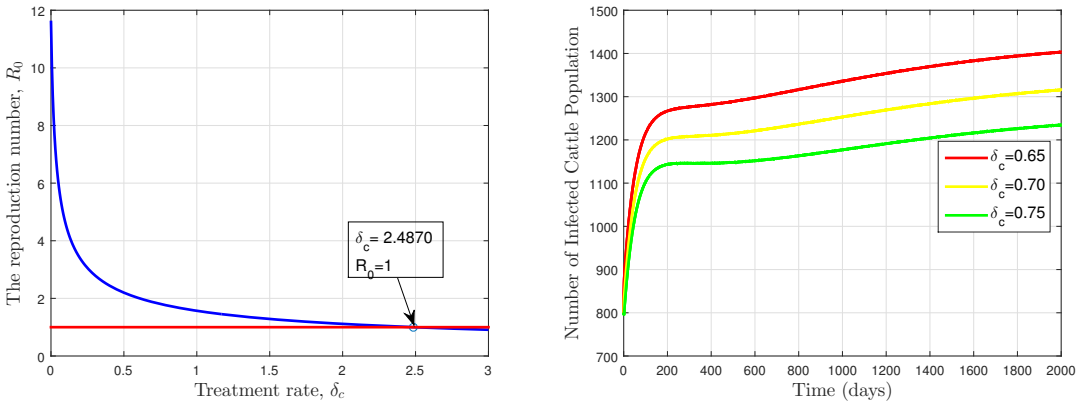

Figure 3.12: Effect of treatment rate on reproduction number and infected cattle for model (3.1).

mortality rate is below $\mu_s = 0.00306999$, the reproduction number exceeds one, allowing the *F. hepatica* disease to persist. In contrast, when the snail mortality rate is higher than $\mu_s = 0.00306999$, R_0 falls below one, eliminating the disease. Controlling the snail population reduces cattle infection and the density of metacercariae in the ecosystem. Therefore, additional measures should be implemented to decrease the number of snails and eliminate the spread of *Fasciola hepatica* in cattle.

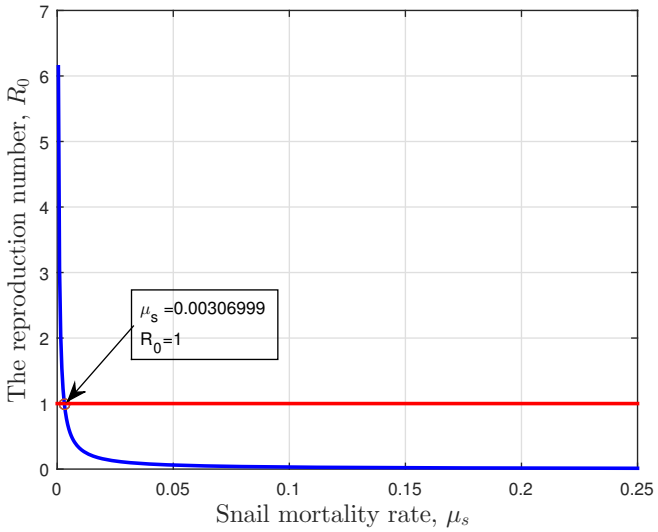

Figure 3.13: Effect of snail mortality rate on the reproduction number for model (3.1).

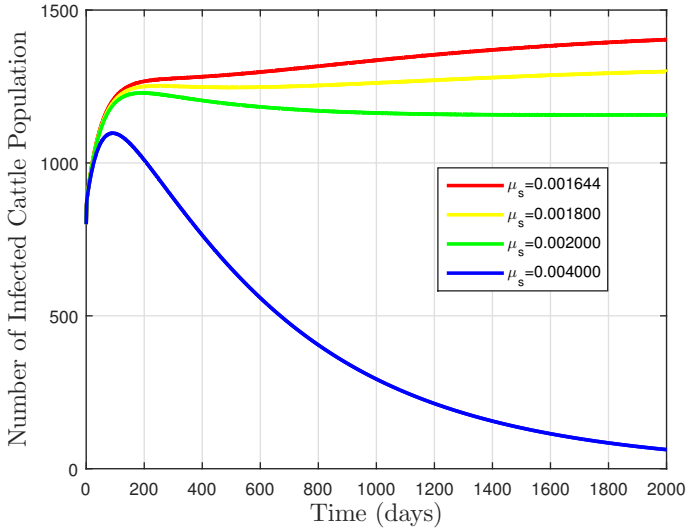

Figure 3.14: Effect of snail mortality rate on infected cattle for model (3.1).

3.6 Conclusion

In this chapter, a deterministic mathematical model is developed for the transmission dynamics of *F. hepatica*. Mathematical analysis and numerical simulations demonstrate that the disease-free equilibrium is locally and globally asymptotically stable when $R_0 < 1$. It has also been shown that the endemic equilibrium point is locally and globally stable when $R_0 > 1$. The model exhibits a forward bifurcation. This

situation occurs when the *Fasciola hepatica*-free equilibrium starts to lose its stability and a steady endemic equilibrium emerges while R_0 tends to increase through one. In models exhibiting forward bifurcation, having $R_0 < 1$ is a necessary and sufficient condition for eradication of *F. hepatica* disease (Gumel 2012).

The sensitivity analysis is used to assess the impact of various parameters on *F. hepatica*. The results reveal that recruitment rates, transmission rates among cattle and snail populations and shedding rates of miracidia and metacercariae directly affect the prevalence of *F. hepatica* in the cattle population. Furthermore, the mortality rates of the miracidia, metacercariae and snail populations, as well as the treatment rate of infected cattle, indirectly influence the spread of the *F. hepatica* parasite.

Numerical simulations show that treatment alone is insufficient to prevent disease transmission in cattle and requires additional control measures. Combining effective treatment with lower transmission and higher snail mortality rates significantly improves disease management. This finding is consistent with a study by (Diaby et al. 2019), which found that the percentage of animals receiving medical treatment is not as important as combination of quarantine with treatment to prevent the disease. Furthermore, a study by (Kadaleka et al. 2021) suggests that combinations of molluscicide and treatment in a contaminated environment can effectively decrease the spread of disease, outperforming individual control methods. This integrated approach targeting both snail hosts and infected cattle could significantly reduce the disease burden and improve animal health outcomes, suggesting the importance of implementing such strategies in endemic regions for sustainable disease control and elimination. Therefore, stakeholders should reduce transmission rates, improve treatment rates and increase mortality rates in the snail population to control this disease.

Chapter 4

4 Optimal Control and Cost-Effectiveness Analysis of *Fasciola Hepatica* Model

4.1 Introduction

This chapter develops a dynamic integrated control model from the core *fascioliasis* transmission model (3.1) by incorporating intervention measures. Sensitivity analysis of the prior model pinpointed snail mortality as a critical epidemiological parameter, underscoring the inherent limitation of relying solely on anthelmintic treatment. This result provides the quantitative justification for advancing an integrated control framework, where combined tactics achieve a more effective and resilient suppression of transmission. We present the mathematical formulation for the combined effects of targeted treatment, pasture management, and molluscicide use. This refined model serves as a decision-support system, enabling evaluation of control strategies, resource allocation optimization, and long-term sustainability assessment regarding anthelmintic resistance. Effective *fascioliasis* control, requires reducing intermediate host populations or using anthelmintics. Consequently, this chapter presents an optimal control problem, assessing the impact and cost-effectiveness of three time-dependent preventive and control strategies on *fascioliasis* transmission dynamics in cattle, using a deterministic model. The Pontryagin maximum principle is applied to identify optimal conditions for disease control via interventions.

4.2 Optimal Control Model Formulation

Optimal control theory optimizes the behavior of dynamic systems (Bat et al. 2010). Based on the sensitivity analysis in Chapter 3, we extend the optimal control model, focusing on control variables: $u_1(t)$, which represents pasture management to reduce

the risk of metacercariae infection in cattle. Similarly, $u_2(t)$ represents measures for the treatment of cattle and $u_3(t)$ quantifies efforts to control snails using molluscicide to mitigate *F. hepatica* disease. By integrating these control variables into the model (3.1), we derive the following formulation.

$$\begin{cases} S'_C(t) = \Lambda_c - (1-u_1(t))\gamma_c S_C(t)P(t) - \mu_c S_C(t) + \lambda T_C(t), \\ I'_C(t) = (1-u_1(t))\gamma_c S_C(t)P(t) - (\delta_c + u_2(t) + \mu_c)I_C(t), \\ T'_C(t) = (\delta_c + u_2(t))I_C(t) - (\lambda + \mu_c)T_C(t), \\ M'(t) = \gamma_m I_C(t) - \mu_m M(t), \\ S'_S(t) = \Lambda_s - \gamma_s S_S(t)M(t) - (\mu_s + u_3(t))S_S(t), \\ I'_S(t) = \gamma_s S_S(t)M(t) - (\mu_s + u_3(t))I_S(t), \\ P'(t) = \gamma_p I_S(t) - \mu_p P(t), \end{cases} \tag{4.1}$$

subject to initial conditions of the model (3.1).

Nonlinear control interventions are used due to the non-linear costs of health-care prevention measures (Ogunmiloro 2022, Asamoah, Jin, Sun, Seidu, Yankson, Abidemi, Oduro, Moore & Okyere 2021). We aim to decrease the number of infected cattle, manage the snail population and minimize the costs of these interventions. The cost of interventions is defined as follows:

$$J(u_1,u_2,u_3) = \int_0^{t_f} \left(A_1 I_C + A_2 N_S + \frac{1}{2}C_1 u_1^2 + \frac{1}{2}C_2 u_2^2 + \frac{1}{2}C_3 u_3^2 \right) dt, \tag{4.2}$$

where A_1 and A_2 are positive weights used to balance factors related to the number of infected cattle and the total snail population, respectively. Likewise, C_1, C_2 and C_3 denote the weights assigned to the costs of the control programs over t_f days, which represents the time frame for implementing the control strategy.

The objective is to identify the optimal controls, u_1^*, u_2^* and u_3^* that satisfy the following condition:

$$J(u_1^*,u_2^*,u_3^*) = \min_{\mathscr{U}} J(u_1,u_2,u_3), \tag{4.3}$$

where the control set $\mathscr{U}$ consists of Lebesgue-measurable bounded functions and is defined as follows:

$$\mathscr{U} = \{u : 0 \le u_1(t) \le 1, 0 \le u_2(t) \le 1, 0 \le u_3(t) \le 1, \text{for} \quad t \in [0,t_f]\}.$$

4.2.1 Existence of an Optimal Control

Theorem 4.1. *For Equation (4.3) to be valid, it is required to meet the following conditions A–D. These conditions are necessary to identify an optimal control* (u_1^*, u_2^*, u_3^*) *that minimizes the objective functional* $J(u_1, u_2, u_3)$ *while satisfying the constraints of the control model (4.1).*

(A) The admissible control set $\mathscr{U}$ *must be both convex and closed.*

(B) The control system must be bounded by a linear function involving the state and control variables.

(C) The integrand of the objective functional in (4.2) must exhibit convexity with respect to the controls.

(D) The Lagrangian must be bounded below by

$$a_0\Big(\sum_{i=1}^{3}|u_i|^2\Big)^{\frac{a_2}{2}} - a_1,$$

where $a_0 > 0$, $a_1 > 0$ *and* $a_2 > 1$.

Proof. To establish the existence of an optimal control (u_1^*, u_2^*, u_3^*), we assign the right-hand side of the system (4.1) as $f(t, \mathscr{X}, u)$, where $\mathscr{X} = (S_C, I_C, T_C, M, S_S, I_S, P)$, $u = (u_1, u_2, u_3) \in \mathscr{U} = [0,1] \times [0,1] \times [0,1]$ and

$$f(t,\mathscr{X},u) = \begin{pmatrix} \Lambda_c - (1-u_1(t))\gamma_c S_C(t)P(t) - \mu_c S_C(t) + \lambda T_C(t) \\ (1-u_1(t))\gamma_c S_C(t)P(t) - (\delta_c + u_2(t) + \mu_c)I_C(t) \\ (\delta_c + u_2(t))I_C(t) - (\lambda + \mu_c)T_C(t) \\ \gamma_m I_C(t) - \mu_m M(t) \\ \Lambda_s - \gamma_s S_S(t)M(t) - (\mu_s + u_3(t))S_S(t) \\ \gamma_s S_S(t)M(t) - (\mu_s + u_3(t))I_S(t) \\ \gamma_p I_S(t) - \mu_p P(t) \end{pmatrix}. \tag{4.4}$$

Following the approach outlined in Mwamtobe et al. (2014), we proceed to verify the satisfaction of the essential conditions.

(A) By definition, it is clear that the control set $\mathscr{U}$ exhibits the closure property. Let $v = (v_1, v_2, v_3)$ and $w = (w_1, w_2, w_3)$ represent arbitrary elements belonging to $\mathscr{U}$. Consequently, based on the definition of a convex set, it can be inferred that

$$(1-t)v + tw \in \mathscr{U} \quad \text{for all} \quad t \in [0,1].$$

Let us take two arbitrary corresponding coordinates, v_i and w_i, such that $0 \leq v_i \leq 1$ and $0 \leq w_i \leq 1$. For any value of t between 0 and 1, the convex combination $(1-t) * v_i + t * w_i$ is within the interval [0, 1]. As a result, the expression $(1-t)v + tw$ belongs to $\mathscr{U}$, indicating the convexity of $\mathscr{U}$.

(B) It can be demonstrated that there are functions g and h such that

$$f(t, \mathscr{X}, u) = g(t, \mathscr{X}) + h(t, \mathscr{X})u, \tag{4.5}$$

where, $f(t, \mathscr{X}, u)$ is in Equation (4.4) and

$$g(t, \mathscr{X}) = \begin{pmatrix} \Lambda_c - \gamma_c S_C(t)P(t) - \mu_c S_C(t) + \lambda T_C(t) \\ \gamma_c S_C(t)P(t) - (\delta_c + \mu_c)I_C(t) \\ \delta_c I_C(t) - (\lambda + \mu_c)T_C(t) \\ \gamma_m I_C(t) - \mu_m M(t) \\ \Lambda_s - \gamma_s S_S(t)M(t) - \mu_s S_S(t) \\ \gamma_s S_S(t)M(t) - \mu_s I_S(t) \\ \gamma_p I_S(t) - \mu_p P(t) \end{pmatrix},$$

$$h(t, \mathscr{X}) = \begin{pmatrix} \gamma_c S_C(t)P(t) & 0 & 0 \\ -\gamma_c S_C(t)P(t) & -I_C(t) & 0 \\ 0 & I_C(t) & 0 \\ 0 & 0 & 0 \\ 0 & 0 & -S_S(t) \\ 0 & 0 & -I_S(t) \\ 0 & 0 & 0 \end{pmatrix}.$$

Applying the norm inequality stated in Equation (4.5) yields that

$$|f(t, \mathscr{X}, u)| \leq |g(t, \mathscr{X})| + |h(t, \mathscr{X})||u|.$$

The functions g and h are continuous for the state variables and each state variable is constrained; it becomes evident that both $|g|$ and $|h|$ are bounded functions. This implies that there exist numbers a and b such that $|g| \leq a$ and $|g| \leq b$.

This provides,

$$\begin{aligned} |f(t,\mathscr{X},u)| &\leq |g(t,\mathscr{X})| + |h(t,\mathscr{X})||u| \\ &\leq a + b|u| \\ &\leq \max\{a,b\}(1+|u|). \end{aligned}$$

Therefore, $||f(t,\mathscr{X},u)|| \leq c(1+|u|)$, where $c = \max\{a,b\}$. This demonstrates that condition (B) is fulfilled.

(C) Initially, it is important to observe that the objective function (4.2), possesses an integrand with characteristics similar to that of the Lagrangian form.

$$\mathscr{L} = A_1 I_C + A_2 N_S + \frac{1}{2} C_1 u_1^2 + \frac{1}{2} C_2 u_2^2 + \frac{1}{2} C_3 u_3^2. \tag{4.6}$$

Assume $v = (v_1, v_2, v_3)$ and $w = (w_1, w_2, w_3)$ be to arbitrary elements of $\mathscr{U}$, $\lambda \in [0,1]$ then it is necessary to prove that

$$\mathscr{L}(t,\mathscr{X},(1-\lambda)v + \lambda w) \leq (1-\lambda)\mathscr{L}(t,\mathscr{X},v) + \lambda(\mathscr{L}(t,\mathscr{X},w).$$

$$\mathscr{L}(t,\mathscr{X},(1-\lambda)v + \lambda w) = A_1 I_C + A_2 N_S + \frac{1}{2}\sum_{i=1}^{3}\Big(C_i((1-\lambda)v_i + \lambda w_i)\Big)^2. \tag{4.7}$$

Also, we have,

$$(1-\lambda)\mathscr{L}(t,\mathscr{X},v) + \lambda(\mathscr{L}(t,\mathscr{X},w) = A_1 I_C + A_2 N_S + \frac{1}{2}(1-\lambda)\sum_{i=1}^{3} C_i v_i^2 + \frac{1}{2}\lambda\sum_{i=1}^{3} C_i w_i^2. \tag{4.8}$$

Subtracting Equation (4.8) from Equation (4.7)

$$\mathscr{L}(t,\mathscr{X},(1-\lambda)v + \lambda w) - \Big((1-\lambda)\mathscr{L}(t,\mathscr{X},v) + \lambda(\mathscr{L}(t,\mathscr{X},w)\Big) = \frac{1}{2}(\lambda^2 - \lambda)\sum_{i=1}^{3} C_i(v_i - w_i)^2 \leq 0$$

Since λ is in the interval $[0,1]$, the right-hand side of the equation is nonpositive. Therefore, $\mathscr{L}$ is a convex function.

(D) Furthermore, it is evident that there exists a value $a_2 > 1$, along with positive

numbers a_1 and a_0, which satisfy the given conditions:

$$\begin{aligned}\mathscr{L} = A_1 I_C + A_2 N_S + \frac{1}{2}C_1 u_1^2 + \frac{1}{2}C_2 u_2^2 + \frac{1}{2}C_3 u_3^2 &\geq \frac{1}{2}(C_1 u_1^2 + C_2 u_2^2 + C_3 u_3^2) \\ &\geq \frac{1}{2}\min\{C_1, C_2, C_3\}\left(u_1^2 + u_2^2 + u_3^2\right) \\ &\geq \frac{1}{2}\min\{C_1, C_2, C_3\}\left(u_1^2 + u_2^2 + u_3^2\right) - a_1 \\ &= a_0\left(u_1^2 + u_2^2 + u_3^2\right)^{\frac{a_2}{2}} - a_1,\end{aligned}$$

where $a_2 = 2$, $a_1 > 0$, and $a_0 = \frac{1}{2}\min\{C_1, C_2, C_3\}$. This implies that

$$\mathscr{L} \geq a_0\left(u_1^2 + u_2^2 + u_3^2\right)^{\frac{a_2}{2}} - a_1.$$

Therefore, the Lagrangian is bounded below by $a_0\left(\sum_{i=1}^{3}|u_i|^2\right)^{\frac{a_2}{2}} - a_1$, where $a_0 > 0$, $a_1 > 0$ and $a_2 > 1$. □

4.2.2 Characterization of the Optimal Control Problem

To solve the above-formulated problem of optimal control, we use Pontryagin's maximum principle, described in studies (Pontryagin 2018, Asamoah et al. 2022). This principle provides the necessary conditions for optimal control. With this principle, we can convert differential equations (4.1) and (4.6) into problems of Hamiltonian minimization concerning control variables (u_1, u_2, u_3), which gives the conditions for optimality of control. This generally involves the search for a control strategy that minimizes a cost function subject to some constraints; this can be rephrased in terms of a Lagrangian function $\mathscr{L}$ as defined by (4.6), which includes both the cost function and the constraints. Using a Hamiltonian function $\mathscr{H}$, the control problem can be expressed as:

$$\mathscr{H} = \mathscr{L} + \delta_1\frac{dS_C}{dt} + \delta_2\frac{dI_C}{dt} + \delta_3\frac{dT_C}{dt} + \delta_4\frac{dM}{dt} + \delta_5\frac{dS_S}{dt} + \delta_6\frac{dI_S}{dt} + \delta_7\frac{dP}{dt}.$$

The notation δ_i for $i = 1$ to 7 indicates seven adjoint variables corresponding to the state equations S_C, I_C, T_C, M, S_S, I_S and P. Simplifying the Hamiltonian function

results in a more concise form.

$$\begin{aligned}\mathscr{H} &= A_1 I_C + A_2 N_S + \frac{1}{2}[C_1 u_1^2 + C_2 u_2^2 + C_3 u_3^2] + \delta_1[\Lambda_c - (1-u_1)\gamma_c S_C P - \mu_c S_C + \lambda T_C] \\ &+ \delta_2[(1-u_1)\gamma_c S_C P - (\delta_c + u_2 + \mu_c) I_C] + \delta_3[(\delta_c + u_2) I_C - (\lambda + \mu_c) T_c] \\ &+ \delta_4[\gamma_m I_C - \mu_m M] + \delta_5[\Lambda_s - \gamma_s S_S M - (\mu_s + u_3) S_S] \\ &+ \delta_6[\gamma_s S_S M - (\mu_s + u_3) I_S] + \delta_7[\gamma_p I_S - \mu_p P].\end{aligned} \tag{4.9}$$

Theorem 4.2. *The optimal control variables, $u_1^*(t)$, $u_2^*(t)$ and $u_3^*(t)$, along with the solutions $\mathscr{X} := (S_C, I_C, T_C, M, S_S, I_S, P)$ of the system (4.1), are associated with adjoint variables δ_i (where i ranges from 1 to 7), which satisfy*

$$\frac{d\delta}{dt} = -\frac{\partial \mathscr{H}(t, \mathscr{X}, u, \delta)}{\partial \mathscr{X}},$$

with transversality conditions $\delta_i(t_f) = 0,\ i = 1, 2, ..., 7$.

Additionally, the optimality conditions for the problem are given by

$$\left.\begin{aligned} u_1^* &= \max\left\{0, \min\left\{1, \frac{(\delta_2 - \delta_1)\gamma_c S_C P}{C_1}\right\}\right\}, \\ u_2^* &= \max\left\{0, \min\left\{1, \frac{(\delta_2 - \delta_3) I_C}{C_2}\right\}\right\}, \\ u_3^* &= \max\left\{0, \min\left\{1, \frac{(\delta_5 S_S + \delta_6 I_S)}{C_3}\right\}\right\}. \end{aligned}\right\}$$

Proof. If $(\mathscr{X}, u)$ denotes an optimal solution for an optimal control problem, then the existence of a nontrivial vector function $\delta = (\delta_1, \delta_2, \delta_3, \delta_4, \delta_5, \delta_6, \delta_7)$ is guaranteed. This vector function satisfies the following set of equations.

$$\frac{d\delta}{dt} = -\frac{\partial \mathscr{H}(t, \mathscr{X}, u, \delta)}{\partial \mathscr{X}},$$

where $\mathscr{X} = (S_C, I_C, T_C, M, S_S, I_S, P)$, with transversality conditions: $\delta_i(t_f) = 0,\ i = 1, 2, ..., 7$.

Therefore, the corresponding adjoint system can be expressed as:

$$\begin{cases} \frac{d\delta_1}{dt} = \gamma_c(1-u_1)P(\delta_1-\delta_2)+\mu_c\delta_1, \\ \frac{d\delta_2}{dt} = -A_1+(\delta_c+u_2+\mu_c)\delta_2-(\delta_c+u_2)\delta_3-\gamma_m\delta_4, \\ \frac{d\delta_3}{dt} = -\lambda\delta_1+(\lambda+\mu_c)\delta_3, \\ \frac{d\delta_4}{dt} = \mu_m\delta_4+(\gamma_s S_S)(\delta_5-\delta_6), \\ \frac{d\delta_5}{dt} = -A_2+\gamma_s M(\delta_5-\delta_6)+(\mu_s+u_3)\delta_5, \\ \frac{d\delta_6}{dt} = -A_2+(\mu_s+u_3)\delta_6-\gamma_p\delta_7, \\ \frac{d\delta_7}{dt} = \gamma_c(1-u_1)(\delta_1-\delta_2)S_C+\mu_p\delta_7. \end{cases}$$

To derive the optimality conditions, we calculate the derivative of the Hamiltonian function (4.9) for the control variables and solve for the point where the derivative is zero.

$$\frac{\partial\mathscr{H}(t,\mathscr{X},u,\delta)}{\partial u}=0.$$

This leads to the following expression:

$$\begin{cases} \frac{\partial\mathscr{H}}{\partial u_1} = C_1u_1+(\delta_1-\delta_2)\gamma_c S_C P = 0, \\ \frac{\partial\mathscr{H}}{\partial u_2} = C_2u_2+(\delta_3-\delta_2)I_C = 0, \\ \frac{\partial\mathscr{H}}{\partial u_3} = C_1u_1-\delta_5 S_S-\delta_6 I_S = 0. \end{cases}$$

Solving the equations for $u_1^*(t)$, $u_2^*(t)$ and $u_3^*(t)$, we can draw the following conclusion.

$$\begin{aligned} u_1^* &= \max\left\{0,\min\left\{1,\frac{(\delta_2-\delta_1)\gamma_c S_C P}{C_1}\right\}\right\}, \\ u_2^* &= \max\left\{0,\min\left\{1,\frac{(\delta_2-\delta_3)I_C}{C_2}\right\}\right\}, \\ u_3^* &= \max\left\{0,\min\left\{1,\frac{(\delta_5 S_S+\delta_6 I_S)}{C_3}\right\}\right\}. \end{aligned}$$

4.3 Numerical Simulations and Discussions

In this section, we present the results of numerical simulations performed to address the optimal control problem. In addition, we would compare the results under two different scenarios: one incorporating optimal control and the other involving no control at all. The simulations were conducted using the parameter values specified in Table 3.1.

The fourth-order *Runge-Kutta forward-backward scheme* is used to solve the control model numerically. An optimal control simulation was performed using a 100-day time step for time series analysis. The values of the weight constants and the cost constants used in the simulations are $A_1 = 800$, $A_2 = 500$, $C_1 = 100$, $C_2 = 85$ and $C_3 = 90$. To see the impact that each control measure has on the elimination of *F. hepatica* disease, we evaluated the efficiency of four control strategies. Our objective was to determine the most favourable mix of these interventions.

Strategy A: Pasture management (u_1) and cattle treatment (u_2).

Strategy B: Pasture management (u_1) and molluscicides (u_3).

Strategy C: Cattle treatment (u_2) and molluscicides (u_3).

Strategy D: Combine all three controls.

4.3.1 Strategy A: Pasture Management and Cattle Treatment

Integrating pasture management (u_1) and infected cattle treatment (u_2), while omitting molluscicide control ($u_3 = 0$), optimizes the objective function J (Figure 4.1). Figure 4.1a illustrates that the implementation of these combined interventions leads to a decrease in the number of cattle infected with the disease. Figure 4.1c indicates that this approach requires maintaining maximum cattle treatment throughout almost the entire intervention period, while pasture management should be at its peak during the initial 50 days and then gradually decrease to zero. Studies (Rahmann & Seip 2006, Knubben-Schweizer et al. 2010) confirm that effective pasture man-

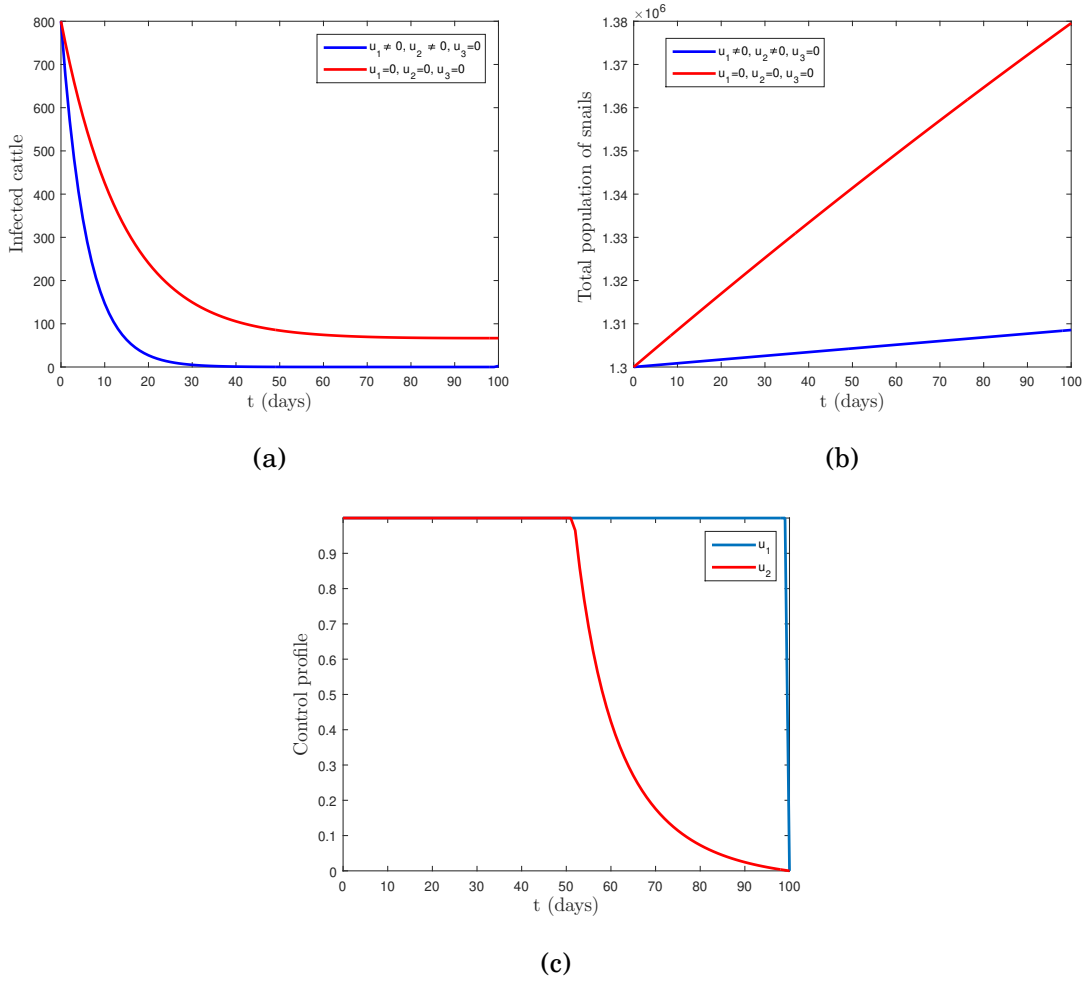

Figure 4.1: The optimal combined effect of implementing pasture management ($u_1(t)$) and cattle treatment ($u_2(t)$) for: (a) infected cattle, (b) total snail and (c) control profile.

agement and regular anthelmintic treatment for infected cattle significantly reduce disease prevalence and transmission.

4.3.2 Strategy B: Pasture Management and Molluscicides

Figure 4.2 shows the simulation results for optima pasture management (u_1) and molluscicides (u_3). Figures 4.2a and 4.2b shows that optimal controls significantly reduce both the number of infected cattle (I_C) and the snail population (N_S) compared to scenarios without controls. As shown in Figure 4.2c, this strategy requires

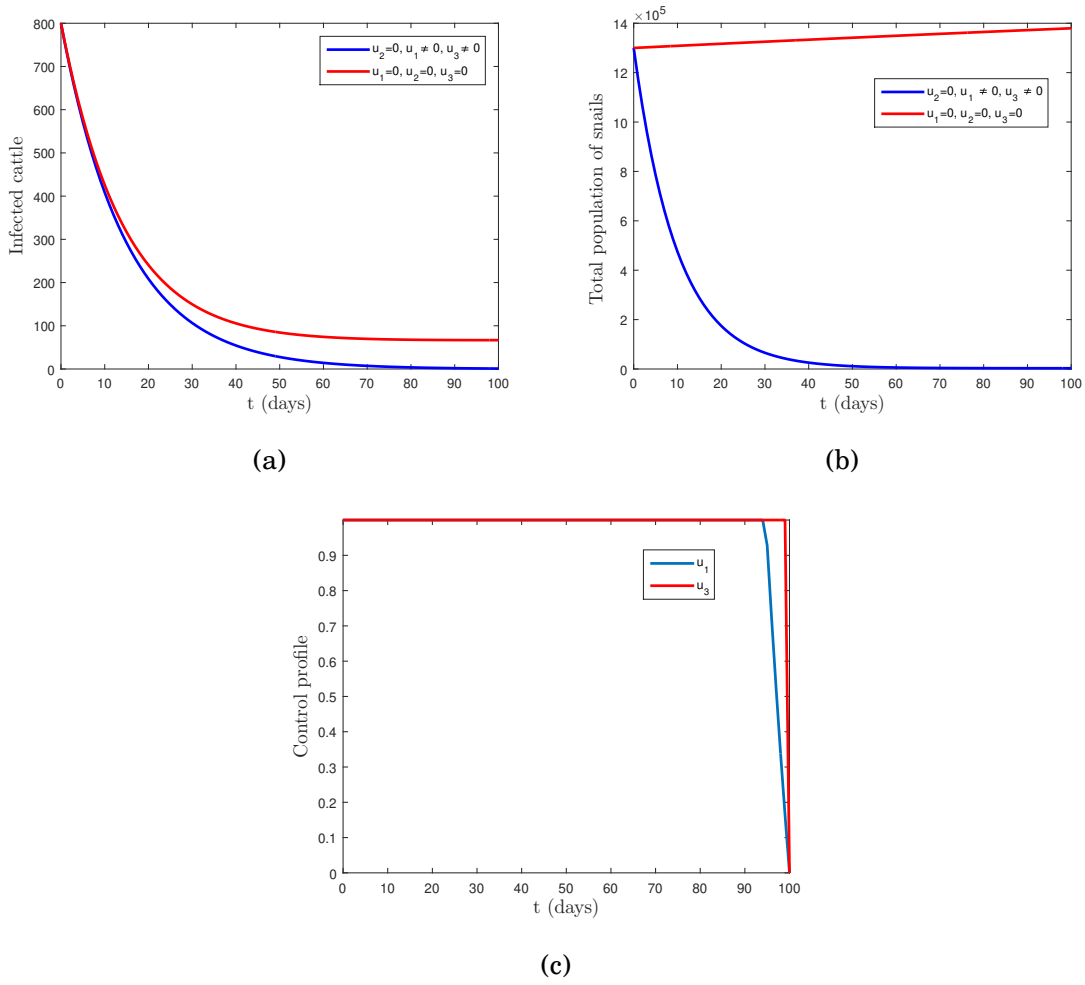

Figure 4.2: The optimal combined effect of implementing pasture management ($u_1(t)$) and molluscicides ($u_3(t)$) for: (a) infected cattle, (b) total snail and (c) control profile.

maintaining the control profile for pasture management (u_1) and the use of molluscicides (u_3) at their maximum levels for approximately 90% and 95% of the 100 days, respectively.

4.3.3 Strategy C: Treatment and Molluscicides

To minimize the objective functional J, we perform simulations in Figure 4.3 that represent the treatment of infected cattle (u_2) combined with the use of molluscicide while setting the pasture management (u_3) practice to zero. Figure 4.3a shows that

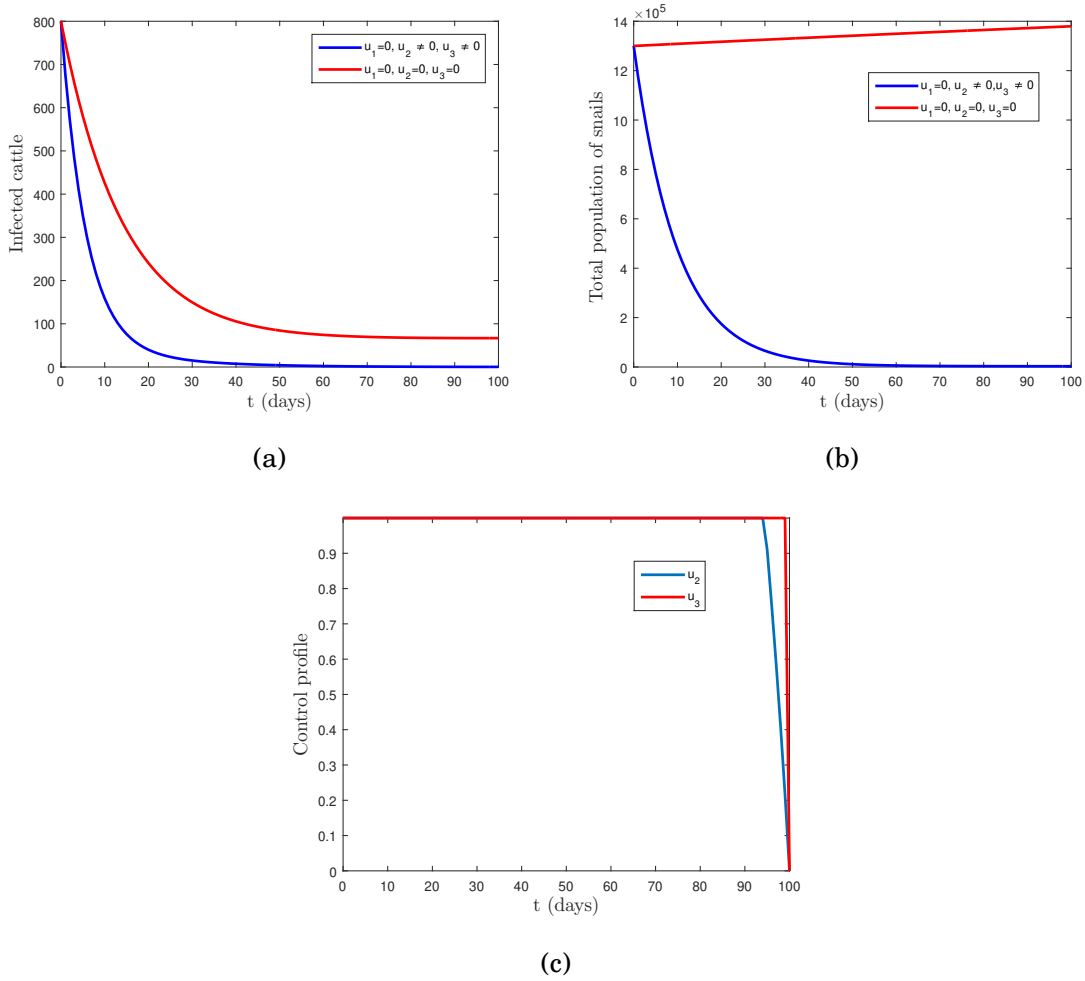

Figure 4.3: The optimal combined effect of implementing cattle treatment ($u_2(t)$) and molluscicides ($u_3(t)$) for: (a) infected cattle, (b) total snail and (c) control profile.

under control, the number of cattle infected by *F. hepatica* drops dramatically. Figure 4.3b shows a substantial decline in snail population when implementing this control strategy. Figure 4.3c also illustrates the control profiles for the treatment of infected cattle (u_2) and molluscicides (u_3). The analysis suggests that the treatment control consistently maintains its upper bound of 100% for 95 days. On the other hand, the molluscicide control reaches its maximum level of 100% throughout the entire implementation period.

4.3.4 Strategy D: Pasture Management, Treatment and Molluscicides

In this strategy shown in Figure 4.4, we use the three controls, namely u_1, u_2 and u_3, to optimize the objective function J. Figures 4.4a and 4.4b illustrate that all three of these optimal controls must be used together to eliminate the disease in both cattle and snail populations. In Figure 4.4c, in which pasture management is strictly maintained at a maximum level of 100% for 95 days, treatment administration is at a maximum of 100% for 52 days. The possibility of molluscicide control remains continuously at a maximum level of 100% until the end of 100 days, when the optimal solution can be reached. It is highly effective when these three controls are combined to reduce infected cattle, compared to a combination of two control measures.

4.4 Cost-Effectiveness Analysis

Cost-effectiveness analysis balances costs against outcomes to guide resource allocation and policy decision-making for the control of *F. hepatica* infection in cattle. An incremental cost-effectiveness ratio was used in a cost-effectiveness analysis comparing the differences in total costs to indicate the best strategy for controlling *F. hepatica* in cattle. When strategy i outperforms strategy j, the incremental cost-effectiveness ratio (ICER) is calculated as:

$$ICER = \frac{TC(i)}{TA(i)}.$$

$$ICER(j) = \frac{TC(j) - TC(i)}{TA(j) - TA(i)}.$$

where the total costs (TC) and the total cases averted (TA), during a given period for strategy i for $i = A, B, C, D$.

Based on the simulation results, we arrange the control strategies in ascending order of effectiveness in terms of the averted infections. This ranking procedure reveals that the strategy D resulted in the lowest number of infections averted, followed by the strategies A, C and B (Table 4.1). Using this ranking, we initially

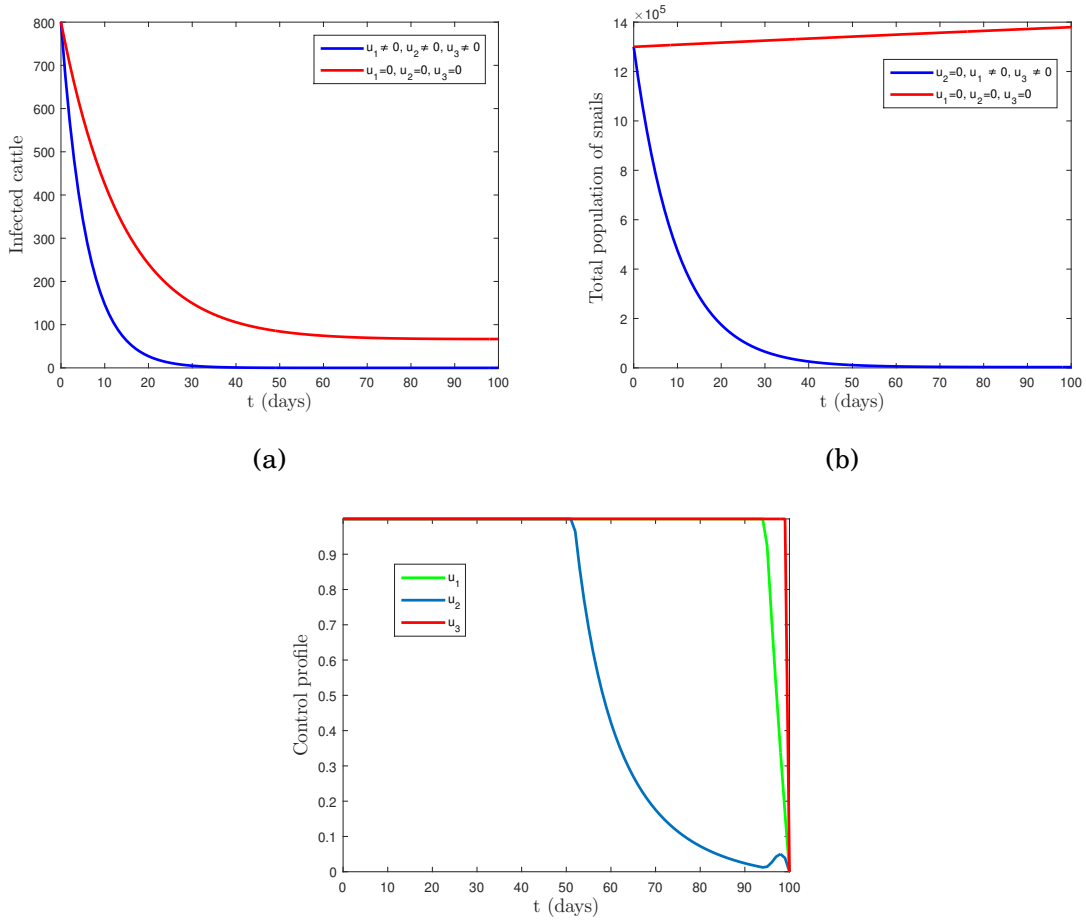

Figure 4.4: The optimal combined effect of implementing pasture management ($u_1(t)$), cattle treatment ($u_2(t)$) and molluscicides ($u_3(t)$) for: (a) infected cattle, (b) total snail and (c) control profile.

compare the ICER between strategy D and strategy A as follows:

$$ICER(D) = \frac{9.6074 \times 10^5}{5.1348 \times 10^3} = 187.202.$$
$$ICER(A) = \frac{6.2737 \times 10^5 - 9.6074 \times 10^5}{5.1369 \times 10^3 - 5.1348 \times 10^3} = -15879.5238.$$

The lower ICER for strategy A indicates that strategy D is strongly dominated by strategy A. It can be inferred that strategy A is more cost-effective than strategy D. Therefore, strategy D is rejected and the analysis focuses on comparing strategy A and strategy C.

$$ICER(A) = \frac{6.2737 \times 10^5}{5.1369 \times 10^3} = 122.087.$$
$$ICER(C) = \frac{6.4329 \times 10^5 - 6.2737 \times 10^5}{5.6423 \times 10^3 - 5.1369 \times 10^3} = 31.521.$$

Strategy A is more expensive and less effective than strategy C. Therefore, strategy A is rejected and the analysis focuses on comparing strategy C with strategy B.

$$ICER(C) = \frac{6.4329 \times 10^5}{5.6423 \times 10^3} = 113.989.$$
$$ICER(B) = \frac{7.1606 \times 10^5 - 6.4329 \times 10^5}{1.2289 \times 10^4 - 5.6423 \times 10^3} = 12.88.$$

These results show that strategy B is more cost-effective and efficient than strategy C. Thus, the strategy B, including pasture management and molluscicides, becomes the best among the four strategies in that order, followed by the strategies C, A and D.

Table 4.1: Total amount of *F. hepatica* infection averted and total cost for all strategies.

Strategies	Total infection averted	Total cost ($)
strategy D (control u_1, u_2 and u_3)	5.1348×10^3	9.6074×10^5
strategy A (control u_1 and u_2)	5.1369×10^3	6.2737×10^5
strategy C (control u_2 and u_3)	5.6423×10^3	6.4329×10^5
strategy B (control u_1 and u_3)	1.2289×10^4	7.1606×10^5

4.5 Conclusion

An optimal control model analyzed control strategies for *Fasciola hepatica* in cattle to identify the most cost-effective approach, considering pasture management, cattle treatment and molluscicide use. Pontryagin's maximum principle defined the necessary conditions for optimal control. Numerical simulations showed that double and triple control strategies effectively reduced infected cattle, with combination of pasture management, treatment and molluscicide proving significantly more effective than double control strategies, consistent with Madubueze et al. (2022). Simulations indicate that maximizing the molluscicide control variable enhances *Fasciola hepatica* control, confirming its importance in interventions, consistent with Nur, Suryanto, Kusumawinahyu et al. (2022). Controlling intermediate snail host populations remains a promising strategy in endemic areas and molluscicides are a potential tool for managing fluke infections (Solomon & Alemu 2019, Feyisa 2021).

The cost-effectiveness analysis was done using the incremental cost-effectiveness ratio (ICER) to see the level of benefit and cost-effectiveness of these intervention strategies. The results indicate that combined pasture management and molluscicides were the most efficient and cost-effective strategies to eliminate *Fasciola hepatica*. Rizwan et al. (2022) suggests that strategic anthelmintic rotations may improve control of both immature and adult flukes, supporting these findings. Finally,

we suggest that policy makers adopt a combined strategy involving pasture management and molluscicide intervention, as it will be the most cost-effective approach to controlling *F. hepatica* disease.

Chapter 5

5 The Impact of Early Diagnosis and Treatment in a *Fasciola Hepatica* Model

5.1 Introduction

Mathematical models of disease transmission often omit the crucial exposed (infected but non-infectious) stage. Incorporating this latent stage improves outbreak prediction and allows timely interventions. Early diagnosis within the exposed group, using advanced equipment, enables prompt treatment, reduces disease burden and transmission. Cattle diagnosis is based on clinical signs, grazing history, seasonal patterns, fecal analysis, postmortem examinations and detection of liver fluke. We are unaware of any deterministic model of *fascioliasis* that accounts for the effect of the latent period. Addressing both exposed individuals and those under treatment optimizes disease control by preventing infectiousness and reducing prevalence, particularly in high-risk populations. Therefore, including the exposed group and prioritizing early diagnosis and treatment significantly improves the control of *fascioliasis*, minimizing its health and economic consequences. This study addresses these gaps by examining exposed snail and cattle populations and evaluating the impact of molluscicides. By integrating these factors, it aims to provide a comprehensive understanding of the transmission dynamics of *F. hepatica* to improve control and prevention strategies.

5.2 Model Formulation

In this section, we formulate a mathematical model to investigate the dynamics of *F. hepatica*. This model considers an ode system to describe the relationship between snail and cattle populations, considering the latency in these populations. The

cattle population is classified into susceptible, exposed, infected and treated subpopulations, while the snail population is divided into susceptible, exposed and infected subpopulations. Furthermore, free-living *Fasciola* larvae consist of two subpopulations: miracidia and metacercariae. We consider nine different state variables and represent them using the abbreviations: susceptible cattle (S_C), exposed cattle (E_C), infected cattle (I_C), treated cattle (T_C), susceptible snail (S_S), exposed snail (E_S), infected snail (I_S), miracidia (M) and metacercariae (P).

Susceptible cattle and snails can contract diseases at a bilinear incidence rate. In our scenario, we consider a homogeneous cattle population in which all animals have an identical chance of having contact with the disease. We assumed that the diagnosis would be confirmed by serological tests and that all cattle exposed and infected with the disease were effectively treated with triclabendazole. It is important to note that the onset of egg production does not occur until 3 to 4 months after exposure, as indicated by previous research (Caravedo & Cabada 2020). Figure 5.1 shows a compartmental model flow diagram that represents the complex dynamics of the *F. hepatica* parasite within cattle and snails. All model parameter values and descriptions are summarized in Table 5.1.

The rate of change in the susceptible cattle population is influenced by the recruitment rate (Λ_c), infection rate (β_c), the natural death rate (δ_c) and the recovery rate from treatment (ρ). The exposed cattle depend on the infection rate (β_c), the treatment rate (τ_1), the natural death (δ_c) and the rate at which exposed cattle transition to infected cattle (σ_c). Infected cattle are influenced by the transition rate from exposed to infected (σ_c), the treatment rate (τ_2) and the removal rate due to natural death and disease-induced deaths (δ_c and d_c). The treated cattle depended on the treatment rates in the exposed and infected stages (τ_1 and τ_2), natural death (δ_c) and the recovery rate (ρ). The dynamics of miracidia are determined by the rate of production of miracidia in an infected cattle (γ_m) and removal due to natural death (δ_m). The dynamics of miracidia are determined by the rate of production of miracidia in cattle (γ_m) of infection and removal due to natural death (δ_m). The dynamics of the susceptible snail depends on the recruitment rate (Λ_s) and the infection rate (β_s).

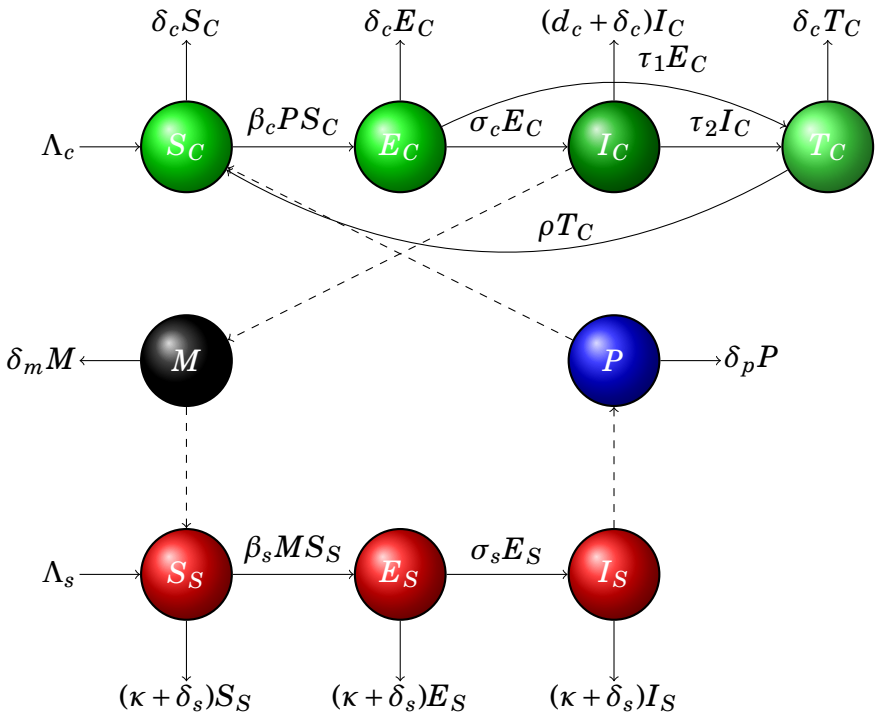

Figure 5.1: Transfer diagram for *F. hepatica* disease model (5.1). Solid lines indicate the movement of individuals between compartments, whereas dotted lines show interactions or influences without direct transfers.

The dynamics of the exposed snail depends on the infection rate (β_s) and the rate of transition from exposed to infected (σ_c). The transition rate (σ_c) from exposed to infected snails influences the dynamics of the infected snail. In addition, all groups of snail populations are influenced by the removal rate due to natural death and the use of molluscicide (δ_s, κ). The metacercariae population depends on the rate of release of metacercariae γ_p and the natural death rate of metacercariae δ_p.

The transmission dynamics of *F. hepatica* is described by the system of differen-

tial equations, which is stated as follows:

$$\begin{cases} \dfrac{dS_C}{dt} = \Lambda_c - \beta_c S_C P - \delta_c S_C + \rho T_C, \\ \dfrac{dE_C}{dt} = \beta_c S_C(t) P - (\tau_1 + \sigma_c + \delta_c) E_C, \\ \dfrac{dI_C}{dt} = \sigma_c E_C - (\tau_2 + d_c + \delta_c) I_C, \\ \dfrac{dT_C}{dt} = \tau_1 E_C + \tau_2 I_C - (\rho + \delta_c) T_C(t), \\ \dfrac{dM}{dt} = \gamma_m I_C - \delta_m M, \\ \dfrac{dS_S}{dt} = \Lambda_s - \beta_s S_S M - (\kappa + \delta_s) S_S, \\ \dfrac{dE_S}{dt} = \beta_s S_S M - (\sigma_s + \kappa + \delta_s) E_S, \\ \dfrac{dI_S}{dt} = \sigma_s E_S - (\kappa + \delta_s) I_S, \\ \dfrac{dP}{dt} = \gamma_p I_S - \delta_p P, \end{cases} \tag{5.1}$$

with initial conditions, $S_C(0) \geq 0$; $E_C(0) \geq 0$; $I_C(0) \geq 0$; $T_C(0) \geq 0$; $M(0) \geq 0$; $S_S(0) \geq 0$; $E_S(0) \geq 0$; $I_S(0) \geq 0$; and $P(0) \geq 0$. The total populations of cattle (N_C) and snail (N_S) populations are given, respectively, by $N_C = S_C + E_C + I_C + T_C$ and $N_S = S_S + E_S + I_S$. All the parameters in equation (5.1) are assumed to be positive.

5.3 Model Analysis

In this section, we investigate the fundamental properties of the model described in Equation (5.1). We analyze the feasible regions of the system, the positivity of solutions, the equilibrium points and their stability. For simplicity of the mathematical proofs and calculations, let us use the following representation: $\eta = \tau_1 + \sigma_c + \delta_c$, $\theta = \tau_2 + d_c + \delta_c$, $\phi = \rho + \delta_c$, $\psi = \kappa + \delta_s$ and $\omega = \sigma_s + \kappa + \delta_s$.

5.3.1 Well-posedness

The system (3.1) can be rewritten as $\frac{dx}{dt} = g(x)$, with $x = (S_C, E_C, I_C, T_C, M, S_S, E_S, I_S, P) \in \mathbb{R}^9$. The right-hand side ($g(x)$) is smooth, it is locally Lipschitz continuous on $\mathbb{R}^9$. Thus, by the Cauchy–Lipschitz theorem, a unique maximal solution exists on $[0, T_{\max}]$ for any initial condition in $\mathbb{R}^9$.

Table 5.1: The description of the model (5.1) parameters and values.

Parameters	Descriptions	Values	Sources
Λ_c	Recruitment rate of cattle	64/day	Assumed
Λ_s	Recruitment rate of snail	3000/day	(Kanyi et al. 2021)
δ_c	Natural death rate of cattle	0.000488/day	Assumed
δ_s	Natural death rate of snails	0.001644/day	(Diaby et al. 2019)
d_c	Death rate due to *Fasciola hepatica* disease in cattle	0.00274/day	(Madubueze et al. 2022)
δ_m	Natural death rate of miracidia	0.9/day	(Kanyi et al. 2021, Chiyaka & Garira 2009)
δ_p	Natural death rate of metacercariae	0.6452/day	(Diaby et al. 2019)
γ_m	Production rate of miracidia	6.96/day	(Chiyaka & Garira 2009)
γ_p	Shedding rate of metacercariae	2.6 /day	(Chiyaka & Garira 2009)
β_c	Rate of transmission of cattle from susceptible to exposed	0.0000008/day	(Diaby et al. 2019)
β_s	Rate of transmission of snails from susceptible to exposed	0.0000004 /day	Assumed
σ_c	Progression rate from exposed to infected cattle	0.0265/day	Assumed
σ_s	Progression rate from exposed to infected snails	0.0575/day	Assumed
τ_1	Treatment rate of exposed cattle	0.15/day	Assumed
τ_2	Treatment rate of infected cattle	0.65/day	Assumed
ρ	Treatment efficiency of the infected cattle	0.9567/day	(Diaby et al. 2019)
κ	Elimination rates of snail by molluscicide	0.025/day	Assumed

5.3.2 Positivity of Solutions

Theorem 5.1. *If the initial values of the system (5.1) are all positive, ($S_C(0) > 0$, $E_C(0) > 0$), $I_C(0) > 0$, $T_C(0) > 0$, $M(0) > 0$, $S_S(0) > 0$, $E_S(0) > 0$, $I_S(0) > 0$, $P(0) > 0$), then any solution of the system (5.1) will be positive for any positive time t.*

Proof. To show the positivity of the model solutions, we start by considering the first equation of the model (5.1),

$$\frac{dS_C(t)}{dt} = \Lambda_c - \beta_c S_C(t)P(t) - \delta_c S_C(t) + \rho T_C(t) \geq -(\beta_c P(t) + \delta_c)S_C(t).$$

This yields

$$S_C(t) \geq S_C(0)e^{-\int_0^t (\beta_c P(\tau)+\delta_c)d\tau} > 0.$$

Hence, $S_C(t)$ is always positive for every positive t.

From the second equation in (5.1), we have

$$\frac{dE_C(t)}{dt} = \beta_c S_C(t)P(t) - \eta E_C(t) \geq -\eta E_C(t). \tag{5.2}$$

Integrating this differential inequality with a positive initial condition yields,

$$E_C(t) \geq E_C(0)e^{-\eta t}. \tag{5.3}$$

Therefore, this proves that $E_C(t)$ is always positive for all positive t.

Similarly, for any positive value of t, the other state variables are always positive.

$$\begin{cases} I_C(t) \geq I_C(0)e^{-\theta t}, \\ T_C(t) \geq T_C(0)e^{-\phi t}, \\ M(t) \geq M(0)e^{-\delta_m t}, \\ S_S(t) \geq S_S(0)e^{-\int_0^t (\beta_s M(\tau)+\psi)d\tau}, \\ E_S(t) \geq E_S(0)e^{-\omega t}, \\ I_S(t) \geq I_S(0)e^{-\psi t}, \\ P(t) \geq P(0)e^{-\delta_p t}. \end{cases} \tag{5.4}$$

Any solutions of system (5.1) with positive initial data should stay positive for every time $t \geq 0$. □

This is important because it ensures that the model will not produce negative values, which could lead to invalid or nonsensical results.

5.3.3 Boundedness of the Solutions

Theorem 5.2. *All solutions to the system (5.1) with positive initial conditions are confined within the bounded interior region*

$$\mathscr{D} = \{(S_C, E_C, I_C, T_C, M, S_S, E_S, I_S, P) \in \mathbb{R}_+^9 : N_C \leq \frac{\Lambda_c}{\delta_c}, N_S \leq \frac{\Lambda_s}{\psi}, M \leq \frac{\Lambda_c \gamma_m}{\delta_c \delta_m}, P \leq \frac{\Lambda_s \gamma_p}{\delta_p \psi}\}. \tag{5.5}$$

Proof. We considered the total number of cattle (N_C) and the total number of snails (N_S), with positive initial conditions $N_C(0)$ and $N_S(0)$. Adding the equations for the cattle populations gives the following equation.

$$\frac{dN_C}{dt} = \Lambda_c - \delta_c N_C - d_c I_C(t). \tag{5.6}$$

This implies that

$$\frac{dN_C}{dt} \leq \Lambda_c - \delta_c N_C(t). \tag{5.7}$$

The solution of the differential inequality (5.7) yields,

$$N_C(t) \leq \frac{\Lambda_c}{\delta_c} + (\frac{\delta_c N_C(0) - \Lambda_c}{\delta_c}) e^{-\delta_c t}. \tag{5.8}$$

As time, t becomes sufficiently large and approaches infinity, the population of cattle will tend to $\frac{\Lambda_c}{\delta_c}$. Consequently, we can conclude that:

$$N_C(t) \leq \frac{\Lambda_c}{\delta_c}. \tag{5.9}$$

Similarly, by bringing together the snail subclass equations, we can determine the entire dynamics of the snail population:

$$\frac{dN_S}{dt} = \Lambda_s - \psi N_S - \delta_s I_S. \tag{5.10}$$

Equation (5.10) provides that

$$\frac{dN_S}{dt} \leq \Lambda_s - \psi N_S. \tag{5.11}$$

The solution to the differential inequality (5.11) provides

$$N_S(t) \leq \frac{\Lambda_s}{\psi} + (\frac{\psi N_S(0) - \Lambda_s}{\psi}) e^{-\psi t}. \tag{5.12}$$

When t approaches infinity, $N_S(t)$ approaches $\frac{\Lambda_s}{\psi}$. As a result, we have

$$N_S(t) \leq \frac{\Lambda_s}{\psi}. \tag{5.13}$$

Combining equation (5.9) with the fourth equation of the system (5.1) yields,

$$M(t) \leq \frac{\Lambda_c \gamma_m}{\delta_c \delta_m}. \tag{5.14}$$

Likewise, by using equation (5.13) and the ninth equation of the system (5.1), we get:

$$P(t) \leq \frac{\Lambda_s \gamma_p}{\delta_p \psi}. \tag{5.15}$$

As a result, the feasible region of the system becomes

$$\mathscr{D} = \{(S_C, E_C, I_C, T_C, M, S_S, E_S, I_S, P) \in \mathbb{R}^9 : N_C \leq \frac{\Lambda_c}{\delta_c}, N_S \leq \frac{\Lambda_s}{\psi}, M \leq \frac{\Lambda_c \gamma_m}{\delta_c \delta_m}, P \leq \frac{\Lambda_s \gamma_p}{\delta_p \psi}\}.\square$$

5.3.4 Disease-Free Equilibrium Point and Effective Reproduction Number

Disease-Free Equilibrium Point

The disease-free equilibrium point of the system (5.1) exists when the populations of metacercaria, miracidia, exposed and treated cattle, as well as exposed and infected snails, all become zero. This is achieved by substituting $E_C = 0$, $I_C = 0$, $T_C = 0$, $M = 0$, $E_S = 0$, $I_S = 0$ and $P = 0$ into equation (5.1) and it yields the following result:

$$\begin{cases} \frac{dS_C}{dt} = \Lambda_c - \delta_c S_C = 0, \\ \frac{dS_S}{dt} = \Lambda_s - \psi S_S = 0. \end{cases} \tag{5.16}$$

Thus, the disease-free equilibrium is given by

$$E_0 = \left(S_C^0, E_C^0, I_C^0, T_C^0, M^0, S_S^0, E_S^0, I_S^0, P^0\right) = \left(\frac{\Lambda_c}{\delta_c}, 0, 0, 0, 0, \frac{\Lambda_s}{\psi}, 0, 0, 0\right). \tag{5.17}$$

Effective Reproduction Number

In order to estimate the effective reproduction number, R_0, for a compartmental-design transmissible disease, the next-generation matrix approach is often used. This method allows calculation of the reproductive number by considering different groups or compartments within the population, such as E_C, I_C, T_C, M, E_S, I_S and P,

which represent disease compartments. The disease group can then be represented as a differential system to study its dynamics and make predictions.

$$\begin{cases} \dfrac{dE_C}{dt} = \beta_c S_C P - \eta E_C, \\ \dfrac{dI_C}{dt} = \sigma_c E_C - \theta I_C, \\ \dfrac{dT_C}{dt} = \tau_1 E_C + \tau_2 I_C - \phi T_C, \\ \dfrac{dM}{dt} = \gamma_m I_C - \delta_m M, \\ \dfrac{dE_S}{dt} = \beta_s S_S M - \omega E_S, \\ \dfrac{dI_S}{dt} = \sigma_s E_S - \psi I_S, \\ \dfrac{dP}{dt} = \gamma_p I_S - \delta_p P. \end{cases} \tag{5.18}$$

Let $X = (E_C, I_C, T_C, M, E_S, I_S, P)$, $g(X)$ denote the rates of appearance of new infections in compartments and $u(X)$ represent the rate at which the cattle are moved into the compartments. Thus, equation (5.18) is expressed as,

$$\frac{dX}{dt} = g(X) - u(X), \tag{5.19}$$

where, $g = \begin{pmatrix} \beta_c S_C P \\ 0 \\ 0 \\ 0 \\ \beta_s S_S M \\ 0 \\ 0 \end{pmatrix}$ and $u = \begin{pmatrix} \eta E_C \\ -\sigma_c E_C + \theta I_C \\ -\tau_1 E_C - \tau_2 I_C + \phi T_C \\ -\gamma_m I_C + \delta_m M \\ \omega E_S \\ -\sigma_s E_S + \psi I_S \\ -\gamma_p I_S + \delta_p P \end{pmatrix}$.

We compute the Jacobian matrices, G and U, by evaluating g and u derivatives to the disease class variables at DFE.

$$G = \begin{pmatrix} 0 & 0 & 0 & 0 & 0 & 0 & \frac{\beta_c \Lambda_c}{\delta_c} \\ 0 & 0 & 0 & 0 & 0 & 0 & 0 \\ 0 & 0 & 0 & 0 & 0 & 0 & 0 \\ 0 & 0 & 0 & 0 & 0 & 0 & 0 \\ 0 & 0 & 0 & \frac{\beta_s \Lambda_s}{\psi} & 0 & 0 & 0 \\ 0 & 0 & 0 & 0 & 0 & 0 & 0 \\ 0 & 0 & 0 & 0 & 0 & 0 & 0 \end{pmatrix} \text{ and} \tag{5.20}$$

$$U = \begin{pmatrix} \eta & 0 & 0 & 0 & 0 & 0 & 0 \\ -\sigma_c & \theta & 0 & 0 & 0 & 0 & 0 \\ -\tau_1 & -\tau_2 & \phi & 0 & 0 & 0 & 0 \\ 0 & -\gamma_m & 0 & \delta_m & 0 & 0 & 0 \\ 0 & 0 & 0 & 0 & \omega & 0 & 0 \\ 0 & 0 & 0 & 0 & -\sigma_s & \psi & 0 \\ 0 & 0 & 0 & 0 & 0 & -\gamma_p & \delta_p \end{pmatrix}. \tag{5.21}$$

The inverse of the matrix U becomes,

$$U^{-1} = \begin{pmatrix} \frac{1}{\eta} & 0 & 0 & 0 & 0 & 0 & 0 \\ \frac{\sigma_c}{\eta\theta} & \frac{1}{\theta} & 0 & 0 & 0 & 0 & 0 \\ \frac{\theta\tau_1 + \sigma_c\tau_2}{\eta\theta\phi} & \frac{\tau_2}{\theta\phi} & \frac{1}{\psi} & 0 & 0 & 0 & 0 \\ \frac{\gamma_m\sigma_c}{\eta\theta\delta_m} & \frac{\gamma_m}{\theta\delta_m} & 0 & \frac{1}{\delta_m} & 0 & 0 & 0 \\ 0 & 0 & 0 & 0 & \frac{1}{\omega} & 0 & 0 \\ 0 & 0 & 0 & 0 & \frac{\sigma_s}{\psi\omega} & \frac{1}{\psi} & 0 \\ 0 & 0 & 0 & 0 & \frac{\gamma_p\sigma_s}{\psi\omega\delta_p} & \frac{\gamma_p}{\psi\delta_p} & \frac{1}{\delta_p} \end{pmatrix}. \tag{5.22}$$

The multiplication of matrices G and U^{-1} yields the following results:

$$GU^{-1} = \begin{pmatrix} 0 & 0 & 0 & 0 & \frac{\beta_c\gamma_p\Lambda_c\sigma_s}{\omega\psi\delta_c\delta_p} & \frac{\beta_c\gamma_p\Lambda_c}{\psi\delta_c\delta_p} & \frac{\beta_c\Lambda_c}{\delta_c\delta_p} \\ 0 & 0 & 0 & 0 & 0 & 0 & 0 \\ 0 & 0 & 0 & 0 & 0 & 0 & 0 \\ 0 & 0 & 0 & 0 & 0 & 0 & 0 \\ \frac{\beta_s\gamma_m\Lambda_s\sigma_c}{\eta\theta\psi\delta_m} & \frac{\beta_s\gamma_m\Lambda_s}{\theta\psi\delta_m} & 0 & \frac{\beta_s\Lambda_s}{\psi\delta_m} & 0 & 0 & 0 \\ 0 & 0 & 0 & 0 & 0 & 0 & 0 \\ 0 & 0 & 0 & 0 & 0 & 0 & 0 \end{pmatrix}. \tag{5.23}$$

The eigenvalues of GU^{-1} are 0, 0, 0 and $\pm\sqrt{\frac{\beta_c\beta_s\gamma_m\gamma_p\Lambda_c\Lambda_s\sigma_c\sigma_s}{\eta\theta\psi^2\omega\delta_c\delta_m\delta_p}}$.

Therefore, the effective reproduction number, which is the spectral radius of $\rho(GU^{-1})$, is

$$R_0 = \sqrt{\frac{\beta_c\beta_s\gamma_m\gamma_p\Lambda_c\Lambda_s\sigma_c\sigma_s}{\eta\theta\psi^2\omega\delta_c\delta_m\delta_p}}. \tag{5.24}$$

$$R_0 = \sqrt{\frac{\beta_c\beta_s\gamma_m\gamma_p\Lambda_c\Lambda_s\sigma_c\sigma_s}{(\tau_1+\sigma_c+\delta_c)(\tau_2+d_c+\delta_c)(\kappa+\delta_s)^2(\sigma_s+\kappa+\delta_s)\delta_c\delta_m\delta_p}}.$$

The basic reproduction number, R_b, is the effective reproduction number when all control parameters are zero. This occurs when there is no treatment ($\tau_1 = 0$ and $\tau_2 = 0$) and no snail control ($\kappa = 0$). Therefore, the basic reproduction number is

$$R_b = \sqrt{\frac{\beta_c\beta_s\gamma_m\gamma_p\Lambda_c\Lambda_s\sigma_c\sigma_s}{(\sigma_c+\delta_c)(d_c+\delta_c)(\delta_s)^2(\sigma_s+\delta_s)\delta_c\delta_m\delta_p}}.$$

5.3.5 Stability of Disease-Free Equilibrium Point

Local Stability of Disease-Free Equilibrium

Theorem 5.3. *The disease-free equilibrium point, (5.17) is locally asymptotically stable when* $R_0 < 1$

Proof. The Jacobian matrix of the system (5.1) at the disease-free equilibrium

point E_0 is

$$J(E_0) = \begin{pmatrix} -\delta_c & 0 & 0 & \rho & 0 & 0 & 0 & 0 & -\frac{\Lambda_s \beta_c}{\delta_c} \\ 0 & -\eta & 0 & 0 & 0 & 0 & 0 & 0 & \frac{\Lambda_s \beta_c}{\delta_c} \\ 0 & \sigma_c & -\theta & 0 & 0 & 0 & 0 & 0 & 0 \\ 0 & \tau_1 & \tau_2 & -\phi & 0 & 0 & 0 & 0 & 0 \\ 0 & 0 & -\gamma_m & 0 & \delta_m & 0 & 0 & 0 & 0 \\ 0 & 0 & 0 & 0 & -\frac{\beta_s \Lambda_s}{\psi} & -\psi & 0 & 0 & 0 \\ 0 & 0 & 0 & 0 & \frac{\beta_s \Lambda_s}{\psi} & 0 & -\omega & 0 & 0 \\ 0 & 0 & 0 & 0 & 0 & 0 & \sigma_s & -\psi & 0 \\ 0 & 0 & 0 & 0 & 0 & 0 & 0 & \gamma_p & -\delta_p \end{pmatrix}. \tag{5.25}$$

The eigenvalues of the Jacobian matrix J are $-\delta_c$, $-\phi$, $-\psi$ and the rest are roots of the polynomial equation,

$$\psi\delta_c(X+\eta)(X+\theta)(X+\omega)(X+\psi)(X+\delta_m)(X+\delta_p) - \beta_c\beta_s\gamma_m\gamma_p\Lambda_c\Lambda_s\sigma_c\sigma_s = 0. \tag{5.26}$$

Equation (5.26) will have roots with negative real parts if all coefficients are positive (Heffernan et al. 2005). All coefficients for terms X^6, X^5, X^4, X^3, X^2 and X are positive because all expressions in the products are positive. The constant term in the equation will also be positive if the following condition is met:

$$\eta\theta\psi^2\omega\delta_c\delta_m\delta_p - \beta_c\beta_s\gamma_m\gamma_p\Lambda_c\Lambda_s\sigma_c\sigma_s = \eta\theta\psi^2\omega\delta_c\delta_m\delta_p(1-R_0^2) > 0.$$

This implies that the constant term is positive if $R_0 < 1$. It satisfies the Routh-Hurwitz conditions and provides that all eigenvalues of this characteristic polynomial have negative real part roots.

Global Stability of Disease-Free Equilibrium

The method proposed by Castillo-Chavez et al. (2002) stated in Lemma 5.4 is used to analyse the global stability of the disease-free equilibrium point within the feasible region $\mathscr{D} \in \mathscr{R}^9_+$.

The system (5.1) can be expressed in the following form:

$$\begin{cases} \frac{dU}{dt} &= R(U,V), \\ \frac{dV}{dt} &= T(U,V),\ T(U,0) = 0, \end{cases} \tag{5.27}$$

where $U = (S_C, S_S)$ and $V = (E_C, I_C, T_C, M, E_S, I_S, P)$ represent the infected and infected compartments, respectively.

Lemma 5.4. *(Castillo-Chavez et al. 2002) The fixed point $E_0 = (U^*, 0)$ is a globally asymptotically stable equilibrium of the system (5.27) if and only if $R_0 < 1$ (locally asymptotically stable) and conditions (C1) and (C2) are satisfied.*

The two conditions (C1) and (C2) are:

C1 : For $\frac{dU}{dt} = R(U,0)$, U^* is globally asymptotically stable.

C2 : $T(U,V) = BV - \hat{T}(U,V)$, $\hat{T}(U,V) \geq 0$ for $(U,V) \in \mathscr{D}$.

with $B = D_V T(U^*, 0)$ being the M-matrix, the off-diagonal entries of B are nonnegative and $\mathscr{D}$ is the set at which the system becomes feasible.

Theorem 5.5. *The disease-free equilibrium, $E_0 = \left(\frac{\Lambda_c}{\delta_c}, 0, 0, 0, 0, \frac{\Lambda_s}{\psi}, 0, 0, 0\right)$, is globally asymptotically stable when $R_0 < 1$.*

Proof. We prove this using the lemma 5.4. From the system described by equation (5.27), we obtain the following:

$$R(U,V) = \begin{pmatrix} \Lambda_c - \beta_c S_C(t) P(t) - \delta_c S_C(t) + \rho T_C(t) \\ \Lambda_s - \beta_s S_S(t) M(t) - \psi S_S(t) \end{pmatrix}. \tag{5.28}$$

Based on equation (5.28), we have,

$$\frac{dU}{dt} = R(U,0) = \begin{pmatrix} \Lambda_c - \delta_c S_C \\ \Lambda_s - \psi S_S \end{pmatrix}. \tag{5.29}$$

The solution to equation (5.29), for disease-free variables becomes, $S_C(t) = \frac{\Lambda_c}{\delta_c} - [\frac{\Lambda_c}{\delta_c} - S_C(0)]e^{-\delta_c t}$ and $S_C(t) = \frac{\Lambda_S}{\psi} - [\frac{\Lambda_s}{\psi} - S_S(0)]e^{-\psi t}$. As t goes to infinity, the values of S_C and S_S converge to $\frac{\Lambda_c}{\delta_c}$ and $\frac{\Lambda_c}{\psi}$, respectively. Thus, $U^* = (\frac{\Lambda_c}{\delta_c}, \frac{\Lambda_s}{\psi})$ is the globally asymptotically stable equilibrium point for equation (5.29). As a result, condition C1 is satisfied.

The disease class differential equation in equation (5.27) can be expressed as follows:

$$\frac{dV}{dt} = T(U,V) = \begin{pmatrix} \beta_c S_C(t)P(t) - \eta E_C(t) \\ \sigma_c E_C(t) - \theta I_C(t) \\ \tau_1 E_C(t) + \tau_2 I_C(t) - \phi T_C(t) \\ \gamma_m I_C(t) - \delta_m M(t) \\ \beta_s S_S(t) M(t) - \omega E_S(t) \\ \sigma_s E_S(t) - \psi I_S(t) \\ \gamma_p I_S(t) - \delta_p P(t) \end{pmatrix}.$$

$$T(U,V) = BU - \hat{T}(U,V),$$

where

$$B = \begin{pmatrix} -\eta & 0 & 0 & 0 & 0 & 0 & \frac{\beta_c \Lambda_c}{\delta_c} \\ \sigma_c & -\theta & 0 & 0 & 0 & 0 & 0 \\ \tau_1 & \tau_2 & -\phi & 0 & 0 & 0 & 0 \\ 0 & \gamma_m & 0 & -\delta_m & 0 & 0 & 0 \\ 0 & 0 & 0 & \frac{\beta_s \Lambda_s}{\psi} & -\omega & 0 & 0 \\ 0 & 0 & 0 & 0 & \sigma_s & -\psi & 0 \\ 0 & 0 & 0 & 0 & 0 & \gamma_p & -\delta_p \end{pmatrix},$$

$$\hat{T}(U,V) = \begin{pmatrix} \beta_c P(\frac{\Lambda_c}{\delta_c} - S_C) \\ 0 \\ 0 \\ 0 \\ \beta_s M(\frac{\Lambda_s}{\psi} - S_S) \\ 0 \\ 0 \end{pmatrix}.$$

Thus, $\hat{T}(U,V) \geq 0,\ \forall (U,V) \in \mathscr{D}$ for $S_C \leq \frac{\Lambda_c}{\delta_c}$ and $S_S \leq \frac{\Lambda_s}{\psi}$. Furthermore, the non-negativity of the off-diagonal entries implies that B is an M-matrix. This also suggests that condition C2 is satisfied. Therefore, the disease-free equilibrium is globally asymptotically stable whenever $R_0 < 1$. □

5.3.6 Endemic Equilibrium Point and its Stability

Existence of Endemic Equilibrium Point

After computation, the model has an endemic equilibrium point E_e^* given by

$$E_e^* = \left(S_C^*, E_C^*, T_C^*, I_C^*, M^*, S_S^*, E_S^*, I_S^*, P^*\right),$$

where the components are expressed in terms of the steady state of I_C^* and given by the following equations,

$$\begin{cases} M^* = \dfrac{\gamma_m}{\delta_m} I_C^*, \\ S_S^* = \dfrac{\delta_m \Lambda_s}{\beta_s \gamma_m I_C^* + \psi \delta_m}, \\ E_S^* = \dfrac{I_C^* \beta_s \gamma_m \Lambda_s}{\omega(\beta_s \gamma_m I_C^* + \psi \delta_m)}, \\ I_S^* = \dfrac{\sigma_s I_C^* \beta_s \gamma_m \Lambda_s}{\psi\omega(\beta_s \gamma_m I_C^* + \psi \delta_m)}, \\ P^* = \dfrac{\gamma_p \sigma_s I_C^* \beta_s \gamma_m \Lambda_s}{\psi\omega\delta_p(\beta_s \gamma_m I_C^* + \psi \delta_m)}, \\ E_C^* = \dfrac{\theta}{\sigma_c} I_C^*, \\ T_C^* = \left(\dfrac{\theta\tau_1 + \sigma_c\tau_2}{\phi\sigma_c}\right) I_C^*, \\ S_C^* = \dfrac{\eta\theta\omega\psi\delta_p\left(I_C^*\beta_s\gamma_m + \psi\delta_m\right)}{\beta_c\beta_s\gamma_m\gamma_p\Lambda_s\sigma_c\sigma_s}, \\ I_C^* = \dfrac{\eta\theta\phi\psi^2\omega\delta_c\delta_m\delta_p\left(R_0^2 - 1\right)}{\beta_s\gamma_m(\eta\theta\phi\psi\omega\delta_c\delta_p + \beta_c\gamma_p\Lambda_s\sigma_s(\eta\theta\phi - (\theta\rho\tau_1 + \rho\sigma_c\tau_2)))}, \end{cases} \tag{5.30}$$

such that, $\eta\theta\phi - (\theta\rho\tau_1 + \rho\sigma_c\tau_2) = (d_c + \delta_c)\left(\left(\delta_c + \rho\right)(\delta_c + \sigma_c) + \tau_1\delta_c\right) + \tau_2\delta_c\left(\delta_c + \sigma_c + \rho + \tau_1\right) > 0$. Therefore, if the effective reproduction number, $R_0 > 1$, it can be seen that $S_C^* > 0$, $E_C^* > 0$, $I_C^* > 0$, $T_C^* > 0$, $M^* > 0$, $S_S^* > 0$, $I_S^* > 0$ and $P^* > 0$. This shows that the disease becomes endemic when $R_0 > 1$.

Global Stability of Endemic Equilibrium Point

Theorem 5.6. *The endemic equilibrium is globally asymptotically stable if* $R_0 > 1$.

Proof. We use the Lyapunov method with a Volterra-Lyapunov stable matrix. We define a Lyapunov function defined as follows:

$$\begin{aligned} L = \frac{1}{2}[&k_1(S_C - S_C^*)^2 + k_2(E_C - E_C^*)^2 + k_3(I_C - I_C^*)^2 + k_4(T_C - T_C^*)^2 \\ &+ k_5(M - M^*)^2 + k_6(S_S - S_S^*)^2 + k_7(E_S - E_S^*)^2 + k_8(I_S - I_S^*)^2 + k_9(P - P^*)^2], \end{aligned} \tag{5.31}$$

where each k_i, $i = 1,2,...,9$, is a positive constant. We compute the time derivative of L along the trajectories of system (5.1) and obtain:

$$\begin{aligned} \frac{dL}{dt} = &k_1(S_C - S_C^*)\frac{dS_C}{dt} + k_2(E_C - E_C^*)\frac{dE_C}{dt} + k_3(I_C - I_C^*)\frac{dI_C}{dt} \\ &+ k_4(T_C - T_C^*)\frac{dT_C}{dt} + k_5(M - M^*)\frac{dM}{dt} + k_6(S_S - S_S^*)\frac{dS_S}{dt} \\ &+ k_7(E_S - E_S^*)\frac{dE_S}{dt} + k_8(I_S - I_S^*)\frac{dI_S}{dt} + k_9(P - P^*)\frac{dP}{dt}. \end{aligned} \tag{5.32}$$

After mathematical calculations and simplifications, equation (5.32) is written as

$$\frac{dL}{dt} = X(DA + A^T D)X^T, \tag{5.33}$$

where $X = (S_C - S_C^*, E_C - E_C^*, I_C - I_C^*, T_C - T_C^*, M - M^*, S_S - S_S^*, E_S - E_S^*, I_S - I_S^*, P - P^*)$, $D = diag(k_1, k_2, ..., k_9)$ and

$$A = \begin{pmatrix} -P^*\beta_c - \delta_c & 0 & 0 & \rho & 0 & 0 & 0 & 0 & -S_C^*\beta_c \\ P^*\beta_c & -\eta & 0 & 0 & 0 & 0 & 0 & 0 & S_C^*\beta_c \\ 0 & \sigma_c & -\theta & 0 & 0 & 0 & 0 & 0 & 0 \\ 0 & \tau_1 & \tau_2 & -\phi & 0 & 0 & 0 & 0 & 0 \\ 0 & 0 & \gamma_m & 0 & -\delta_m & 0 & 0 & 0 & 0 \\ 0 & 0 & 0 & 0 & -S_S^*\beta_s & -\psi - M^*\beta_s & 0 & 0 & 0 \\ 0 & 0 & 0 & 0 & S_S^*\beta_s & M^*\beta_s & -\omega & 0 & 0 \\ 0 & 0 & 0 & 0 & 0 & 0 & \sigma_s & -\psi & 0 \\ 0 & 0 & 0 & 0 & 0 & 0 & 0 & \gamma_p & -\delta_p \end{pmatrix}. \tag{5.34}$$

Theorem 5.7. *The matrix A in (5.34) is Volterra–Lyapunov stable.*

Proof. To verify this, we claim and demonstrate that the matrix, $C = -A$ in equation (5.35), is diagonally stable, which confirms the Volterra-Lyapunov stability of the matrix A.

$$C = \begin{pmatrix} P^*\beta_c+\delta_c & 0 & 0 & -\rho & 0 & 0 & 0 & 0 & S_C^*\beta_c \\ -P^*\beta_c & \eta & 0 & 0 & 0 & 0 & 0 & 0 & -S_C^*\beta_c \\ 0 & -\sigma_c & \theta & 0 & 0 & 0 & 0 & 0 & 0 \\ 0 & -\tau_1 & -\tau_2 & \phi & 0 & 0 & 0 & 0 & 0 \\ 0 & 0 & -\gamma_m & 0 & \delta_m & 0 & 0 & 0 & 0 \\ 0 & 0 & 0 & 0 & S_S^*\beta_s & \psi+M^*\beta_s & 0 & 0 & 0 \\ 0 & 0 & 0 & 0 & -S_S^*\beta_s & -M^*\beta_s & \omega & 0 & 0 \\ 0 & 0 & 0 & 0 & 0 & 0 & -\sigma_s & \psi & 0 \\ 0 & 0 & 0 & 0 & 0 & 0 & 0 & -\gamma_p & \delta_p \end{pmatrix} \tag{5.35}$$

Lemma 5.8. *The matrix C described in Equation (5.35) is diagonally stable.*

Proof. The principal minors of C can be easily examined and all are positive. By Lemma 3.12, there exists a 9×9 diagonal matrix D such that DC has simple and positive eigenvalues. Since all eigenvalues of DC are positive , it can be concluded that DC is positive definite. Thus, there must be a nonzero vector x for which $x^TDCx > 0$. Therefore, by Lemma 3.13, the matrix C is Lyapunov diagonally stable.

If a matrix C is diagonally stable, it means that, according to Definition 3.10, a positive diagonal matrix D exists such that $DC + C^TD^T > 0$. Furthermore, replacing C with $-A$ leads to the conclusion that $DA + A^TD^T < 0$, thus establishing the Volterra-Lyapunov stability of A, as defined in Definition 3.11. □

In summary, based on previous discussions, if $R_0 > 1$, the endemic equilibrium point E_e^* of the model (5.1) is globally asymptotically stable.

5.3.7 Bifurcation Analysis

In a dynamical system, a bifurcation occurs when the value of a parameter in the system changes, causing rapid qualitative changes in its behaviour (McCann 2013). Bifurcation analysis can be used to analyze qualitative changes in steady-state solutions (Sharma et al. 2015). A stable equilibrium point loses stability as a parameter

is changed in a forward bifurcation, resulting in the formation of two new equilibrium points, one stable and the other unstable.

Theorem 5.9. *The model (5.1) has a forward bifurcation at* $R_0 = 1$ *and the endemic equilibrium is locally stable when* $R_0 > 1$.

Proof. To prove this theorem, we use the centre-manifold theorem. In model (5.1), the following variable modifications are applied for calculation purposes: $S_C = y_1, E_C = y_2, I_C = y_3, T_C = y_4, M = y_5, S_S = y_6, E_S = y_7, I_S = y_8$ and $P = y_9$. Thus, the model (5.1) becomes

$$\begin{cases} \frac{dy_1}{dt} = \Lambda_c - \beta_c y_1 y_9 - \delta_c y_1 + \rho y_4 := h_1, \\ \frac{dy_2}{dt} = \beta_c y_1 y_9 - \eta y_2 := h_2, \\ \frac{dy_3}{dt} = \sigma_c y_2 - \theta y_3 := h_3, \\ \frac{dy_4}{dt} = \tau_1 y_2 + \tau_2 y_3 - \phi y_4 := h_4, \\ \frac{dy_5}{dt} = \gamma_m y_3 - \delta_m y_5 := h_5, \\ \frac{dy_6}{dt} = \Lambda_s - \beta_s y_6 y_5 - \psi y_6 := h_6, \\ \frac{dy_7}{dt} = \beta_s y_6 y_5 - \omega y_7 := h_7, \\ \frac{dy_8}{dt} = \sigma_s y_7 - \psi y_8 := h_8, \\ \frac{dy_9}{dt} = \gamma_p y_8 - \delta_p y_9 := h_9. \end{cases} \tag{5.36}$$

With these modified variables, the disease-free equilibrium of (5.36) is $(y_1, y_2, y_3, y_4, y_5, y_6, y_7, y_8, y_9) = (\frac{\Lambda_c}{\delta_c}, 0, 0, 0, 0, \frac{\Lambda_s}{\psi}, 0, 0, 0)$. Let $\nu = \beta_c^*$ be the bifurcation parameter in $R_0 = 1$ (5.3.4). Solving for this the bifurcating parameter provides,

$$\nu = \beta_c^* = \frac{\eta\theta\psi^2\omega\delta_c\delta_m\delta_p}{\Lambda_c\Lambda_s\beta_s\gamma_m\gamma_p\sigma_c\sigma_s}. \tag{5.37}$$

The Jacobian matrix for equation (5.36) at the disease-free equilibrium when $\nu =$

β_c^* becomes,

$$J_v(E_0) = \begin{pmatrix} -\delta_c & 0 & 0 & \rho & 0 & 0 & 0 & 0 & -\frac{\nu\Lambda_c}{\delta_c} \\ 0 & -\eta & 0 & 0 & 0 & 0 & 0 & 0 & \frac{\nu\Lambda_c}{\delta_c} \\ 0 & \sigma_c & -\theta & 0 & 0 & 0 & 0 & 0 & 0 \\ 0 & \tau_1 & \tau_2 & -\phi & 0 & 0 & 0 & 0 & 0 \\ 0 & 0 & -\gamma_m & 0 & \delta_m & 0 & 0 & 0 & 0 \\ 0 & 0 & 0 & 0 & -\frac{\beta_s\Lambda_s}{\psi} & -\psi & 0 & 0 & 0 \\ 0 & 0 & 0 & 0 & \frac{\beta_s\Lambda_s}{\psi} & 0 & -\omega & 0 & 0 \\ 0 & 0 & 0 & 0 & 0 & 0 & \sigma_s & -\psi & 0 \\ 0 & 0 & 0 & 0 & 0 & 0 & 0 & \gamma_p & -\delta_p \end{pmatrix}. \tag{5.38}$$

The eigenvalues of J_v are 0, $-\delta_c$, $-\phi$, $-\psi$ and the remaining eigenvalues are the solutions of the following equation.

$$\begin{aligned}&(\eta+x)(\theta+x)(\omega+x)(\psi+x)(x+\delta_p)+\delta_m((\eta+x)(\theta+x)(\omega+x)(\psi+x)\\&+((\theta+x)(\omega+x)(\psi+x)+\eta((\omega+x)(\psi+x)+\theta(\omega+\psi+x)))\delta_p)=0.\end{aligned} \tag{5.39}$$

Expanding equation (5.39) would give a polynomial equation of five degrees with positive coefficients. Thus, J_v has simple zero eigenvalues, with all remaining eigenvalues having negative real components by Routh-Hurwitz criterion. As a result, the centre manifold theory can be used to examine the behavior of the model.

Consider $z = (z_1, z_2, z_3, z_4, z_5, z_6, z_7, z_8, z_9)$ to be a left eigenvector of J_v. Its is obtained by multiplying z by J_v and equating it to 0. So after evaluation, the left eigenvector becomes

$$z = (0, \frac{z_9\beta_s\gamma_m\gamma_p\Lambda_s\sigma_c\sigma_s}{\eta\theta\psi^2\omega\delta_m}, \frac{z_9\beta_s\gamma_m\gamma_p\Lambda_s\sigma_s}{\theta\psi^2\omega\delta_m}, 0, \frac{z_9\beta_s\gamma_p\Lambda_s\sigma_s}{\psi^2\omega\delta_m}, 0, \frac{z_9\gamma_p\sigma_s}{\omega\psi}, \frac{z_9\gamma_p}{\psi}, z_9).$$

Let $w = (w_1, w_2, w_3, w_4, w_5, w_6, w_7, w_8, w_9)$ be the right eigenvector of J_v. Similarly, the right eigenvector is obtained by multiplying J_v by w and equating it with 0. After

computation, the components of the right eigenvector w are given by

$$\begin{cases} w_1 = -\dfrac{\psi^2\omega w_9\delta_m\delta_p(\eta\theta\phi - \eta\rho\tau_1 - \rho\sigma_c\tau_2)}{\phi\beta_s\gamma_m\gamma_p\delta_c\Lambda_s\sigma_c\sigma_s}, \\ w_2 = \dfrac{\psi^2\omega w_9\delta_m\delta_p}{\beta_s\gamma_m\gamma_p\Lambda_s\sigma_c\sigma_s}, \\ w_3 = \dfrac{\psi^2\omega w_9\delta_m\delta_p}{\beta_s\gamma_m\gamma_p\Lambda_s\sigma_s}, \\ w_4 = \dfrac{\psi^2\omega w_9\delta_m\delta_p(\theta\tau_1 + \sigma_c\tau_2)}{\phi\beta_s\gamma_m\gamma_p\Lambda_s\sigma_c\sigma_s}, \\ w_5 = \dfrac{\psi^2\omega w_9\delta_p}{\beta_s\gamma_p\Lambda_s\sigma_s}, \\ w_6 = -\dfrac{\omega w_9\delta_p}{\gamma_p\sigma_s}, \\ w_7 = \dfrac{\psi w_9\delta_p}{\gamma_p\sigma_s}, \\ w_8 = \dfrac{w_9\delta_p}{\gamma_p}, \\ w_9 = w_9. \end{cases} \tag{5.40}$$

The functions $h_1 = \Lambda_c - \beta_c y_1 y_9 - \delta_c y_1 + \rho y_4$, $h_2 = \beta_c y_1 y_9 - \eta y_2$, $h_6 = \Lambda_s - \beta_s y_6 y_5 - \psi y_6$ and $h_7 = \beta_s y_6 y_5 - \omega y_7$ have the following non-zero partial derivatives at the disease-free equilibrium,

$\frac{\partial^2 h_1(E_0)}{\partial y_1 \partial y_9} = -\beta_c$, $\frac{\partial^2 h_2(E_0)}{\partial y_1 \partial y_9} = \beta_c$, $\frac{\partial^2 h_6(E_0)}{\partial y_6 \partial y_5} = -\beta_s$ and $\frac{\partial^2 h_7(E_0)}{\partial y_6 \partial y_5} = \beta_s$.

Suppose a and b are the standard form coefficients describing the system dynamics in the centre manifold theorem. Using the centre manifold theorem, after some computations, the bifurcation coefficients are given by

$$a = w_9^2 z_9 \delta_p \left(\frac{\omega\psi\delta_p}{\gamma_p\Lambda_s\sigma_s} + \frac{\beta_c(\eta\theta\phi - \theta\rho\tau_1 - \rho\sigma_c\tau_2)}{\eta\theta\phi\delta_c}\right),$$
$$b = w_9 z_9 \left(\frac{\delta_p}{\beta_s} + \frac{\beta_s\gamma_m\gamma_p\Lambda_c\Lambda_s\sigma_c\sigma_s}{\eta\theta\psi^2\omega\delta_c\delta_m}\right),$$

where, $\eta\theta - \phi\rho\tau_1 - \rho\sigma_c\tau_2 = (d_c + \delta_c)[(\rho + \delta_c)(\delta_c + \sigma_c) + \delta_c\tau_1] + \delta_c\tau_2(\rho + \delta_c + \sigma_c + \tau_1) > 0$.

Thus, $a < 0$ and $b > 0$ for $z_9 > 0$ and $w_9 > 0$ and hence a forward bifurcation occurs at $R_0 = 1$ by the Theorem B.12. □

Furthermore, the presence of a forward bifurcation ensures that the endemic equilibrium is locally stable for $R_0 > 1$ (Madubueze et al. 2022).

5.4 Sensitivity Analysis

The normalized forward sensitivity index method (3.36) is used to calculate the sensitivity indices of the model parameters. The results given in Table 5.2 and Figure 5.2 indicate that specific parameters, including recruitment rates, miracidia and metacercariae production rates and incidence rates of cattle and snails, directly influence the value of R_0. These parameters, specifically related to the transmission rates and the production of miracidia and metacercariae by cattle and snails, are biologically important in determining the severity of *F. hepatica* in cattle.

The findings also indicate that the mortality rates of miracidia, metacercaria and snail populations and the treatment rate of exposed and infected cattle indirectly influence the effective reproduction number. Moreover, it shows that the use of molluscicide (κ) is the most sensitive parameter, which can reduce disease transmission. Stakeholders play an important role in reducing the spread of *F. hepatica* disease by implementing a range of preventive measures and improving the values of these parameters. Specific parameters with a positive index must be decreased. Keeping the other parameters constant will decrease the value of R_0 and ultimately contribute to the eradication of the disease.

Similarly, increasing the value of parameters with a negative index while keeping all other parameters constant will reduce the value of R_0 and contribute to the eradication of *F. hepatica* disease. If the incidence rate of cattle diseases increases by 10%, it will cause an increase of 5% in R_0. Similarly, if the use of molluscicide is increased by 10%, it will decrease R_0 by 10.706%.

5.5 Numerical Simulations

This section presents a numerical simulation of the *Fasciola hepatica* model to characterize its quantitative and qualitative dynamics. Table 5.1 summarizes the parameters used for numerical simulation in the model. Most of these parameter values have been sourced from previous studies, while some have been estimated or assumed.

Table 5.2: Sensitivity indices of model (5.1).

Parameter	Sensitivity indices
κ	-1.0706
δ_c	-0.5018
δ_m	-0.5
δ_p	-0.5
τ_2	-0.4975
τ_1	-0.4250
δ_s	-0.0715
d_c	-0.0021
Λ_c	+0.5
Λ_s	+0.5
β_s	+0.5
β_c	+0.5
γ_s	+0.5
γ_c	+0.5

5.5.1 Contour Plots of (R_0) as a Function of Key Model Parameters

Figures 5.3a–5.3d present contour plots of the effective reproduction number (R_0) as a function of key model parameters. Figures 5.3a and 5.3b show R_0 against the treatment rates for exposed cattle (τ_1) and infected cattle (τ_2) under two fixed molluscicide application rates: $\kappa = 0.025$ and $\kappa = 0.045$, respectively. In both figures, R_0 decreases monotonically with increasing values of τ_1 and τ_2, demonstrating that higher treatment intensity reduces transmission potential. Comparing the two figures, the contours for $\kappa = 0.045$ are shifted toward lower R_0 values relative to those for $\kappa = 0.025$, indicating that combining treatment with molluscicide application has a synergistic effect on suppressing R_0.

Figure 5.3c displays the dependence of R_0 on the parasite contact rates from susceptible to exposed cattle (β_c) and snails (β_s). Here, R_0 increases with both β_c and

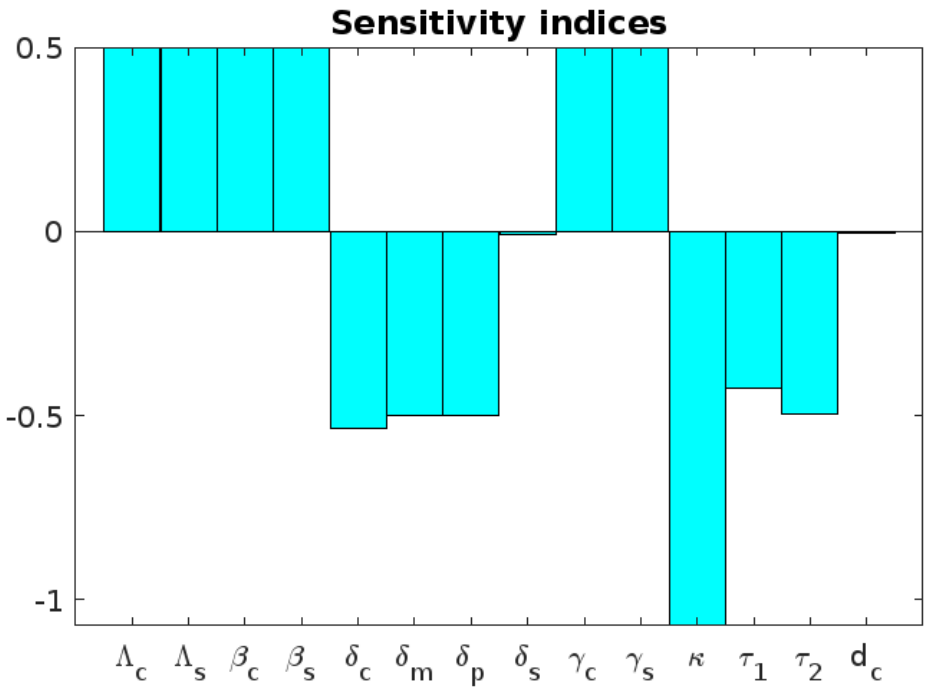

Figure 5.2: Sensitivity indices for model 5.1.

β_s, confirming that higher host parasite contact rates elevate the risk of outbreak persistence. Figure 5.3d illustrates the relationship between $\mathscr{R}_e$ and the progression rates from exposed to infected cattle (σ_c) and snails (σ_s). Similarly, R_0 rises with increasing σ_c and σ_s, indicating that faster progression through exposed stages enhances overall transmission.

5.5.2 Forward Bifurcation Behaviour

Figure 5.4 shows that the model (5.1) has a forward bifurcation at $R_0 = 1$. This bifurcation describes a scenario in which the equilibrium point changes its stability as the parameter R_0 increases through one. This phenomenon involves the effective reproduction number is one. If the effective reproduction number satisfies $R_0 < 1$, then the disease-free equilibrium (DFE) is locally asymptotically stable, and the infection will eventually be eliminated from the population. In contrast, when the effective reproduction number is greater than one, the disease-free equilibrium becomes unstable and a stable endemic equilibrium emerges, indicating that the disease persists. Epidemiologically, in models that exhibit forward bifurcation, it is essential to

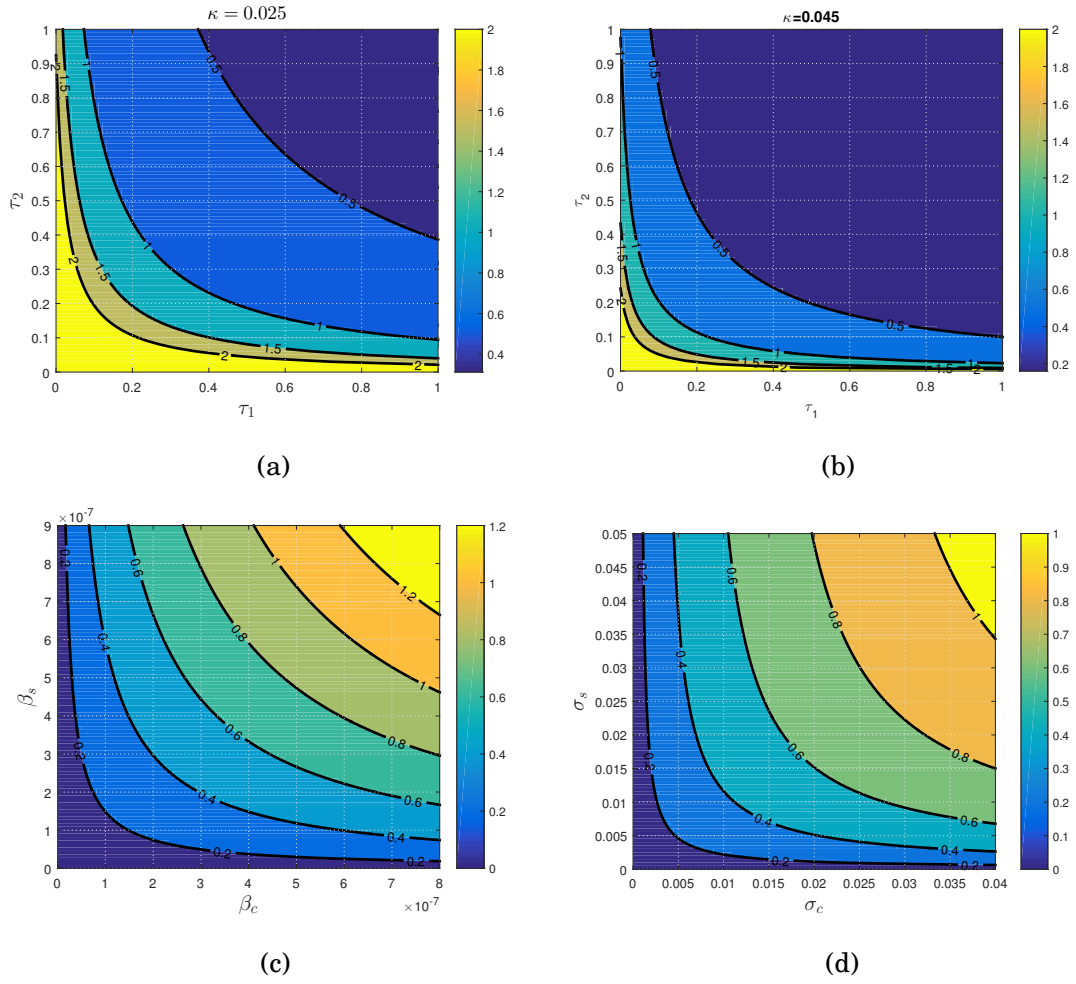

Figure 5.3: Contour plots of R_0 as a function of the combinations: (a) τ_1 and τ_2 for $\kappa = 0.025$, (b) τ_1 and τ_2 for $\kappa = 0.045$, (c) β_c and β_s, and (d) σ_c and σ_s.

maintain the value of R_0 below 1 to achieve disease elimination (Gumel 2012). This bifurcation guarantees that an endemic equilibrium is locally asymptotically stable whenever $R_0 > 1$ (Madubueze et al. 2022), as shown in Figure 5.5b.

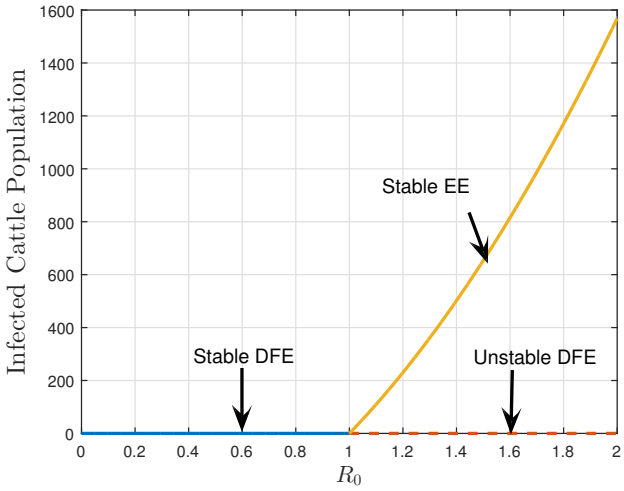

Figure 5.4: Forward bifurcation diagram for model 5.1.

5.5.3 Verifying the Stability of Disease-Free Equilibrium Numerically

Simulations have been conducted to observe the evolution of snail and cattle populations, using the initial conditions given $[(S_C(0), E_C(0), I_C(0), T_C(0), M(0), S_S(0), E_S(0), I_S(0), P(0)) = (1000, 400, 800, 600, 6500, 1000000, 10000, 300000, 1200000)]$. For the parameter values listed in Table 5.1, the reproduction number will be $R_0 = 0.921628$. As a result, the system described in equation (5.1) will possess a disease-free equilibrium point given by $E_0 = (131148, 0, 0, 0, 0, 112596, 0, 0, 0)$, which is an asymptotically stable equilibrium point.

Figure 5.5a indicates that all solution trajectories in the model tend to converge towards the disease-free equilibrium (DFE) as time progresses. This observation suggests that the DFE is locally asymptotically stable, implying that small perturbations or deviations from the equilibrium point will eventually return to the disease-free state. In Figure 5.6, it can be seen that the equilibrium number of infected cattle decreases to zero over time for different initial conditions. This result shows that the

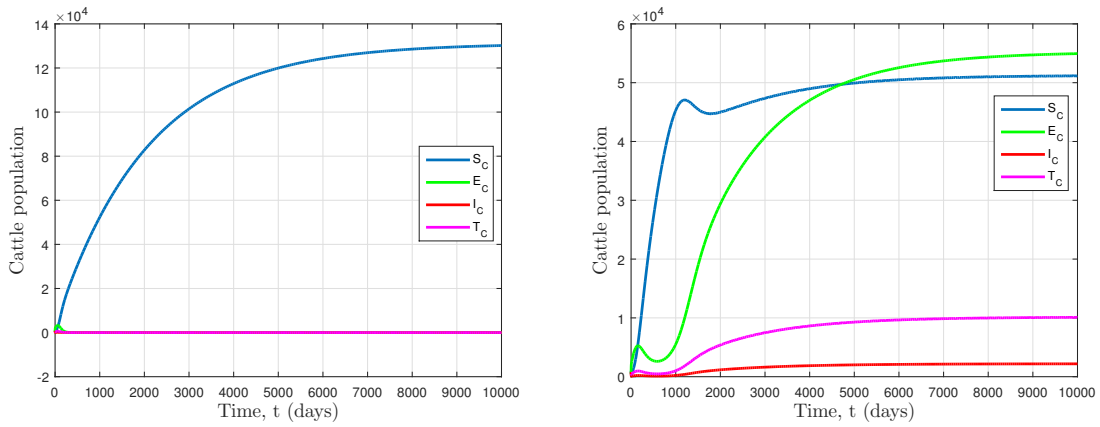

(a) when $R_0 < 1$ (b) when $R_0 > 1$

Figure 5.5: Time series evolution of cattle populations.

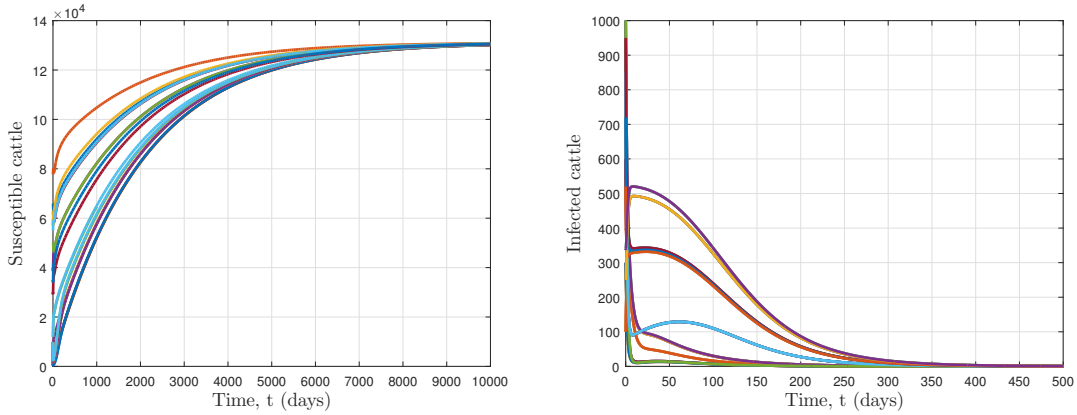

Figure 5.6: The global stability behaviour of the disease-free equilibrium point for various randomly selected initial conditions.

DFE is globally asymptotically stable. Moreover, biologically it shows that the *Fasciola hepatica* disease will eventually be eliminated in cattle, while the population of susceptible cattle will reach their maximum value.

Elimination of *Fasciola hepatica* in cattle requires maintaining the reproduction number, R_0, below 1. This requires interventions such as snail control and treatment to reduce infected cattle and accelerate eradication.

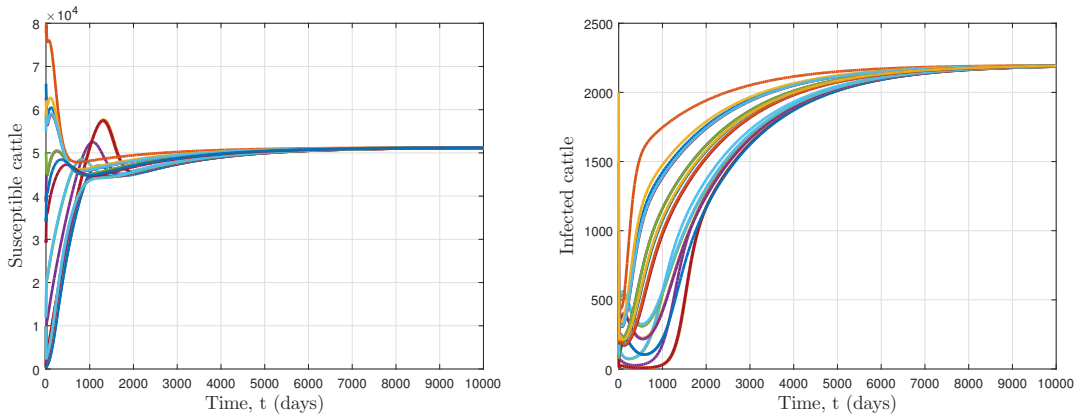

Figure 5.7: The global stability behaviour of the endemic equilibrium point for various randomly selected initial conditions.

5.5.4 Verifying Stability of Endemic Equilibrium Point Numerically

From 0.025 to 0.015, a reduction in the use of molluscicides would result in an increase in the reproduction number to $R_0 = 1.0706$. In addition, using the other values of the parameters listed in Table 5.1 would result in the occurrence of the endemic equilibrium,

$$E_e^* = (S_C^*, E_C^*, I_C^*, T_C^*, M^*, S_S^*, E_S^*, I_S^*, P*)$$

$$= (51236.9, 55224.2, 2198.05, 10146.8, 16998.3, 146747, 14124.1, 59005.6, 237778).$$

Figure 5.5b depicts the numerical simulation of the model (5.1) in endemic equilibrium under the initial conditions described in Section 5.5.3. All solutions approach the estimated value of the endemic equilibrium, E_e^*.

Figure 5.7 demonstrates the phase diagram of the cattle populations with different initial conditions. This figure shows that the endemic equilibrium point, E_e^*, is globally asymptotically stable. Moreover, regardless of the initial conditions, all solutions converge to the endemic equilibrium point. The global stability of this endemic equilibrium in epidemiology refers to the long-term behaviour of the *F. hepatica* disease that persists in the cattle population without dying out or growing uncontrollably. This means that once the hepatica disease reaches a certain prevalence level, the disease would continue indefinitely in the population.

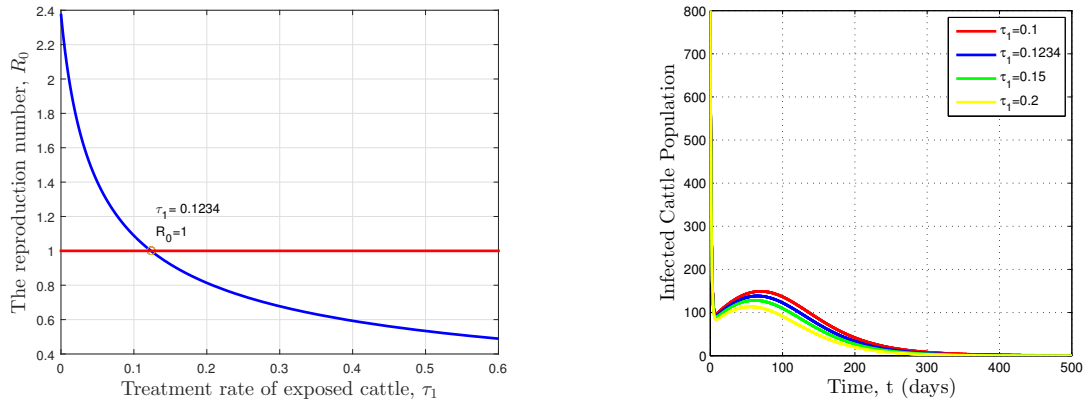

Figure 5.8: Effect of exposed cattle treatment on reproduction number and infected cattle.

5.5.5 Treatment and Molluscicide Effects on R_0 and Infected Cattle

Effects of treatments ***(τ_1 and τ_2)***: Based on the parameter values provided in Table 5.1, we can establish the correlation between the reproduction number (R_0) and the treatment rates (τ_1 and τ_2) given by $R_0 = \frac{0.38718}{\sqrt{0.026488+\tau_1}}$ and $R_0 = \frac{0.744883}{\sqrt{0.003228+\tau_2}}$. Figures 5.8 and 5.9 demonstrate the influence of treatment rates on disease propagation. It is observed that as treatment rates increase, both the reproduction number (R_0) and the infected cattle population decrease. Better treatment practices can reduce the number of infected cattle when treatment rates are down, specifically when $\tau_1 < 0.1234$ or $\tau_2 < 0.5516$, the value of R_0 is greater than 1, indicating that the infection will remain endemic. However, increasing treatment rates reduces the incidence of disease. Figure 5.10a illustrates that the number of infected cattle can be significantly reduced in a short period by improving treatments for the populations of exposed and infected cattle.

Molluscicide Effects: On the basis of equation (5.3.4), the relation between the use of mollucicide (κ) and the reproduction number is given by $R_0 = \frac{0.00710187}{(0.001644+\kappa)\sqrt{0.058644+\kappa}}$. Figure 5.11 illustrates the use of molluscicide to influence the reproduction number and the population of infected cattle. It shows that when the snail removal rate by the molluscicide intervention increases, both the number of infected cattle and the reproduction number decrease. Moreover, Figure 5.11 indicates a significant increase

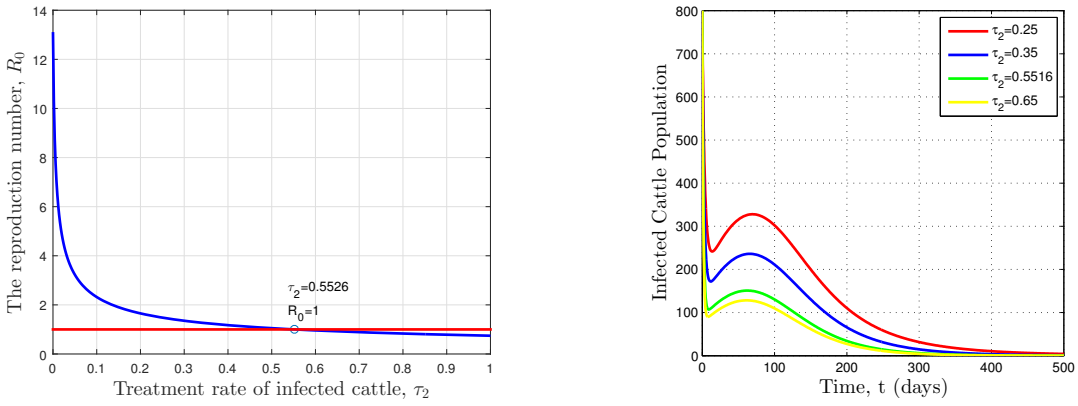

Figure 5.9: Effect of treatment on reproduction number and infected cattle.

in infected cattle within a short period, but it is reduced over longer time intervals. It ensured that the effectiveness of molluscicides in the control of *Fasciola* snails depends on several factors, such as the specific chemical used, the dose of application, the time, the environmental conditions and the susceptibility of the snail population (Rizwan et al. 2022).

Furthermore, the long-term effectiveness of molluscicide can be based on integrated approaches that involve combining it with other control measures. These measures can include treatment options, strategic deworming of cattle, pasture management practices and biological control methods (Maqbool et al. 2017). In Figure 5.10b, combination treatments with the molluscicide intervention improve long-term effectiveness in controlling *F. hepatica* disease. Thus, it is imperative to improve efforts to reduce the snail population and boost treatments, thus eradicating the disease in cattle.

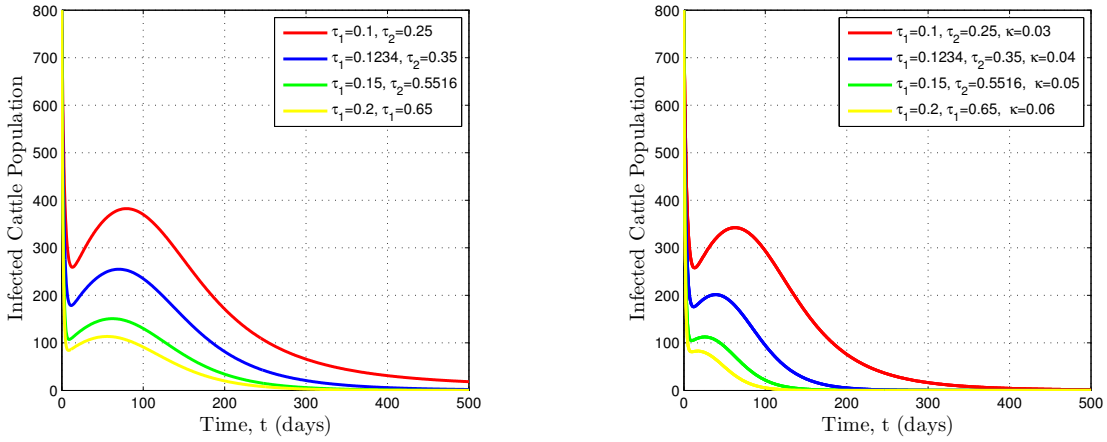

Figure 5.10: Infected cattle populations for (a) the impact of administering treatments to both exposed and infected cattle, and (b) the impact of administering treatments and molluscicide.

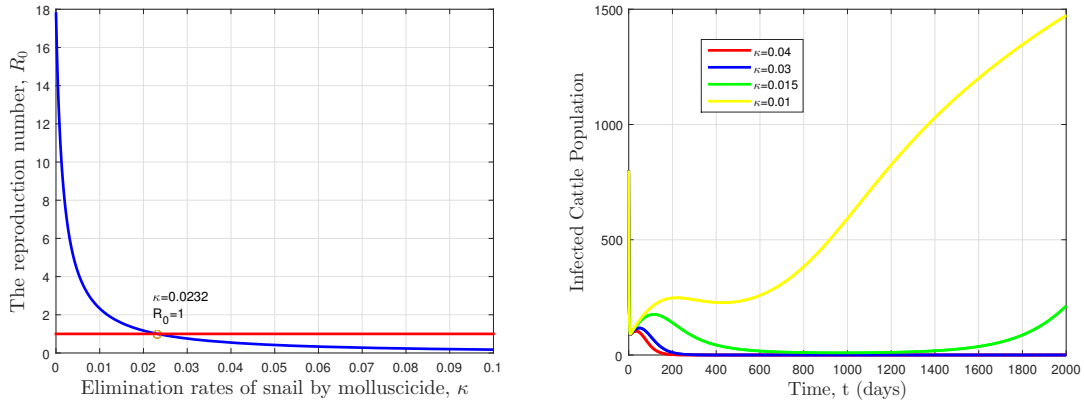

Figure 5.11: Effect of molluscicide on reproduction number and infected cattle.

5.6 Conclusion

This chapter developed and analyzed a deterministic compartmental model to understand the transmission dynamics of *F. hepatica*. In the model, both exposed and infected cattle populations receive treatment. When the effective reproduction number, R_0, is less than 1, the model has a disease-free equilibrium point that is asymptotically stable both locally and globally. The global asymptotically stable state of the endemic equilibrium is investigated using the Volterra-Lyapunov method. The model exhibits a forward bifurcation. It occurs when a disease transmission system undergoes a qualitative change, leading to the coexistence of disease-free and endemic states. It suggests that even in the absence of external factors, the disease can transition from a state of low or no transmission to a state of sustained and epidemic-level transmission.

The sensitivity analysis is conducted using the normalized sensitivity index and the results indicate that the transmission rates for snail and cattle populations, as well as the rates at which miracidia and metacercariae are shed, have the most significant direct influence on the spread of the disease. It shows that the most sensitive parameter to reduce disease transmission or reproduction number is the use of molluscicide (κ). Preventing the growth and development of the parasite can be achieved by eliminating the snail or destroying the stages of *Fasciola* larvae within the snail (Ayele & Hiko 2016). The contour plots suggest that improving the use of molluscicide and integrating it with the treatments of exposed and infected cattle reduces the transmission of the disease. This finding aligns with the result mentioned in (Yadav 2015), which suggests that the use of molluscicides to control the population of snail vectors is an innovative and highly efficient approach in integrated vector management strategies. It shows that the use of molluscicides effectively reduces snail populations by disrupting the life cycle of *F. hepatica* and lowering infection rates in cattle that graze in contaminated vegetation.

The simulation results also show that elimination of snail populations using molluscicide and improving treatments for exposed and infected cattle significantly de-

crease the prevalence of *F. hepatica* disease in the cattle population. Therefore, stakeholders should focus on applying an adequate combination of molluscicide use and treatment implementation in the management of the disease.

Chapter 6

6 Analyzing Human-Cattle Dynamics for Effective *Fasciola Hepatica* Management

6.1 Introduction

Fasciola hepatica, poses a health risk to humans and livestock. Treatment relies on anthelmintics like triclabendazole (Kelley et al. 2016), while prevention involves sanitation, safe water, proper food preparation and livestock deworming. Mass drug administration is used in endemic regions (Mollinedo et al. 2019). Research efforts are focused on epidemiology, host-parasite interactions, diagnostics, treatment and vaccine development (Webb & Cabada 2018). This chapter presents a model to assess disease spread, control strategies and intervention impacts, informing optimized control measures for *Fasciola hepatica* transmission between cattle and humans. This research models transmission dynamics and evaluates anthelmintic treatment, health education and snail control interventions to manage the disease and minimize its impact.

6.2 Model Formulation

The model focuses on the spread of *Fasciola hepatica* disease among cattle and human populations. This model employs a series of differential equations to describe the transmission dynamics of the disease. The model considers populations of humans, cattle, snails and the larval stages (miracidia and metacercariae) of the *Fasciola* parasite. It divides the human, cattle and snail populations into susceptible and infected categories. Table 6.1 details the nine variables used to represent this dynamic system.

Incidence rates are critical in the mathematical modeling of disease (Shao & Shateyi 2021, Xiao & Ruan 2007). Although bilinear rates are common in epidemiological models, they become impractical with large susceptible populations. Furthermore, high contact rates between infected and susceptible individuals result in a nonlinear incidence (Kuddus & Rahman 2021). Therefore, we model disease transmission in cattle and humans using linear (βI) and nonlinear ($\frac{\beta I}{1+\alpha I}$) incidence rates, respectively. The saturated incidence rate, $\frac{\beta I}{1+\alpha I}$, approaches a saturation point at high values of I. Here, βI represents the force of infection in a fully susceptible population and $\frac{\beta I}{1+\alpha I}$ accounts for the inhibitory effect of behavioral changes among susceptible individuals. Introducing a non-linear incidence rate is therefore justified, as crowding within the infected population can saturate influential contacts between infected and susceptible individuals at high levels. The transmission diagram for *F. hepatica* is shown in Figure 6.1. Table 6.2 gives all values along with a biological description of all parameters in the system.

Table 6.1: Description of the model variables.

Variables	Description
$S_C(t)$	Number of susceptible cattle at time t
$I_C(t)$	Number of infected cattle at time t
$S_H(t)$	Number of susceptible humans at time t
$I_H(t)$	Number of infected humans at time t
$S_S(t)$	Number of susceptible snails at time t
$I_S(t)$	Number of infected snails at time t
$M(t)$	Number of mercidia at time t
$P(t)$	Number of metacercariae at time t

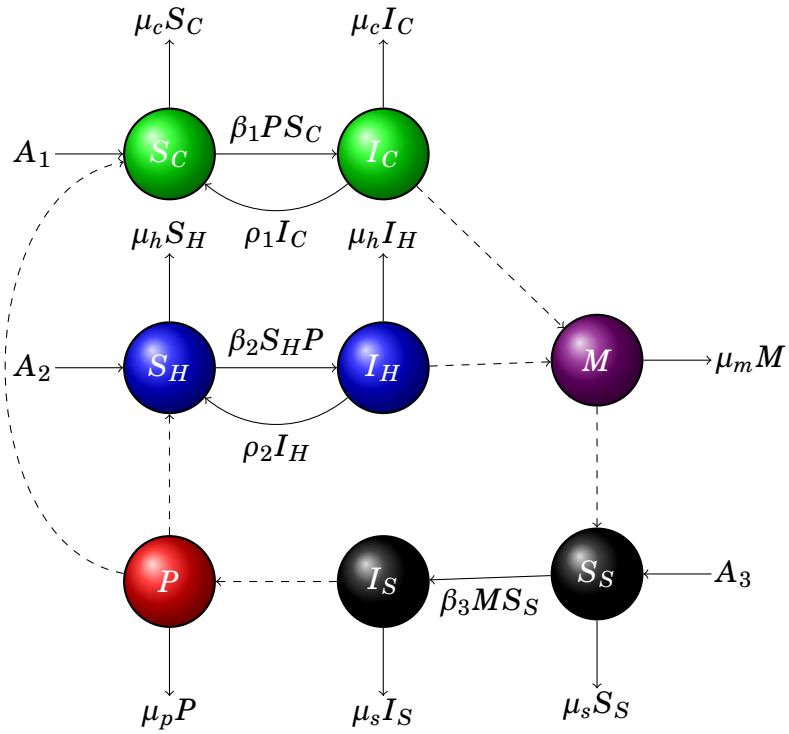

Figure 6.1: Transfer diagram for *Fasciola hepatica* disease model (6.1).

Based on the description above and Figure 6.1, the model is defined by a series of ordinary differential equations:

$$\begin{cases} \dfrac{dS_C}{dt} = A_1 - \beta_1 S_C P - \mu_c S_C + \rho_1 I_C, \\ \dfrac{dI_C}{dt} = \beta_1 S_C P - (\rho_1 + \mu_c) I_C, \\ \dfrac{dS_H}{dt} = A_2 - \dfrac{\beta_2 P S_H}{1+\alpha P} - \mu_h S_H + \rho_2 I_H, \\ \dfrac{dI_H}{dt} = \dfrac{\beta_2 P S_H}{1+\alpha P} - (\mu_h + \rho_2) I_H \\ \dfrac{dS_S}{dt} = A_3 - \beta_3 S_S M - \mu_s S_S, \\ \dfrac{dI_S}{dt} = \beta_3 S_S M - \mu_s I_S, \\ \dfrac{dM}{dt} = \gamma_1 I_C + \gamma_2 I_H - \mu_m M, \\ \dfrac{dP}{dt} = \gamma_3 I_S - \mu_p P. \end{cases} \tag{6.1}$$

The model parameters are assumed to be non-negative. Furthermore, since the model (6.1) monitors living populations, it is assumed that all state variables are non-negative at time $t = 0$.

Table 6.2: The description of the model (6.1) parameters and values.

Parameters	Descriptions	Values	Sources
A_1	The recruitment rate of the cattle population	64/day	Assumed
A_2	The recruitment rate of the human population	$\frac{2247}{365}$/day	(Mwasunda et al. 2022)
A_3	The recruitment rate of the snail population	3000/day	(Kanyi et al. 2021)
β_1	Cattle infection rate due to metacercariae	0.0000058/day	Assumed
β_2	Humans infection rate due to metacercariae	0.00002/day	(Nur, Trisilowati, Suryanto & Kusumawinahyu 2022)
β_3	Snail infection rate due to miracidia	0.0000078/day	Assumed
μ_h	The mortality rate of human due to natural causes	0.014/365/day	(Qi et al. 2014, 2018)
μ_c	The mortality rate of cattle due to natural causes	0.00488/day	Assumed
μ_s	The mortality rate of snails due to natural causes	0.01644/day	(Diaby et al. 2019)
μ_m	The mortality rate of miracidia due to natural causes	0.9/day	(Chiyaka & Garira 2009, Kanyi et al. 2021)
μ_p	The mortality rate of metacercariae due to natural causes	0.6452/day	(Diaby et al. 2019)
ρ_1	Treatment efficiency of the infected cattle	0.35/day	Assumed
ρ_2	Treatment efficiency of the infected human	0.225/day	Assumed
γ_1	Miracidia production rate in infected cattle.	6.96 /day	(Chiyaka & Garira 2009)
γ_2	Miracidia production rate in infected human	0.8/day	Assumed
γ_3	Metacercariae production rate in infected snail.	2.6 /day	(Chiyaka & Garira 2009)
α	The force of infection saturates level	0.02	Assumed

6.3 Model Analysis

6.3.1 Feasibility of Solutions

We define the total populations of cattle, humans and snails as $N_C = S_C + I_C$, $N_H = S_H + I_H$ and $N_S = S_S + I_S$, respectively. It can be easily verified that the system of equations (6.1) exhibits invariant positivity: for all nonnegative initial conditions, the solutions remain nonnegative for all $t \geq 0$.

Lemma 6.1. *For all $t \geq 0$, all solutions of model (6.1) bounded in region Ω where*

$$\Omega = \Omega_1 \cup \Omega_2 \cup \Omega_3 \cup \Omega_4 \cup \Omega_5$$

where, $\Omega_1 = \left\{(S_C, I_C) \in \mathbb{R}^2 : 0 \leq N_C \leq \frac{A_1}{\mu_c}\right\}$, $\Omega_2 = \left\{(S_H, I_H) \in \mathbb{R}^2 : 0 \leq N_H \leq \frac{A_2}{\mu_h}\right\}$,
$\Omega_3 = \left\{(S_S, I_S) \in \mathbb{R}^2 : 0 \leq N_S \leq \frac{A_3}{\mu_s}\right\}$, $\Omega_4 = \left\{M \in \mathbb{R} : 0 \leq M \leq \frac{\gamma_1 A_1}{\mu_c \mu_m} + \frac{\gamma_2 A_2}{\mu_h \mu_m}\right\}$,
and $\Omega_5 = \left\{P(t) \in \mathbb{R} : 0 \leq P \leq \frac{A_3 \lambda_3}{\mu_s \mu_p}\right\}$.

Proof. Adding the first two equations of model (3.1) provides

$$\frac{dN_C}{dt} = A_1 - \mu_c S_C - \mu_c I_C = A_1 - \mu_c N_C.$$

Thus

$$\frac{dN_C}{dt} \leq A_1 - \mu_c N_C.$$

After integration, as in model (3.1), standard comparison yields,

$$\limsup_{t \to \infty} N_C(t) \leq \frac{A_1}{\mu_c}.$$

$$0 \leq N_C(t) \leq \frac{A_1}{\mu_c} \quad \text{for large } t.$$

Thus, Ω_1 is positively invariant.

Adding the third and fourth equations:

$$\frac{dN_H}{dt} = A_2 - \mu_h N_H.$$

Hence, $\limsup_{t \to \infty} N_H(t) \leq \frac{A_2}{\mu_h}$.

$$0 \leq N_H(t) \leq \frac{A_2}{\mu_h}.$$

Adding the fifth and sixth equations:

$$\frac{dN_S}{dt} = A_3 - \mu_s N_S.$$

Therefore, $\limsup_{t\to\infty} N_S(t) \le \frac{A_3}{\mu_s}$.

$$0 \le N_S(t) \le \frac{A_3}{\mu_s}.$$

So, Ω_2 is positively invariant.

From the M-equation:

$$\frac{dM}{dt} = \gamma_1 I_C + \gamma_2 I_H - \mu_m M.$$

Since $0 \le I_C \le \frac{A_1}{\mu_c}$ and $0 \le I_H \le \frac{A_2}{\mu_h}$ eventually, we have

$$\gamma_1 I_C + \gamma_2 I_H \le \gamma_1 \frac{A_1}{\mu_c} + \gamma_2 \frac{A_2}{\mu_h}.$$

Thus

$$\frac{dM}{dt} \le \left(\gamma_1 \frac{A_1}{\mu_c} + \gamma_2 \frac{A_2}{\mu_h}\right) - \mu_m M.$$

By comparison,

$$\limsup_{t\to\infty} M(t) \le \frac{\gamma_1 A_1}{\mu_c \mu_m} + \frac{\gamma_2 A_2}{\mu_h \mu_m}.$$

Thus, Ω_3 is positively invariant.

From the P-equation:

$$\frac{dP}{dt} = \gamma_3 I_S - \mu_p P.$$

Since $0 \le I_S \le \frac{A_3}{\mu_s}$ eventually,

$$\gamma_3 I_S \le \gamma_3 \frac{A_3}{\mu_s}.$$

Thus

$$\frac{dP}{dt} \le \gamma_3 \frac{A_3}{\mu_s} - \mu_p P.$$

By comparison,

$$\limsup_{t\to\infty} P(t) \le \frac{\gamma_3 A_3}{\mu_s \mu_p}.$$

Therefore, Ω_4 is positively invariant.

Since each subregion Ω_i is positively invariant and attracts all solutions, the union Ω is a positively invariant bounded region for the system. This completes the proof. □

This implies that the model is both epidemiologically meaningful and mathematically well-posed.

6.3.2 Local Stability of the Disease-Free Equilibrium

The disease-free equilibrium (DFE) of the model (6.1) is defined as

$$E_0 = \left(S_C^0, I_C^0, S_H^0, I_H^0, S_S^0, I_S^0, M^0, P^0\right) = \left(\frac{A_1}{\mu_c}, 0, \frac{A_2}{\mu_h}, 0, \frac{A_3}{\mu_s}, 0, 0, 0\right).$$

We begin by calculating the reproduction number (R_0) to analyze the stability of the disease-free equilibrium. This number represents the average number of new infections generated by an infectious individual in a fully susceptible population (Mwasunda et al. 2022). The next generation matrix method, introduced by van den Driessche & Watmough (2002), is commonly used to determine (R_0). The infected compartments in the model (6.1) can be described as follows:

$$\begin{cases} \dfrac{dI_C}{dt} = \beta_1 S_C P - (\rho_1 + \mu_c) I_C, \\ \dfrac{dI_H}{dt} = \dfrac{\beta_2 P S_H}{1 + \alpha P} - (\mu_h + \rho_2) I_H \\ \dfrac{dI_S}{dt} = \beta_3 S_S M - \mu_s I_S, \\ \dfrac{dM}{dt} = \gamma_1 I_C + \gamma_2 I_H - \mu_m M, \\ \dfrac{dP}{dt} = \gamma_3 I_S - \mu_p P, \end{cases} \tag{6.2}$$

Rewrite Equation (6.2) and consider f_i represents new infections in compartment i and v_i^+ and v_i^- represent transfer terms into and out of compartment i, respectively;

$$\frac{dX_i}{dt} = f_i(x) + v_i^+ - v_i^-$$

where, $f_i = \begin{pmatrix} \beta_1 S_C P \\ \frac{\beta_2 P S_H}{1+\alpha P} \\ \beta_3 S_S M \\ 0 \\ 0 \end{pmatrix}$ and $v_i = \begin{pmatrix} (\rho_1+\mu_c) I_C \\ (\mu_h+\rho_2) I_H \\ \mu_s I_S \\ -\gamma_1 I_C - \gamma_2 I_H + \mu_m M \\ -\gamma_3 I_S + \mu_p P \end{pmatrix}$

The matrices used in the next generation method, denoted as F and V, are defined as follows:

$$F = \begin{pmatrix} 0 & 0 & 0 & 0 & \frac{\beta_1 A_1}{\mu_c} \\ 0 & 0 & 0 & 0 & \frac{\beta_2 A_2}{\mu_h} \\ 0 & 0 & 0 & \frac{\beta_3 A_3}{\mu_h} & 0 \\ 0 & 0 & 0 & 0 & 0 \\ 0 & 0 & 0 & 0 & 0 \end{pmatrix} \text{and} \quad V = \begin{pmatrix} \rho_1+\mu_c & 0 & 0 & 0 & 0 \\ 0 & \mu_h+\rho_2 & 0 & 0 & 0 \\ 0 & 0 & \mu_s & 0 & 0 \\ -\gamma_1 & -\gamma_2 & 0 & \mu_m & 0 \\ 0 & 0 & -\gamma_3 & 0 & \mu_p \end{pmatrix}.$$

Therefore, the reproduction number is the spectral radius of the matrix FV^{-1} and is given by

$$R_0 = \sqrt{\frac{A_3\beta_3\gamma_3\left(A_2\beta_2\gamma_2\mu_c\left(\mu_c+\rho_1\right)+A_1\beta_1\gamma_1\mu_h\left(\mu_h+\rho_2\right)\right)}{\mu_c\mu_h\mu_m\mu_p\mu_s^2\left(\mu_c+\rho_1\right)\left(\mu_h+\rho_2\right)}}.$$

$$R_0 = \sqrt{\frac{A_3\beta_3\gamma_3A_1\beta_1\gamma_1}{\mu_c\mu_m\mu_p\mu_s^2\left(\mu_c+\rho_1\right)}+\frac{A_3\beta_3\gamma_3A_2\beta_2\gamma_2}{\mu_h\mu_m\mu_p\mu_s^2\left(\mu_h+\rho_2\right)}},$$

where $R_c = \sqrt{\frac{A_3\beta_3\gamma_3A_1\beta_1\gamma_1}{\mu_c\mu_m\mu_p\mu_s^2(\mu_c+\rho_1)}}$ and $R_h = \sqrt{\frac{A_3\beta_3\gamma_3A_2\beta_2\gamma_2}{\mu_h\mu_m\mu_p\mu_s^2(\mu_h+\rho_2)}}$ represent the average number of secondary infections caused by a single infected cattle and human, respectively, in a completely susceptible population.

Theorem 6.2. *The disease-free equilibrium of the Fasciola hepatica model (6.1) is locally asymptotically stable if* $R_0 < 1$.

Proof: The Jacobian of the model (6.1) at the disease-free equilibrium point is

determined as:

$$J = \begin{pmatrix} -\mu_c & \rho_1 & 0 & 0 & 0 & 0 & 0 & -\frac{A_1\beta_1}{\mu_c} \\ 0 & -\mu_c-\rho_1 & 0 & 0 & 0 & 0 & 0 & \frac{A_1\beta_1}{\mu_c} \\ 0 & 0 & -\mu_h & \rho_2 & 0 & 0 & 0 & -\frac{A_2\beta_2}{\mu_h} \\ 0 & 0 & 0 & -\mu_h-\rho_2 & 0 & 0 & 0 & \frac{A_2\beta_2}{\mu_h} \\ 0 & 0 & 0 & 0 & -\mu_s & 0 & -\frac{A_3\beta_3}{\mu_s} & 0 \\ 0 & 0 & 0 & 0 & 0 & -\mu_s & \frac{A_3\beta_3}{\mu_s} & 0 \\ 0 & \gamma_1 & 0 & \gamma_2 & 0 & 0 & -\mu_m & 0 \\ 0 & 0 & 0 & 0 & 0 & \gamma_3 & 0 & -\mu_p \end{pmatrix}.$$

The eigenvalues of J include $x = -\mu_c$, $x = -\mu_h$ and $x = -\mu_s$. The remaining eigenvalues can be found by solving the characteristic equation:

$$X^5 + A_4X^4 + A_3X^3 + A_2X^2 + A_1X + A_0 = 0, \tag{6.3}$$

where,

$$\begin{aligned}
A_4 &= \mu_c + \mu_h + \mu_m + \mu_p + \rho_1 + \rho_2 + \mu_s, \\
A_3 &= \mu_c\left(\mu_h + \mu_m + \mu_p + \rho_2 + \mu_s\right) + \mu_h\left(\mu_m + \mu_p + \rho_1 + \mu_s\right) + \rho_1\mu_m + \mu_m\mu_p \\
&\quad + \rho_2\left(\mu_m + \mu_p + \rho_1 + \mu_s\right) + \mu_m\mu_s + \rho_1\mu_p + \mu_p\mu_s + \rho_1\mu_s, \\
A_2 &= \mu_m\mu_p\mu_s + \rho_1\mu_m\mu_p + \rho_1\mu_m\mu_s + \rho_1\mu_p\mu_s + \mu_h\left(\mu_m\left(\mu_p + \rho_1 + \mu_s\right) + \mu_p\left(\rho_1 + \mu_s\right) + \rho_1\mu_s\right) \\
&\quad + \mu_c\left(\mu_h\left(\mu_m + \mu_p + \mu_s\right) + \mu_m\left(\mu_p + \rho_2 + \mu_s\right) + \rho_2\left(\mu_p + \mu_s\right) + \mu_p\mu_s\right) \\
&\quad + \rho_2\left(\mu_m\left(\mu_p + \rho_1 + \mu_s\right) + \mu_p\left(\rho_1 + \mu_s\right) + \rho_1\mu_s\right), \\
A_1 &= \frac{(1-R_h^2)}{\mu_c\mu_h\mu_m\mu_p\mu_s^2\left(\mu_h + \rho_2\right)} + \mu_h\mu_s\left(\mu_c + \rho_1\right)\left(\mu_h + \rho_2\right)\left(\mu_m\left(\mu_p + \mu_s\right) + \mu_p\mu_s\right), \\
A_0 &= \frac{(1-R_0^2)}{\mu_c\mu_h\mu_m\mu_p\mu_s^2\left(\mu_c + \rho_1\right)\left(\mu_h + \rho_2\right)}.
\end{aligned}$$

The Routh-Hurwitz stability criterion is employed to assess the stability of non-linear, time-invariant systems.

(i) By directly noting that A_4, A_3, A_2 and A_1 are real positive numbers and given that $R_0 < 1$, $R_c < 1$ and $R_h < 1$, it follows that A_0 is also positive. As a result, the solutions to the auxiliary equation (6.3) have a negative real value.

(ii) The conditions of the Routh-Hurwitz stability criterion, $A_4A_3A_2 - A_2^2 + A_4^2A_1 > 0$ and $(A_4A_1 - A_0)(A_4A_3A_2 - A_2^2 - A_4^2A_1) > A_0(A_4A_3 - A_2)^2 + A_4A_0^2$, are satisfied after simplification. Therefore, all the requirements of the Routh-Hurwitz stability criterion are met, indicating that all the eigenvalues of the model will be negative when $R_c < 1$, $R_h < 1$ and $R_0 < 1$. This conclusively proves the theorem. □

6.3.3 Global Stability of the Disease-Free Equilibrium

Theorem 6.3. *The disease-free equilibrium point is globally asymptotically stable if* $R_0 < 1$.

To investigate the global behavior of the model (6.1), we employ the theorem of (Castillo-Chavez et al. 2002) and summarize it as follows.
Consider the system:

$$\begin{cases} \dfrac{dX}{dt} = F(X,Y), \\ \dfrac{dY}{dt} = G(X,Y),\ G(X,0) = 0, \end{cases} \tag{6.4}$$

where the elements of the column vector $X \in \mathbb{R}^m$ represent the number of uninfected individuals and the elements of the vector $Y \in \mathbb{R}^n$ represent the number of infected individuals. The point $U_0 = (X^*, 0)$ denotes the disease-free equilibrium of the system. This fixed point $U_0 = (X^*, 0)$ is globally asymptotically stable if $R_0 < 1$ (indicating local asymptotic stability) and the following two conditions are met:

(C1) For $\frac{dX}{dt} = F(X,0)$, X^* is globally asymptotically stable.

(C2) $G(X,Y) = AY - \hat{G}(X,Y)$ and $\hat{G}(X,Y) \geq 0$ hold for $(X,Y) \in \Omega$, where $A = D_Y G(X_0, 0)$ is a Metzler matrix and Ω is the feasible region of the model (6.1).

With the notation provided earlier in equation 6.4, we can re-frame our model (6.1) in the following manner: $X = (S_C, S_H, S_S)$, $Y = (I_C, I_H, I_S, M, P)$, $X_0 = (\frac{A_1}{\mu_c}, \frac{A_2}{\mu_h}, \frac{A_3}{\mu_s})$,

$$F(X,Y) = \begin{pmatrix} A_1 - \beta_1 S_C P - \mu_c S_C + \rho_1 I_C \\ A_2 - \frac{\beta_2 P S_H}{1+\alpha P} - \mu_h S_H + \rho_2 I_H \\ A_3 - \beta_3 S_S M - \mu_s S_S \end{pmatrix},$$

$$F(X,0) = \begin{pmatrix} A_1 - \mu_c S_C \\ A_2 - \mu_h S_H \\ A_3 - \mu_s S_S \end{pmatrix},$$

$$G(X,Y) = \begin{pmatrix} \beta_1 S_C P - (\rho_1 + \mu_c) I_C \\ \frac{\beta_2 P S_H}{1+\alpha P} - (\mu_h + \rho_2) I_H \\ \beta_3 S_S M - \mu_s I_S \\ \gamma_1 I_C + \gamma_2 I_H - \mu_m M \\ \gamma_3 I_S - \mu_p P \end{pmatrix},$$

$$A = D_Y G(X_0,0) = \begin{pmatrix} -(\rho_1+\mu_c) & 0 & 0 & 0 & \frac{\beta_1 A_1}{\mu_c} \\ 0 & -(\rho_2+\mu_h) & 0 & 0 & \frac{\beta_2 A_2}{\mu_h} \\ 0 & 0 & -\mu_s & \frac{\beta_3 A_3}{\mu_s} & 0 \\ \gamma_1 & \gamma_2 & 0 & -\mu_m & 0 \\ 0 & 0 & \gamma_3 & 0 & -\mu_p \end{pmatrix}. \tag{6.5}$$

It is evident that $X^* = (\frac{A_1}{\mu_c}, \frac{A_2}{\mu_h}, \frac{A_3}{\mu_s})$ serves as the global asymptote for $F(X,0)$, thus fulfilling condition (C1). The matrix shown in equation (6.5) is categorized as a Metzler matrix, with all the off-diagonal elements being non-negative.

Condition (C2) specifies that, $\hat{G}(X,Y) = AY - G(X,Y)$ and

$$\hat{G}(X,Y) = \begin{pmatrix} P\beta_1(\frac{A_1}{\mu_c} - S_C) \\ P\beta_2(\frac{A_2}{\mu_h} - \frac{S_H}{1+\alpha P}) \\ M\beta_3(\frac{A_3}{\mu_s} - S_S) \\ \\ 0 \\ 0 \end{pmatrix}. \tag{6.6}$$

Therefore, by referencing equation (6.6), it can be observed that $\hat{G}(X,Y) \geq 0$ is valid within the feasible region. Consequently, this analysis verifies the global stability of the Disease-Free Equilibrium (DFE) when $R_0 < 1$. □

6.3.4 Forward Bifurcation

The model (6.1), undergoes a forward bifurcation when $R_0 = 1$. Applying the principles of Castillo-Chavez & Song (2004), we perform a bifurcation analysis on the model equation (6.1) when $R_0 = 1$. In this analysis, we consider the transmission rate of cattle disease, indicated as β_1, as the key parameter that triggers the bifurcation. The condition $R_0 = 1$ holds true if and only if

$$\phi := \beta_1 = \frac{\mu_c\mu_h\mu_m\mu_p\mu_s^2\left(\mu_c+\rho_1\right)\left(\mu_h+\rho_2\right) - A_2A_3\beta_2\beta_3\gamma_2\gamma_3\mu_c\left(\mu_c+\rho_1\right)}{A_3\beta_3\gamma_1\gamma_3\mu_c\mu_h\left(\mu_h+\rho_2\right)}.$$

The Jacobian matrix for model (6.1) at the disease-free equilibrium, concerning ϕ, can be written as follows,

$$J_\phi = \begin{pmatrix} -\mu_c & \rho_1 & 0 & 0 & 0 & 0 & 0 & -\frac{A_1\phi}{\mu_c} \\ 0 & -\mu_c-\rho_1 & 0 & 0 & 0 & 0 & 0 & \frac{A_1\phi}{\mu_c} \\ 0 & 0 & -\mu_h & \rho_2 & 0 & 0 & 0 & -\frac{A_2\beta_2}{\mu_h} \\ 0 & 0 & 0 & -\mu_h-\rho_2 & 0 & 0 & 0 & \frac{A_2\beta_2}{\mu_h} \\ 0 & 0 & 0 & 0 & -\mu_s & 0 & -\frac{A_3\beta_3}{\mu_s} & 0 \\ 0 & 0 & 0 & 0 & 0 & -\mu_s & \frac{A_3\beta_3}{\mu_s} & 0 \\ 0 & \gamma_1 & 0 & \gamma_2 & 0 & 0 & -\mu_m & 0 \\ 0 & 0 & 0 & 0 & 0 & \gamma_3 & 0 & -\mu_p \end{pmatrix}.$$

The eigenvalues of the matrix J_ϕ are $\lambda_1 = 0$, $\lambda_2 = -\mu_c$,$\lambda_3 = -\mu_h$, $\lambda_4 = -\mu_s$ and the remaining eigenvalues can be obtained by solving the following equation for λ;

$$\lambda^4 + b_3\lambda^3 + b_2\lambda^2 + b_1\lambda + b_0 = 0,$$

where,

$$
\begin{aligned}
b_3 &= \mu_c + \mu_h + \mu_m + \mu_p + \rho_1 + \rho_2 + \mu_s,\\
b_2 &= \mu_c\left(\mu_h + \mu_m + \mu_p + \rho_2 + \mu_s\right) + \mu_h\left(\mu_m + \mu_p + \rho_1 + \mu_s\right) + \rho_1\mu_m + \mu_m\mu_p\\
&\quad + \rho_2\left(\mu_m + \mu_p + \rho_1 + \mu_s\right) + \mu_m\mu_s + \rho_1\mu_p + \mu_p\mu_s + \rho_1\mu_s,\\
b_1 &= \mu_c\left(\mu_h(\mu_m + \mu_p + \mu_s) + \mu_m(\mu_p + \rho_2 + \mu_s) + \rho_2(\mu_p + \mu_s) + \mu_p\mu_s\right)\\
&\quad + \mu_h\left(\mu_m(\mu_p + \rho_1 + \mu_s) + \mu_p(\rho_1 + \mu_s) + \rho_1\mu_s\right)\\
&\quad + \rho_1\mu_m\mu_p + \rho_2\left(\mu_m(\mu_p + \rho_1 + \mu_s) + \mu_p(\rho_1 + \mu_s) + \rho_1\mu_s\right) + \mu_m\mu_p\mu_s + \rho_1\mu_m\mu_s + \rho_1\mu_p\mu_s,\\
b_0 &= (\mu_h + \rho_2)\left(\mu_m\mu_p\mu_s(1 - R_h^2) + \frac{A_2A_3\beta_2\beta_3\gamma_2\gamma_3\left(\mu_c + \rho_1\right)}{\mu_h\mu_s\left(\mu_h + \rho_2\right)} + \mu_c\mu_m\mu_p + \mu_c\mu_m\mu_s\right)\\
&\quad + (\mu_h + \rho_2)\left(\mu_c\mu_p\mu_s + \rho_1\mu_m\mu_p + \rho_1\mu_m\mu_s + \rho_1\mu_p\mu_s\right).
\end{aligned}
$$

With all coefficients (b_i) are positive and the condition, $b_1^2 + b_3^2 b_0 - b_3 b_2 b_1 < 0$ met, the Routh-Hurwitz stability criterion indicates that J_ϕ has simple zero eigenvalues, with the remaining eigenvalues having negative real parts. Since one of the calculated eigenvalues is negative, a bifurcation occurs at $R_0 = 1$.

We determine both a right eigenvector and a left eigenvector for the matrix J_ϕ, represented as $x = (x_1, x_2, x_3, x_4, x_5, x_6, x_7, x_8)^T$ and $z = (z_1, z_2, z_3, z_4, z_5, z_6, z_7, z_8)$, respectively. Upon evaluation, we derive the following results:

$$
\begin{cases}
x_1 = -x_2,\\
x_3 = \dfrac{A_2A_3\beta_2\beta_3\gamma_1\gamma_3x_2}{A_2A_3\beta_2\beta_3\gamma_2\gamma_3 - \mu_h\mu_m\mu_p\mu_s^2\left(\mu_h + \rho_2\right)},\\
x_4 = \dfrac{-A_2A_3\beta_2\beta_3\gamma_1\gamma_3x_2}{A_2A_3\beta_2\beta_3\gamma_2\gamma_3 - \mu_h\mu_m\mu_p\mu_s^2\left(\mu_h + \rho_2\right)},\\
x_5 = \dfrac{A_3\beta_3\gamma_1x_2\mu_h\mu_p\left(\mu_h + \rho_2\right)}{A_2A_3\beta_2\beta_3\gamma_2\gamma_3 - \mu_h\mu_m\mu_p\mu_s^2\left(\mu_h + \rho_2\right)},\\
x_6 = \dfrac{-A_3\beta_3\gamma_1x_2\mu_h\mu_p\left(\mu_h + \rho_2\right)}{A_2A_3\beta_2\beta_3\gamma_2\gamma_3 - \mu_h\mu_m\mu_p\mu_s^2\left(\mu_h + \rho_2\right)},\\
x_7 = \dfrac{\gamma_1x_2\mu_h\mu_p\mu_s^2\left(\mu_h + \rho_2\right)}{\mu_h\mu_m\mu_p\mu_s^2\left(\mu_h + \rho_2\right) - A_2A_3\beta_2\beta_3\gamma_2\gamma_3},\\
x_8 = \dfrac{-A_3\beta_3\gamma_1\gamma_3x_2\mu_h\left(\mu_h + \rho_2\right)}{A_2A_3\beta_2\beta_3\gamma_2\gamma_3 - \mu_h\mu_m\mu_p\mu_s^2\left(\mu_h + \rho_2\right)}.
\end{cases}
\tag{6.7}
$$

$$
z = (0, z_2, 0, \frac{\gamma_2z_2\left(\mu_c + \rho_1\right)}{\gamma_1\left(\mu_h + \rho_2\right)}, 0, \frac{z_2\mu_m\mu_s\left(\mu_c + \rho_1\right)}{A_3\beta_3\gamma_1}, \frac{z_2\left(\mu_c + \rho_1\right)}{\gamma_1}, \frac{z_2\mu_m\mu_s^2\left(\mu_c + \rho_1\right)}{A_3\beta_3\gamma_1\gamma_3}). \tag{6.8}
$$

Assuming a and b are the standard form coefficients representing the system dynamics according to the Castillo-Chavez and Song theorem, the computation process enables us to determine the bifurcation coefficients as follows:

$$a = -x_2^2 z_2 \left(\frac{\mu_c \left(\mu_c + \rho_1\right)}{A_1} + \frac{A_2 A_3^2 \beta_2^2 \beta_3^2 \gamma_1 \gamma_2 \gamma_3^2 \mu_h \left(\mu_c + \rho_1\right)}{\left(A_2 A_3 \beta_2 \beta_3 \gamma_2 \gamma_3 - \mu_h \mu_m \mu_p \mu_s^2 \left(\mu_h + \rho_2\right)\right)^2} \right)$$
$$- x_2^2 z_2 \left(\frac{\beta_3 \gamma_1 \mu_h^2 \mu_m \mu_p^2 \mu_s^3 \left(\mu_c + \rho_1\right) \left(\mu_h + \rho_2\right)^2}{\left(A_2 A_3 \beta_2 \beta_3 \gamma_2 \gamma_3 - \mu_h \mu_m \mu_p \mu_s^2 \left(\mu_h + \rho_2\right)\right)^2} \right),$$
$$b = \frac{x_2 z_2 \left(A_2 A_3 \beta_3^2 \gamma_2 \gamma_3 \mu_c \left(\mu_c + \rho_1\right) + \mu_h \left(\mu_h + \rho_2\right) \left(A_1 A_3 \beta_3^2 \gamma_1 \gamma_3 + \mu_c \mu_m \mu_p \mu_s^2 \left(\mu_c + \rho_1\right)\right)\right)}{\beta_3 \mu_c \mu_h \mu_m \mu_p \mu_s^2 \left(\mu_h + \rho_2\right) \left(1 - R_h^2\right)}.$$

Therefore, under the conditions where $x_2 > 0$, $z_2 > 0$ and $R_h < 1$, the requirements of $a < 0$ and $b > 0$ are met, leading to a forward bifurcation occurring at $R_0 = 1$. In the context of the *Fasciola hepatica* model, forward bifurcation refers to the scenario where the disease-free equilibrium (DFE) loses stability and an endemic equilibrium (EE) emerges as R_0 increases past 1. This means that for $R_0 < 1$, the DFE is stable and for $R_0 > 1$, the DFE becomes unstable and a stable endemic equilibrium appears.

6.3.5 Existence and Local Stability of Endemic Equilibrium

A forward bifurcation guarantees the existence of an endemic equilibrium point. This occurs when the reproduction number (R_0) crosses the critical threshold of 1 from below. For $R_0 < 1$, the disease-free equilibrium is stable and no endemic equilibrium exists. As R_0 surpasses 1, the disease-free equilibrium becomes unstable and a stable endemic equilibrium emerges, indicating the disease will persist in the population at a steady state. Therefore, a forward bifurcation signifies a stable endemic equilibrium for $R_0 > 1$, ensuring the persistence of the disease.

Theorem 6.4. *The endemic equilibrium is locally asymptotically stable if $R_0 > 1$; otherwise, it is unstable.*

Proof. This results from the existence of a forward bifurcation. A forward bifurcation demonstrates local asymptotic stability for equilibrium points derived from epidemiological models (Cheneke 2023). □

6.4 Sensitivity Analysis

The normalized forward sensitivity index method is used to calculate the model parameter sensitivity indices. Table 6.3 presents the sensitivity indices for the model (6.1), while Figure 6.2 provides a visual representation of these indices. The figure highlights significant positive indices in the model, including infection rates (β_1, β_2, β_3), recruitment rates (A_1, A_2, A_3), miracidia production rate (γ_1) and metacercariae production rates (γ_2, γ_3). These parameters are critical in shaping the dynamics and outcomes of the model, highlighting their importance in understanding and managing the system. This indicates that an decrease or increase) in infection rates (β_1, β_2, β_3) by 5% will lead to a decrease or increase of 2.5% in the reproduction number (R_0).

Figure 6.2 also shows that the negative index of snail mortality (μ_s) has the highest sensitivity. This implies that increasing or decreasing the value of (μ_s) by 5% will result in a 5% decrease or increase in the reproduction number (R_0).

Table 6.3: Sensitivity indices.

Parameter	Sensitivity index value
μ_s	-1
μ_m	-0.5
μ_p	-0.5
μ_c	-0.0586
ρ_1	-0.0570
ρ_2	-0.4421
A_2	+0.4422
β_2	+0.4422
γ_2	+0.4422
μ_h	-0.4423
γ_3	+0.5
A_3	+0.5
β_3	+0.5
A_1	+0.0578
β_1	+0.0578
γ_1	+0.0578

6.5 Optimal Control Model Analysis

This section presents an optimal control model that incorporates four time-dependent strategies: public health education ($w_1(t)$), treatment of infected cattle ($w_2(t)$), treatment of infected humans ($w_3(t)$) and snail removal using chemical molluscicides ($w_4(t)$). Anthelmintic treatments can be applied to infected cattle and humans to eradicate the *F. hepatica* parasite. Since drugs and dosages can vary between species, it is crucial to consider and investigate different treatment options for cattle and humans. The model aims to determine the most effective prevention and control strate-

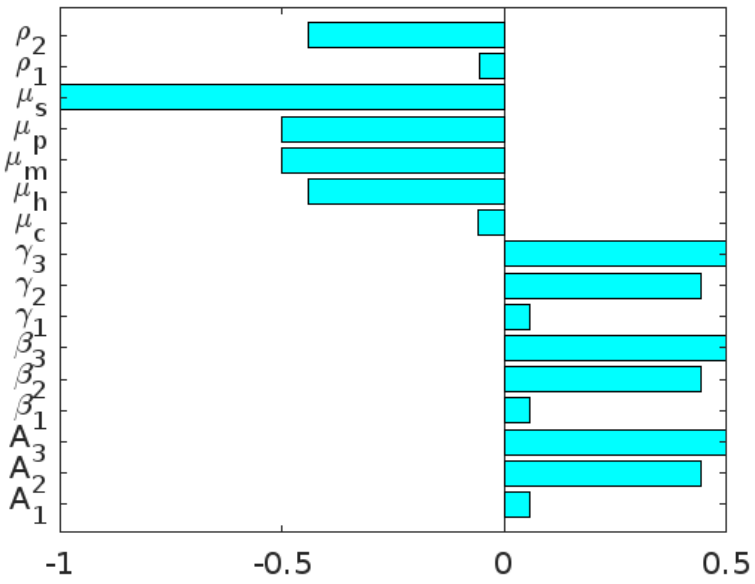

Figure 6.2: Sensitivity indices.

gies to mitigate the impact of *Fasciola hepatica* while minimizing associated costs.

$$\begin{cases} \dfrac{dS_C(t)}{dt} = A_1 - \beta_1 S_C(t)P(t) - \mu_c S_C(t) + (\rho_1 + w_2(t))I_C(t), \\ \dfrac{dI_C(t)}{dt} = \beta_1 S_C(t)P(t) - (\rho_1 + w_2(t) + \mu_c)I_C(t), \\ \dfrac{dS_H(t)}{dt} = A_2 - \dfrac{\beta_2(1-w_1(t))P(t)S_H(t)}{1+\alpha P(t)} - \mu_h S_H(t) + (\rho_2 + w_3(t))I_H(t), \\ \dfrac{dI_H(t)}{dt} = \dfrac{\beta_2(1-w_1 t))P(t)S_H(t)}{1+\alpha P(t)} - (\mu_h + \rho_2 + w_3(t))I_H(t) \\ \dfrac{dS_S(t)}{dt} = A_3 - \beta_3 S_S(t)M(t) - (\mu_s + w_4(t))S_S(t), \\ \dfrac{dI_S(t)}{dt} = \beta_3 S_S(t)M(t) - (\mu_s + w_4(t)))I_S(t), \\ \dfrac{dM(t)}{dt} = \gamma_1 I_C(t) + \gamma_2 I_H(t) - \mu_m M(t), \\ \dfrac{dP(t)}{dt} = \gamma_3 I_S(t) - \mu_p P(t). \end{cases} \tag{6.10}$$

The model incorporates control strategies aimed at identifying the most effective methods to reduce *Fasciola hepatica* infections in both cattle and humans. The objective function outlines the expenses associated with the implementation of these measures as follows:

$$J(w_1, w_2, w_3, w_4) = \int_0^T \left(C_1 I_C + C_2 I_H + \frac{1}{2}C_3 w_1^2 + \frac{1}{2}C_4 w_2^2 + \frac{1}{2}C_5 w_3^2 + \frac{1}{2}C_6 w_4^2 \right) dt, \tag{6.11}$$

where T denotes the specified end time, while C_1 and C_2 represent the cost weights associated with infected humans and infected cattle, respectively. Furthermore, C_3, C_4, C_5 and C_6 correspond to the positive weights assigned to each control measure. The choice to use a quadratic cost function for controls is in line with current research on the costs of managing epidemics (Okosun et al. 2013, Alemneh 2020). We aim to determine the optimal control strategy, w_1^*, w_2^*, w_3^* and w_4^* that minimizes the objective function (J), expressed as:

$$J(w_1^*, w_2^*, w_3^*, w_4^*) = \lim_{\mathcal{W}} J(w_1, w_2, w_3, w_4). \tag{6.12}$$

The control set $\mathcal{W}$ consists of Lebesgue measurable bounded functions and is defined as follows:

$$\mathcal{W} = \{(w_1, w_2, w_3, w_4) : 0 \leq w_i(t) \leq 1,\ i = 1,2,3,4,\ \text{for } t \in [0,T]\}. \tag{6.13}$$

6.5.1 Existence of Optimal Controls

We applied the approach proposed by Nana-Kyere et al. (2022) to demonstrate the existence of optimal control for model (6.10) and Equation (6.11) and subsequently presented the following theorem.

Theorem 6.5. *Consider the system described by equation (6.10) with initial conditions* $(S_C(0), I_C(0), S_H(0), I_H(0), S_S(0), I_S(0), M(0), P(0)) \geq (0,0,0,0,0,0,0,0))$ *and the objective functional (J) given by equation (6.11). There exists an optimal control* $w^*(t) = (w_1^*(t), w_2^*(t), w_3^*(t), w_4^*(t))$ *and corresponding state variables* $(S_C^*, I_C^*, S_H^*, I_H^*, S_S^*, I_s^*, M^*, P^*)$ *that minimize* $J(w)$ *over the set* $\mathcal{W}$*, provided the following conditions are satisfied:*

(a) The set of admissible controls and state variables is non-empty.

(b) The set of admissible controls is convex and closed.

(c) The system defined by equation (6.10) is subject to constraints imposed by a linear function on both the state and control variables.

(d) The integrated objective function ($\mathscr{L}$), as defined in Equation (6.11), is convex with respect to the control variables.

(e) The integrand of the objective function $\mathscr{L}$ satisfies the inequality

$$\mathscr{L} \geq a_1(|w_1|^2 + |w_2|^2 + |w_3|^2 + |w_4|^2)^{\frac{a_3}{2}} - a_2,$$

where a_1 and a_2 are positive constants and $a_3 > 1$.

Proof. (a) For any allowable control function within $\mathscr{W}$, we can assert with certainty that the solutions to the state system are both continuous and bounded. Moreover, the right-hand side functions of equation (6.10) adhere to the Lipschitz condition concerning the state variables. The study presented in Lukes (1982) confirms the existence of solutions for the system (6.10) and validates this property.

(b) The second property, which pertains to the definition of a convex set, is also met because the control set $\mathscr{W} = w_1 \times w_2 \times w_3 \times w_4$ is both convex and closed for all $t \in [0,T]$.

(c) The right-hand side of the system (6.10) is continuous. The state and control variables remain bounded over the interval $[0,T]$. To verify their boundedness, we applied the method described in Burden et al. (2004). The right-hand side of equation (6.10) can be directly expressed as a linear function of w, given by:

$$F(t,X,w) = G(t,X) + H(t,X)w, \tag{6.14}$$

where X and w represent the state and control variables, respectively. The norm inequality given in Equation (6.14) results in,

$$|F(t,X,w)| \leq |G(t,X)| + |H(t,X)||w|.$$

Since the functions G and H are continuous with respect to the state variables and each state variable is bounded, it is evident that both $|G|$ and $|H|$ are bounded functions. Consequently, there exist constants r_1 and r_2 such that $|G| \leq r_1$ and $|H| \leq r_2$. This leads to,

$$|F(t,X,w)| \leq |G(t,X)| + |H(t,X)||w| \leq r_1 + r_2|w| \leq Max\{r_1,r_2\}(1+|w|). \tag{6.15}$$

Thus, $||F(t,X,w)|| \leq r(1+|w|)$, where r is the maximum of r_1 and r_2. This confirms that condition (c) is satisfied.

(d) The integrand in equation (6.10) is given by

$$\mathscr{L}(I_C,I_H,w) = C_1I_C + C_2I_H + \frac{1}{2}(C_3w_1^2 + C_4w_2^2 + C_5w_3^2 + C_6w_4^2).$$

This expression can be broken down into the sum of convex functions, indicating that it is also convex concerning the control variables.

(e) The existence of constants a_1, $a_2 > 0$ and $a_3 > 1$ is established such that the integrand $\mathscr{L}$ of the objective function

$$\mathscr{L}(I_C,I_H,w) = C_1I_C + C_2I_H + \frac{1}{2}(C_3w_1^2 + C_4w_2^2 + C_5w_3^2 + C_6w_4^2) \geq \frac{a_1}{2}(w_1^2 + w_2^2 + w_3^2 + w_4^2)^{\frac{a_3}{2}} - a_2$$

holds true, where $a_1 = \min\{C_3,C_4,C_5,C_6\} > 0$, $a_2 > 0$ and $a_3 = 2$. The assumption made in the original statement is valid, confirming that there exists an optimal control strategy that minimizes the given objective function.

6.5.2 The Hamiltonian and Optimality Control Problem

We transform equation (6.10) and system (6.11) into a specific problem of minimizing the Hamiltonian to the control parameters (w_1,w_2,w_3,w_4) using Pontryagin's Maximum Principle. The Hamiltonian $\mathscr{H}$ associated with this control problem is given by:

$$\mathscr{H} = \mathscr{L} + \lambda_1\frac{dS_C}{dt} + \lambda_2\frac{dI_C}{dt} + \lambda_3\frac{dS_H}{dt} + \lambda_4\frac{dI_H}{dt} + \lambda_5\frac{dS_S}{dt} + \lambda_6\frac{dI_S}{dt} + \lambda_7\frac{dM}{dt} + \lambda_8\frac{dP}{dt}. \quad (6.16)$$

In this optimal control problem, the Hamiltonian function $\mathscr{H}$ incorporates the adjoint variable functions λ_i for $i = 1,2,3,4,5,6,7,8$, which correspond to the respective

state equations.

$$\begin{aligned}\mathscr{H} &= C_1 I_C + C_2 I_H + \frac{1}{2}[C_3 w_1^2 + C_4 w_2^2 + C_5 w_3^2 + C_6 w_4^2] \\ &+ \lambda_1[A_1 - \beta_1 S_C(t)P(t) - \mu_c S_C(t) + (\rho_1 + w_2(t))I_C(t)] + \lambda_2[\beta_1 S_C(t)P(t) - (\rho_1 + w_2(t) + \mu_c)I_C(t)] \\ &+ \lambda_3[A_2 - \frac{\beta_2(1-w_1(t))P(t)S_H(t)}{1+\alpha P(t)} - \mu_h S_H(t) + (\rho_2 + w_3(t))I_H(t)] \\ &+ \lambda_4[\frac{\beta_2(1-w_1 t))P(t)S_H(t)}{1+\alpha P(t)} - (\mu_h + \rho_2 + w_3(t))I_H(t)] \\ &+ \lambda_5[A_3 - \beta_3 S_S(t)M(t) - (\mu_s + w_4(t))S_S(t)] + \lambda_6[\beta_3 S_S(t)M(t) - (\mu_s + w_4(t)))I_S(t)] \\ &+ \lambda_7[\gamma_1 I_C(t) + \gamma_2 I_H(t) - \mu_m M(t)] + \lambda_8[\gamma_3 I_S(t) - \mu_p P(t)].\end{aligned} \tag{6.17}$$

Theorem 6.6. *For an optimal control set* (w_1, w_2, w_3, w_4) *that minimizes the objective function (J) over the set* $\mathscr{W}$*, there exist corresponding adjoint variables* $(\lambda_1, \lambda_2, \lambda_3, \lambda_4, \lambda_5, \lambda_6, \lambda_7, \lambda_8)$ *that satisfy the following :*

$$\begin{cases} \frac{d\lambda_1}{dt} = \left(\beta_1 P(t) + \mu_c\right)\lambda_1 - \left(\beta_1 P(t)\right)\lambda_2, \\ \frac{d\lambda_2}{dt} = -C_1 - \left(\rho_1 + w_2(t)\right)\lambda_1 + \left(\rho_1 + w_2(t) + \mu_c\right)\lambda_2 - \gamma_1\lambda_7, \\ \frac{d\lambda_3}{dt} = \left(\frac{\beta_2(1-w_1(t))P(t)}{1+\alpha P(t)} + \mu_h\right)\lambda_3 - \left(\frac{\beta_2(1-w_1(t))P(t)}{1+\alpha P(t)}\right)\lambda_4, \\ \frac{d\lambda_4}{dt} = -C_2 - \left(\rho_2 + w_3(t)\right)\lambda_3 + \left(\rho_2 + w_3(t) + \mu_h\right)\lambda_4 - \gamma_2\lambda_7 \\ \frac{d\lambda_5}{dt} = \left(\beta_3 M(t) + \mu_s + w_4(t)\right)\lambda_5 - \beta_3 M(t)\lambda_6, \\ \frac{d\lambda_6}{dt} = (w_4(t) + \mu_s)\lambda_6 - \gamma_3\lambda_8, \\ \frac{d\lambda_7}{dt} = \beta_3 S_S\lambda_5 - \beta_3 S_S\lambda_6 + \mu_m\lambda_7, \\ \frac{d\lambda_8}{dt} = \beta_1 S_C\lambda_1 - \beta_1 S_C\lambda_2 + \left(\frac{\beta_2(1-w_1(t))S_H(t)}{(1+\alpha P(t))^2}\right)\lambda_3 - \left(\frac{\beta_2(1-w_1(t))S_H(t)}{(1+\alpha P(t))^2}\right)\lambda_4 + \mu_p\lambda_8, \end{cases} \tag{6.18}$$

with transversality conditions $\lambda_i(T) = 0$*, for* $i = 1, 2, ..., 7$.

Furthermore, the optimal conditions for the problem are given by:

$$\left.\begin{aligned} w_1^* &= \max\left\{0, \min\left\{1, \frac{(\lambda_4-\lambda_3)\beta_2 S_H P}{C_1(1+\alpha P)}\right\}\right\}, \\ w_2^* &= \max\left\{0, \min\left\{1, \frac{(\lambda_2-\lambda_1)I_C}{C_2}\right\}\right\}, \\ w_3^* &= \max\left\{0, \min\left\{1, \frac{(\lambda_4-\lambda_3)I_H}{C_3}\right\}\right\}, \\ w_4^* &= \max\left\{0, \min\left\{1, \frac{\lambda_6 I_S+\lambda_5 S_S}{C_4}\right\}\right\}. \end{aligned}\right\} \tag{6.19}$$

Proof. Pontryagin's maximum principle ensures that for any optimal solution (X,w) to an optimal control problem, there exists a non-trivial adjoint variable vector function $\lambda = (\lambda_1, \lambda_2, \lambda_3, \lambda_4, \lambda_5, \lambda_6, \lambda_7, \lambda_8)$. This adjoint variable vector function (λ) must meet the transversality conditions, where each component $\lambda_i(T) = 0$ at the final time T, for $i = 1$ to 8.

$$\left.\begin{aligned} \frac{d\lambda_1}{dt} &= -\frac{\partial \mathscr{H}}{\partial S_C}, \\ \frac{d\lambda_2}{dt} &= -\frac{\partial \mathscr{H}}{\partial I_C}, \\ \frac{d\lambda_3}{dt} &= -\frac{\partial \mathscr{H}}{\partial S_H}, \\ \frac{d\lambda_4}{dt} &= -\frac{\partial \mathscr{H}}{\partial I_H}, \\ \frac{d\lambda_5}{dt} &= -\frac{\partial \mathscr{H}}{\partial S_S}, \\ \frac{d\lambda_6}{dt} &= -\frac{\partial \mathscr{H}}{\partial I_S}, \\ \frac{d\lambda_7}{dt} &= -\frac{\partial \mathscr{H}}{\partial M}, \\ \frac{d\lambda_8}{dt} &= -\frac{\partial \mathscr{H}}{\partial P}. \end{aligned}\right\} \tag{6.20}$$

The optimality conditions are derived by differentiating the Hamiltonian function from the control variables and identifying the points where these derivatives equal zero.

$$\frac{\partial \mathscr{H}(t, X, w, \lambda)}{\partial w_i} = 0 \tag{6.21}$$

Deriving the adjoint system and differentiating the Hamiltonian function yields the

following expression:

$$\begin{cases} \dfrac{\partial \mathscr{H}}{\partial w_1} = C_1 w_1 + (\dfrac{\beta_2 P(t) S_H(t)}{1+\alpha P(t)})\lambda_3 - (\dfrac{\beta_2 P(t) S_H(t)}{1+\alpha P(t)})\lambda_4 = 0, \\ \dfrac{\partial \mathscr{H}}{\partial w_2} = C_2 w_2 + \lambda_1(I_C) - \lambda_2(I_C) = 0, \\ \dfrac{\partial \mathscr{H}}{\partial w_3} = C_3 w_3 + \lambda_3(I_H) - \lambda_4(I_H) = 0, \\ \dfrac{\partial \mathscr{H}}{\partial w_4} = C_4 w_4 - \lambda_5 S_S - \lambda_6 I_S = 0. \end{cases} \tag{6.22}$$

Solving the equations (6.22) for the control variables (w_i) results in the expression given in equation (6.19).

6.6 Simulations of the Optimal Control Model and Discussion

This section uses numerical simulations to investigate the optimality system for managing *Fasciola hepatica* infections in humans and cattle. The simulations were conducted using the fourth-order Runge-Kutta method and the forward-backwards sweep technique as outlined by Lenhart & Workman ((2007). The parameter values listed in Table 6.2 were used for the simulation and optimization processes to generate visualizations and results. The initial values for simulating the optimality system were set as follows: $S_C = 1000$, $I_C = 250$, $S_H = 3000$, $I_H = 70$, $S_S = 100000$, $I_S = 10000$, $M = 4500$ and $P = 30000$. The associated costs were: $C_1 = 20$, $C_2 = 30$, $C_3 = 30$, $C_4 = 40$, $C_5 = 40$ and $C_6 = 60$. Four scenarios were examined, each representing different configurations or strategies involving the four control variables. These scenarios were categorized as single, double, triple and quadruple interventions.

6.6.1 Scenario 1: Single Intervention

In this scenario, we focus on the individual impact of a specific optimal control variable, w_i, while disregarding the influence of all other optimal controls, w_j, where $i \neq j$, where i and j are in the set $\{1,2,3,4\}$. Figures 6.3a and 6.3b present the results, indicating the impacts of each control strategy on the number of infected cattle and humans. By adopting this approach, we isolate the effects of each optimal control variable, disregarding the presence or influence of the other control variables.

The results demonstrate that the application of these control measures leads to a significant decrease in the population of infected cattle and humans compared to the scenario without any control interventions. This indicates the effectiveness of the implemented control strategies in reducing the number of infections in both populations. Despite the effectiveness of the control strategies in reducing the infected population of both cattle and humans, it is essential to note that the strategies do not eliminate the disease in infected cattle within the first 100 days. However, the infected human population is expected to be eliminated during this time frame.

Figure (6.3c) displays the control profile for individual interventions, showing that w_1 remains at maximum for 10 days, w_2 for 20 days, w_3 for 10 days and w_4 for 5 days. This profile helps to understand the duration and intensity of each control variable during the intervention period, enhancing our comprehension of how control strategies are implemented over time

6.6.2 Scenario 2: Double Intervention

In this scenario, we explore six distinct strategies:

Strategy A: Optimal public health education (w_1) and infected cattle treatment (w_2).

Strategy B: Optimal public health education (w_1) and treatment of infected humans (w_3).

Strategy C: optimal public health education (w_1) and snail removal using chemical molluscicides (w_4).

Strategy D: Optimal treatment of infected cattle (w_2) and treatment of infected humans (w_3).

Strategy E: Optimal treatment of infected cattle (w_2) and snail removal using chemical molluscicides (w_4).

Strategy F: Optimal treatment of infected humans (w_3) and snail removal using chemical molluscicides (w_4).

According to Figure 6.4a, all double strategies contribute to reducing the disease burden in cattle compared to the noncontrol scenario. Although strategy E and strat-

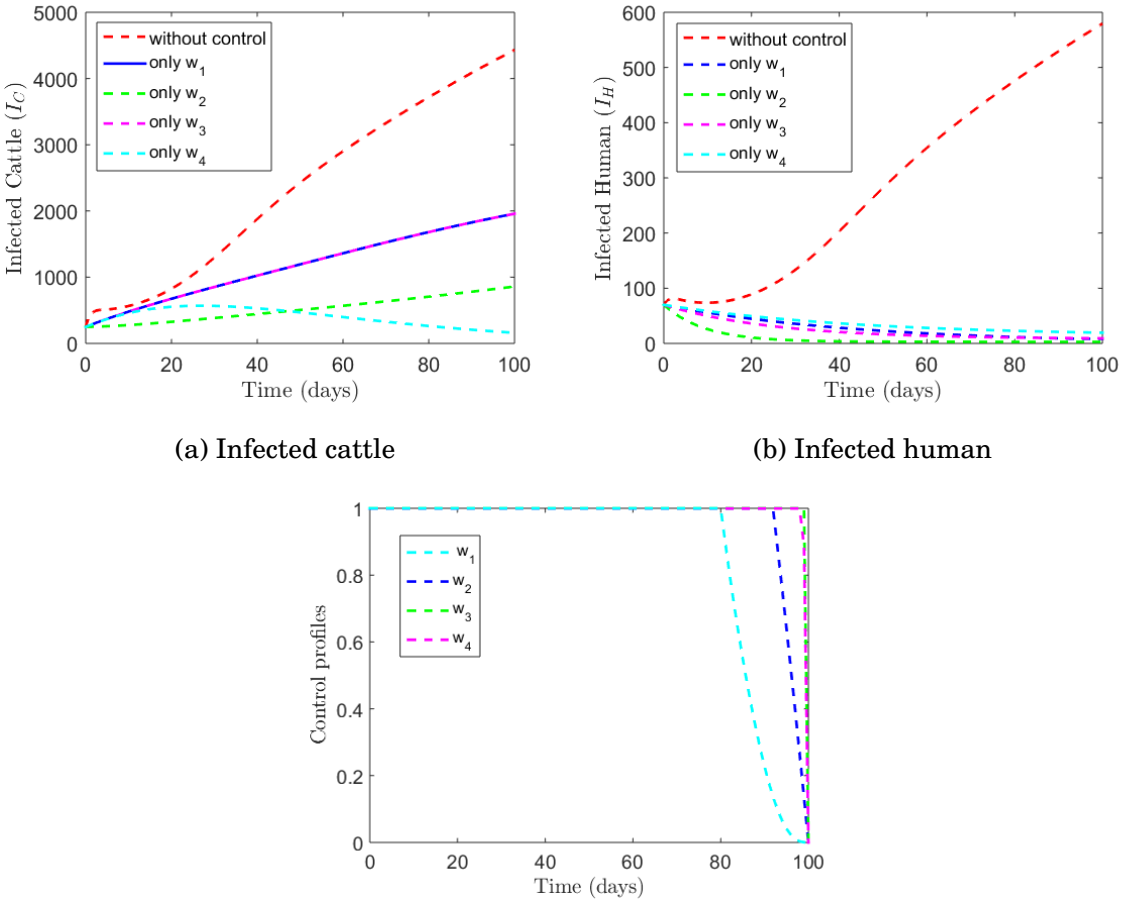

(a) Infected cattle

(b) Infected human

(c) Control profiles

Figure 6.3: The progression of infected humans and cattle, along with the control profile for a single control strategy.

egy F stand out as the most effective in decreasing the number of infected cattle, it is important to note that all three strategies demonstrate a positive impact on mitigating the disease's effects on the cattle population. These two options outperformed the other three strategies to reduce the number of infected cattle.

Figure 6.4b demonstrates the effectiveness of all strategies in reducing the number of infected humans. In particular, strategy A is the most successful approach to eliminating disease in the human population. Although all strategies contribute to reducing human infections, strategy A stands out for its exceptional ability to eradicate the disease. This underscores the effectiveness of strategy A in achieving the

goal of disease elimination in humans, making it the preferred choice among the evaluated strategies.

Figure 6.5 shows the control profiles of the double control strategies, which show the patterns or profiles of control variables for the strategies involving combination of two controls. This figure provides insights into the duration, intensity and interplay of these control variables, providing a visual representation of how the double control strategies are implemented over time.

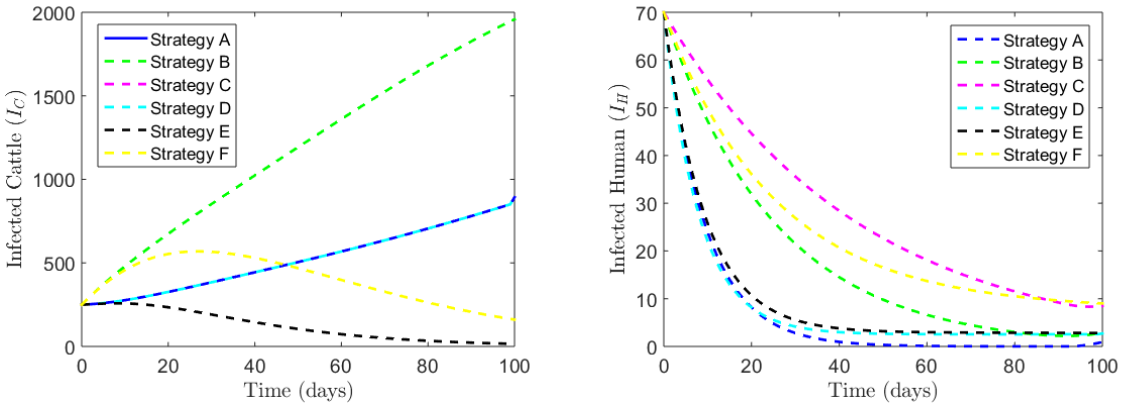

(a) Infected cattle

(b) Infected human

Figure 6.4: The progression of infected humans and cattle for double control.

6.6.3 Scenario 3: Triple Intervention

In this scenario, the main objective is to analyze and evaluate six different strategies by integrating various control measures:

Strategy G: optimal public health education (w_1), treatment of infected cattle (w_2) and treatment of infected humans (w_3).

Strategy H: optimal public health education (w_1), treatment of infected cattle (w_2) and snail removal using chemical molluscicides (w_4).

Strategy I: optimal public health education (w_1), treatment of infected humans (w_3) and snail removal using chemical molluscicides (w_4).

Strategy J: optimal treatment of infected cattle (w_2), treatment of infected humans (w_3) and snail removal using chemical molluscicides (w_4).

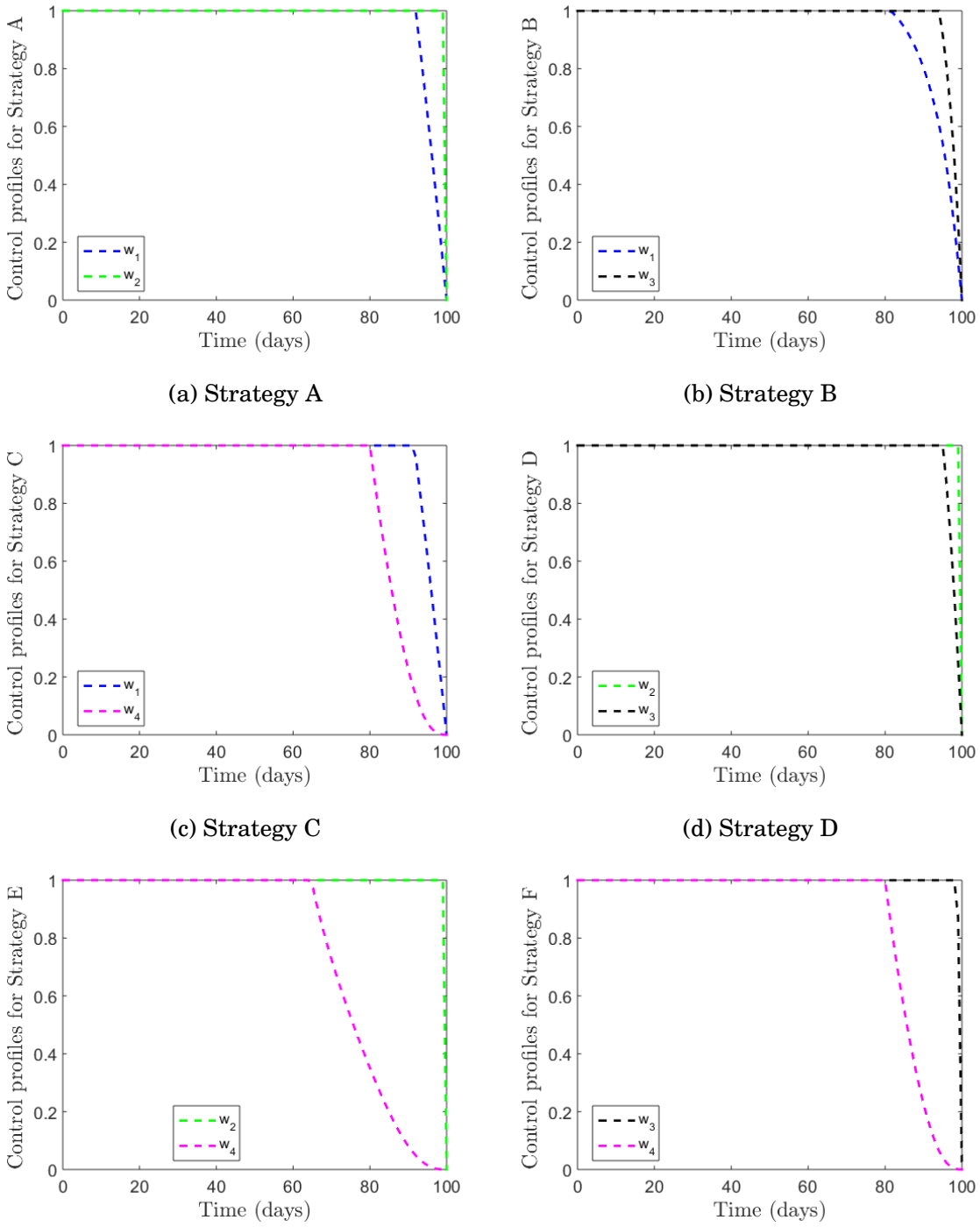

(a) Strategy A

(b) Strategy B

(c) Strategy C

(d) Strategy D

(e) Strategy E

(f) Strategy F

Figure 6.5: The control profiles for the double control strategies.

Figure 6.6a provides evidence of the effectiveness of strategies H, I and J in reducing the number of infected cattle. In particular, both strategy H and strategy J play

an equal role in eradicating disease within the cattle population. These strategies demonstrate comparable effectiveness in achieving the goal of disease elimination among cattle. The results underscore the significant impact of the strategies H and J in reducing the disease burden and successfully removing it within the cattle population.

Figure 6.6b illustrates that all strategies effectively reduce the number of infected humans. However, strategies G and H emerge as the most successful approaches to eliminating disease in the human population. These two strategies demonstrate exceptional effectiveness in achieving the objective of eradication of disease in humans.

Figure 6.7 shows that the control profile for the treatment of infected cattle (w_2) is characterized by a high intensity control strategy. This means that there is a strong emphasis on implementing rigorous measures to treat and manage the infected cattle population. The high-intensity control plan indicates that significant efforts and resources are being directed toward effective treatment of the infection in cattle and minimizing its spread.

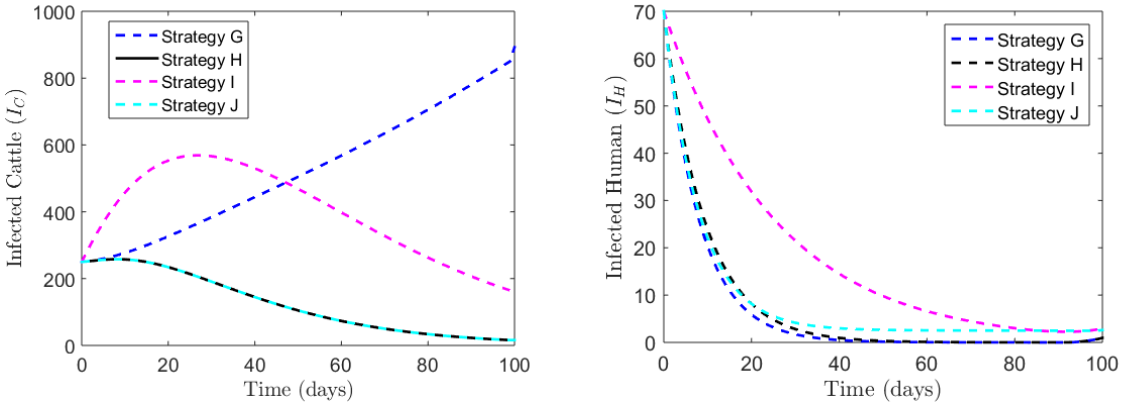

(a) Infected cattle

(b) Infected human

Figure 6.6: The progression of infected humans and cattle for triple control.

6.6.4 Scenario 4: Quadruple Intervention

The last strategy K, which encompasses the four combined individual strategies: optimal public health education (w_1), treatment of infected cattle (w_2), treatment of

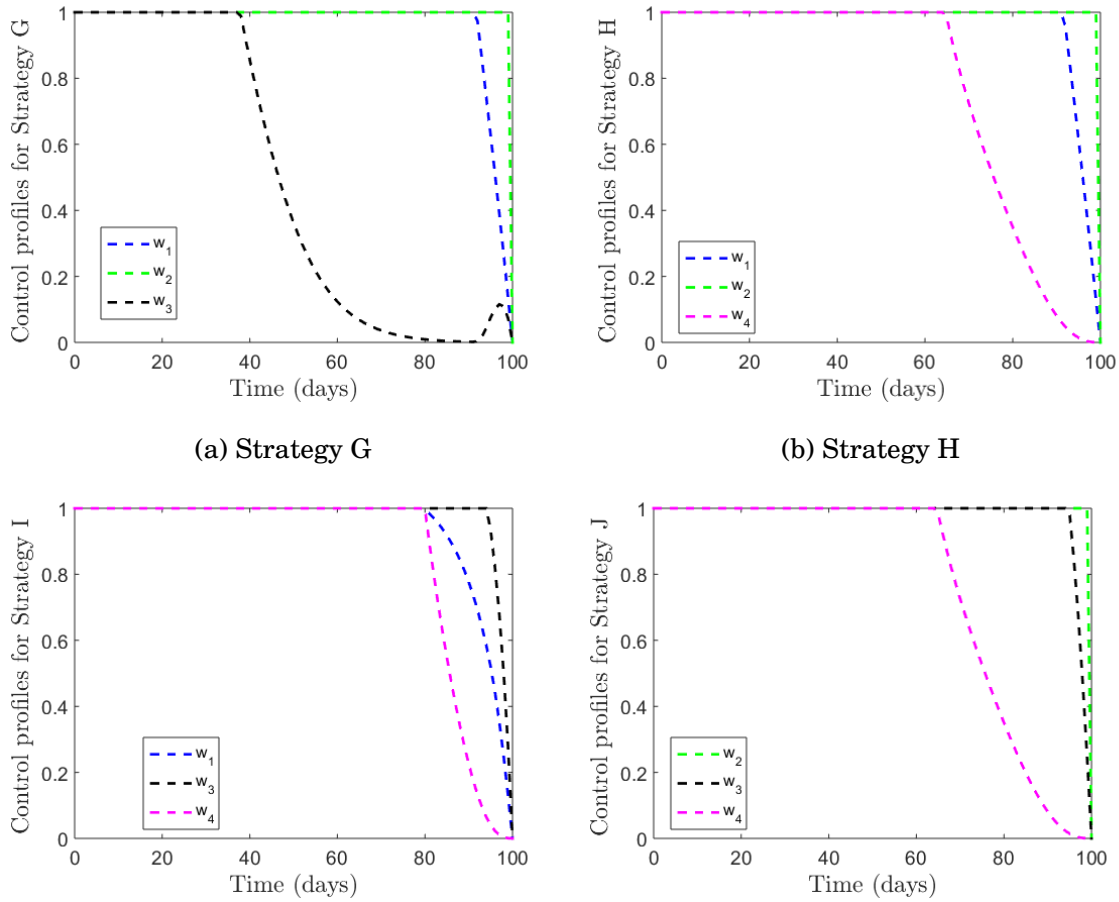

(a) Strategy G

(b) Strategy H

(c) Strategy I

(d) Strategy J

Figure 6.7: The control profiles for the triple control strategies.

infected humans (w_3) and snail removal using chemical molluscicides (w_4). Figures 6.8a and 6.8b demonstrate that the implementation of all control measures (strategy K) effectively reduces the number of infected cattle and successfully eradicates the disease in both the cattle and human populations. The results indicate that strategy K, which combines multiple control measures, is highly effective in mitigating the spread of the disease and achieving the desired results of disease control and elimination in both populations. The figures provide strong evidence of the effectiveness of strategy K in reducing disease burden and ultimately eradicating disease in both cattle and humans. Figure 6.8c further reveals that the control profile for the treatment of infected cattle (w_2) sustains a high intensity control strategy for a duration

of 100 days.

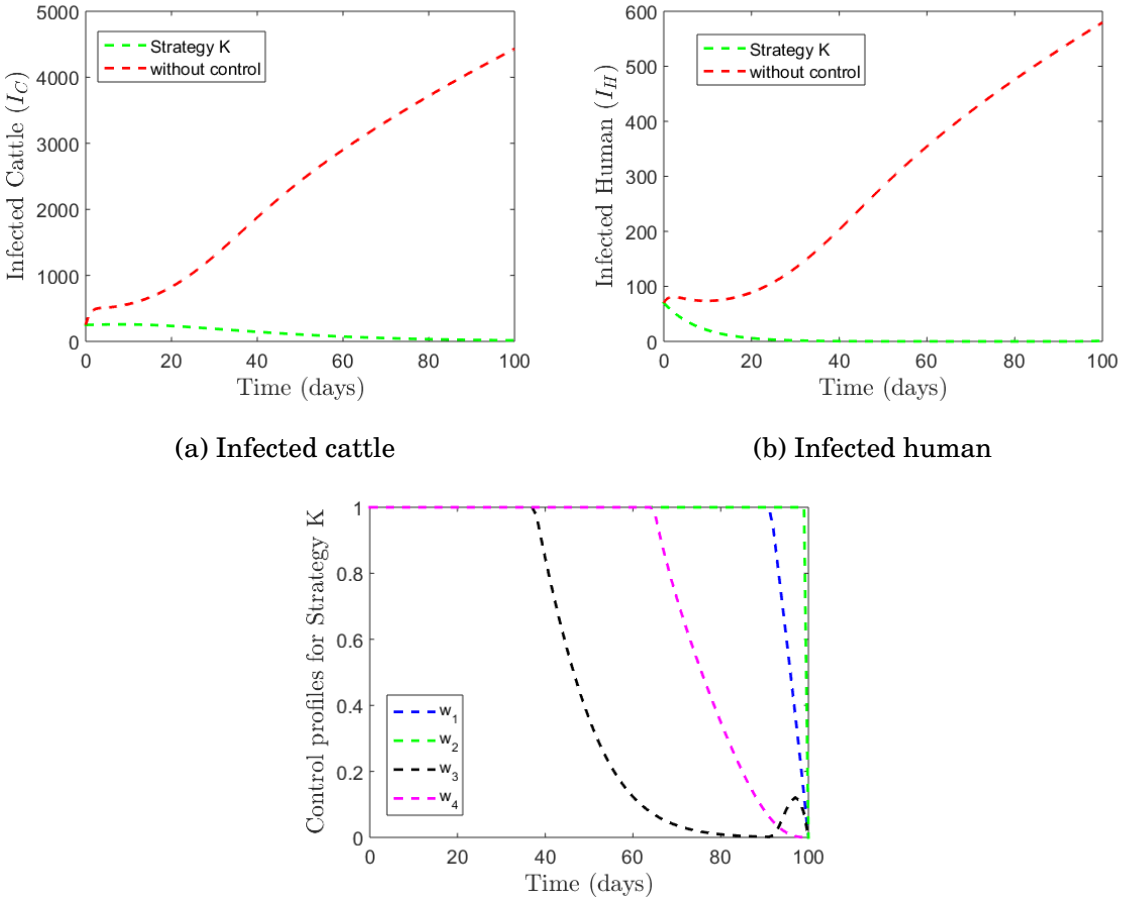

(a) Infected cattle

(b) Infected human

(c) Control profile

Figure 6.8: The progression of infected humans and cattle for quadruple controls.

6.7 Conclusion

This chapter presents a mathematical model of optimal deterministic control to analyze *Fasciola hepatica* transmission dynamics in susceptible or infected cattle, humans and snails. The model used the next-generation matrix approach to calculate the basic reproduction number. The results indicate that if this number is less than one, the disease-free equilibrium is asymptotically stable both locally and globally. Furthermore, the endemic equilibrium is locally asymptotically stable if $R_0 > 1$. The model was expanded to include time-dependent optimal control variables, which were assessed using Pontryagin's maximum principle to evaluate their effectiveness in mitigating the burden of *Fasciola hepatica*.

The numerical simulation results show that combination of control measures in strategy K, which includes public health education, the treatment of infected cattle, the treatment of infected humans and the removal of snails using chemical molluscicides, is exceptionally effective in curbing the transmission of disease. This comprehensive strategy demonstrates significant success in reducing the disease's impact and accomplishing the intended goals of disease control and elimination in both the cattle and human populations. This finding is consistent with the study by [35], which showed that although each control measure individually reduces *fascioliasis* infection, the combined implementation of all control strategies is significantly more effective in reducing the high prevalence of the disease in domestic animals.

The result also indicates that to maximize effectiveness, the treatment intervention for infected cattle should always be set at its highest value. This finding highlights the critical role of treating infected cattle in effectively controlling the spread of *fascioliasis*. Recent studies consistently emphasize the importance of comprehensive and aggressive treatment protocols for the treatment of *Fasciola hepatica*. The result consistent with Charlier et al. (2020) emphasises that high-intensity treatment interventions can significantly reduce the burden of the disease, leading to better health outcomes for both the cattle and human populations. Similarly, Beesley et al. (2018) shows that robust treatment strategies not only improve the immediate health of in-

fected animals, but also contribute to long-term disease control by interrupting the parasite's transmission cycle.

Stakeholders should adopt a comprehensive strategy that includes public health education, treating infected cattle and humans and the use of chemical molluscicides to remove snails. This integrated approach has proven highly effective in controlling the disease, with the recommendation to treat infected cattle as intensively as possible for the best results.

Chapter 7

7 Conclusion, Future Work and Recommendations

7.1 Conclusion

This study developed deterministic mathematical models to analyze the dynamics of *Fasciola hepatica* in cattle and humans. These models characterize host-parasite interactions (cattle, humans, snails and parasites) to predict the spread of *fasciolosis* and its impact under various conditions, providing significant information on the disease. The positivity, boundedness, local and global stability, forward bifurcation and sensitivity analysis of the models were analyzed. Stability analysis reveals conditions for disease equilibrium, which informs the development of sustainable management practices. The models identify key parameters influencing *fasciolosis* transmission and intermediate host survival, thus explaining long-term disease behavior and persistence. Optimal controls were achieved using Pontryagin's maximum principle and cost-effectiveness analysis was performed using the incremental cost-effectiveness ratio.

The first model examined the dynamics of *Fasciola hepatica*, incorporating cattle as the primary host and snails as the intermediate host. Miracidia and metacercariae were included as larval parasite stages within a transmission compartmental model. The results indicate that the snail death rate is a highly sensitive parameter that indirectly influences the spread of the disease. Simulations indicate that reducing the population of miracidia, metacercariae and snails, improving treatment and limiting pathogen transfer between cattle and snails reduce the prevalence of disease in cattle.

The second model employs optimal control to assess the cost-effectiveness of *Fasciola hepatica* control in cattle. The model uses the Pontryagin maximum principle to optimize strategies for pasture management, cattle treatment and the use of mollus-

cicides for snail control. Cost-effectiveness analysis shows that pasture management combined with maximum effort use of molluscicides for snail removal is the most cost-effective disease control strategy.

The third model considers exposed groups in cattle and snails and it addresses treatment for exposed and infected cattle. The global stability of the endemic equilibrium is explored using the Volterra-Lyapunov method and a forward bifurcation indicates the potential coexistence of disease-free and endemic states. The sensitivity analysis identified transmission rates in snails and cattle and shedding rates of miracidia and metacercariae, as key parameters of disease spread. Controlling snail populations with molluscicide and improving treatment for infected cattle effectively reduces the prevalence of *Fasciola hepatica* in cattle.

The fourth model provides a mathematical analysis of *Fasciola hepatica* epidemics to understand disease spread and identify effective prevention and control measures for cattle and humans. It shows that all the control strategies implemented, including public health education, the treatment of infected individuals and the use of molluscicides, significantly reduced infections in both populations. Integrated all control measures led to an immediate and significant decrease in infected cattle and human populations. Maximizing the treatment of infected cattle was identified as a crucial element in the control of *Fasciola hepatica*.

In general, snail mortality rate significantly influences disease transmission. Molluscicides are the most significant intervention to control *Fasciola hepatica*. Model (4.1) is better than model (3.1) because it investigated disease control strategies and identifies the most cost-effective approach. Model (5.1) excels in early diagnosis and treatment, significantly reducing the disease burden. The final model 6.1 is superior due to its inclusive multi-host and multi-control strategies for managing *Fasciola hepatica* in cattle and humans.

7.2 Future Work

Deterministic models offer valuable insights into *fascioliasis* transmission and control in cattle and humans, although their precision can be further enhanced through

future research addressing their limitations.

- Deterministic models of *fascioliasis* transmission often simplify biological and ecological processes with assumptions like homogeneous host mixing and uniform miracidia/metacercariae densities, neglecting real-world complexities.
- These models do not account for random events and variability, which can be important in the transmission of diseases, especially in small populations or at low prevalence levels.
- The models may not fully capture the complexity of the host and vector life cycles, including seasonal variations and environmental influences on their populations.

Further research is needed to address several open mathematical questions.

- As data becomes available, update the models to improve its predictive power and relevance.
- Expanding the models to include multiple host and vector species is a more comprehensive understanding of transmission dynamics.
- Developing stochastic models for improved realism, particularly in low-prevalence or small-population scenarios.
- Integrating climate change and environmental variability effects to predict their impact on snail and main host distribution and transmission dynamics.
- Co-infection studies enhance our understanding of infectious disease dynamics, particularly in cases such as *fascioliasis* and schistosomiasis, and *fascioliasis* and echinococcosis.

7.3 Recommendations

This study analyzes the dynamics of *Fasciola hepatica* disease and evaluates control strategies. The dissertation recommends governments, policymakers and stake-

holders improve disease control in humans and cattle by increasing preventive measures, including public health education, molluscicide use for snail removal, pasture management and treatments. Policymakers and health administrators focused primarily on identifying and forecasting the most cost-effective intervention strategies. This study explored cost-effective analyses to investigate the best disease reduction strategies, found that pasture management combined with the use of molluscicide at the highest level offers the most effective and least expensive option.

Interdisciplinary collaboration across health, agriculture and mathematical modeling is essential. To improve the precision and effectiveness of the model, stakeholders must address the difficulty of accessing national or global *fascioliasis* distribution data in cattle and humans by improving data collection on prevalence, snail distribution and environmental factors. The systematic collection and organization of data within agricultural and health institutions is crucial for effective modeling and simulation. Integrate human, animal and environmental health surveillance with rapid diagnostics for early outbreak detection, facilitating data-driven research and timely disease management.

References

Abdisa, T. & Jilo, K. (2017), 'Review on ovine fasciolosis in ethiopian', *J Vet Sci Res* **2**, 1–10.

Aderyani, S. R., Saadati, R., Abolhassanifar, M. S. & O'Regan, D. (2025), 'Bifurcation analysis of small amplitude unidirectional waves for nonlinear Schrödinger equations with fractional derivatives', *Scientific Reports* **15**(1), 9895.

Admassu, B., Shite, A. & Kinfe, G. (2015), 'A review on bovine fasciolosis', *European Journal of Biological Sciences* **7**(3), 139–146.

Agusto, F. B. & ELmojtaba, I. M. (2017), 'Optimal control and cost-effective analysis of malaria/visceral leishmaniasis co-infection', *PLoS One* **12**(2), e0171102.

Ai, L., Chen, M.-X., Alasaad, S., Elsheikha, H. M., Li, J., Li, H.-L., Lin, R.-Q., Zou, F.-C., Zhu, X.-Q. & Chen, J.-X. (2011), 'Genetic characterization, species differentiation and detection of fasciola spp. by molecular approaches', *Parasites & Vectors* **4**, 101.

Alba, A., Vázquez, A. A., Sánchez, J., Duval, D., Hernández, H. M., Sabourin, E., Vittecoq, M., Hurtrez-Boussés, S. & Gourbal, B. (2018), 'Fasciola hepatica-pseudosuccinea columella interaction: effect of increasing parasite doses, successive exposures and geographical origin on the infection outcome of susceptible and naturally-resistant snails from Cuba', *Parasites & Vectors* **11**(1), 1–9.

Alemneh, H. T. (2020), 'Mathematical modeling, analysis, and optimal control of corruption dynamics', *Journal of Applied Mathematics* **2020**, 1–13.

Alemu, B. (2019), 'Bovine fasciolosis in Ethiopia-a review', *Journal of Veterinary and Animal Research* **2**, 202.

Anderson, R. M. & May, R. M. (1991), *Infectious diseases of humans: dynamics and control*, Oxford university press.

Anggreini, D. (2016), 'Local stability analysis of a mathematical model of the interaction of two populations of differential equations (host-parasitoid)', *Biology, Medicine, & Natural Product Chemistry* **5**(1), 9–14.

Ardo, M. & Aliyara, Y. (2014), 'Prevalence of fasciolosis in small ruminants slaughtered at Yola Modern Abattoir, Adamawa state, Nigeria', *Bayero Journal of Pure and Applied Sciences* **7**, 13–16.

Arrowsmith, D. & Place, C. M. (1992), *Dynamical systems: differential equations, maps, and chaotic behaviour*, Vol. 5, CRC Press.

Asamoah, J. K. K., Jin, Z., Sun, G.-Q., Seidu, B., Yankson, E., Abidemi, A., Oduro, F., Moore, S. E. & Okyere, E. (2021), 'Sensitivity assessment and optimal economic evaluation of a new COVID-19 compartmental epidemic model with control interventions', *Chaos, Solitons & Fractals* **146**, 110885.

Asamoah, J. K. K., Okyere, E., Abidemi, A., Moore, S. E., Sun, G.-Q., Jin, Z., Acheampong, E. & Gordon, J. F. (2022), 'Optimal control and comprehensive cost-effectiveness analysis for COVID-19', *Results in Physics* **33**, 105177.

Asamoah, J. K. K., Yankson, E., Okyere, E., Sun, G.-Q., Jin, Z., Jan, R. et al. (2021), 'Optimal control and cost-effectiveness analysis for dengue fever model with asymptomatic and partial immune individuals', *Results in Physics* **31**, 104919.

Ashrafi, K., Valero, M. A., Peixoto, R. V., Artigas, P., Panova, M. & Mas-Coma, S. (2015), 'Distribution of *Fasciola hepatica* and *F. gigantica* in the endemic area of Guilan, Iran Relationships between zonal overlap and phenotypic traits', *Infection, Genetics and Evolution* **31**, 95–109.

Atalabi, T. E. & Lawal, O. T. (2020), 'Fascioliasis: A foodborne disease of veterinary and zoonotic importance', *Rural Health* .

Avazzadeh, Z., Hassani, H., Agarwal, P., Mehrabi, S., Javad Ebadi, M. & Hosseini Asl, M. K. (2023), 'Optimal study on fractional fascioliasis disease model based on generalized fibonacci polynomials', *Mathematical Methods in the Applied Sciences* **46**(8), 9332–9350.

Ayele, M. & Hiko, A. (2016), 'Review on the biology of fasciola parasites and the epidemiology on small ruminants', *Adv Life Sci Technol* **48**, 19–27.

Bahiru, A. & Assefa, A. (2020), 'Prioritization of economically important cattle diseases using participatory epidemiology tools in Lalibela, Sekota, and Ziquala districts of Amhara region, Northern Ethiopia', *Veterinary Medicine International* **2020**(1), 5439836.

Bakare, E. A., Nwagwo, A. & Danso-Addo, E. (2014), 'Optimal control analysis of an sir epidemic model with constant recruitment', *International Journal of Applied Mathematics Research* **3**(3), 273–285.

Bargues, M. D., Valero, M. A., Trueba, G. A., Fornasini, M., Villavicencio, A. F., Guamán, R., Elías-Escribano, D., Pérez-Crespo, I., Artigas, P., Mas-Coma, S. et al. (2021), 'DNA Multi-Marker Genotyping and CIAS Morphometric Phenotyping of Fasciola gigantica-Sized Flukes from Ecuador, with an Analysis of the Radix Absence in the New World and the Evolutionary Lymnaeid Snail Vector Filter', *Animals* **11**(9), 2495.

Barker, G. P., Berman, A. & Plemmons, R. J. (1978), 'Positive diagonal solutions to the lyapunov equations', *Linear and Multilinear Algebra* **5**(4), 249–256.

Bat, A., Kamil, A. et al. (2010), 'Optimal control of a production inventory system with generalized pareto distributed deterioration items', *Journal of Applied Sciences* **10**(2), 116–123.

Batista, M. (2021), 'On the reproduction number in epidemics', *Journal of Biological Dynamics* **15**(1), 623–634.

Beesley, N., Caminade, C., Charlier, J., Flynn, R., Hodgkinson, J., Martinez-Moreno, A., Perez, J., Rinaldi, L. & Williams, D. (2018), 'Fasciola and fasciolosis in ruminants in Europe: Identifying research needs', *Transboundary and Emerging Diseases* **65**, 199–216.

Bishop, S. C., Axford, R. F., Nicholas, F. W. & Owen, J. B. (2010), *Breeding for disease resistance in farm animals*, CABI.

Brauer, F. (2017), 'Mathematical epidemiology: Past, present, and future', *Infectious Disease Modelling* **2**(2), 113–127.

Bridle, H. (2021), Overview of waterborne pathogens, *in* 'Waterborne pathogens', Elsevier.

Burden, T. N., Ernstberger, J. & Fister, K. R. (2004), 'Optimal control applied to immunotherapy', *Discrete and Continuous Dynamical Systems Series B* **4**(1), 135–146.

Capó-Lugo, P. A. & Bainum, P. M. (2011), 7 - continuous and digital control systems, *in* 'Orbital Mechanics and Formation Flying', Woodhead Publishing.
URL: *https://www.sciencedirect.com/science/article/pii/B9780857090546500076*

Caravedo, M. A. & Cabada, M. M. (2020), 'Human fascioliasis: Current epidemiological status and strategies for diagnosis, treatment, and control', *Research and Reports in Tropical Medicine* **11**, 149.

Castillo-Chavez, C., Feng, Z. & Huang, W. (2002), 'On the computation of R_0 and its role on global stability', *Mathematical Approaches for Emerging and Re-emerging Infection Diseases: An Introduction* **125**, 31–65.

Castillo-Chavez, C. & Song, B. (2004), 'Dynamical models of tuberculosis and their applications', *Mathematical Biosciences and Engineering* **1**(2), 361.

CDC (2019), 'Global health, division of parasitic diseases and malaria: Fascioliasis'.
URL: *https://www.cdc.gov/dpdx/fascioliasis/index.html*

CDC (2020), 'Global health, division of parasitic diseases and malaria: Parasites'.
URL: *https://www.cdc.gov/parasites/fasciola/*

Charlier, J., Rinaldi, L., Musella, V., Ploeger, H. W., Chartier, C., Vineer, H. R., Hinney, B., von Samson-Himmelstjerna, G., Băcescu, B., Mickiewicz, M. et al. (2020), 'Initial assessment of the economic burden of major parasitic helminth infections to the ruminant livestock industry in Europe', *Preventive Veterinary Medicine* **182**, 105103.

Cheneke, K. R. (2023), Forward bifurcation and stability analysis, *in* 'Bifurcation Theory with Applications', IntechOpen.

Chien, F. & Shateyi, S. (2021), 'Volterra–lyapunov stability analysis of the solutions of babesiosis disease model', *Symmetry* **13**(7), 1272.

Chiyaka, E. T. & Garira, W. (2009), 'Mathematical analysis of the transmission dynamics of schistosomiasis in the human-snail hosts', *Journal of Biological Systems* **17**(03), 397–423.

Cuervo, P. F., Bargues, M. D., Artigas, P., Buchon, P., Angles, R. & Mas-Coma, S. (2024), 'Global warming induced spread of the highest human fascioliasis hyperendemic area', *Parasites & Vectors* **17**(1), 434.

Dhar, P. (2016), *Thermal System Design and Simulation*, Academic Press.

Diaby, M., Diop, O., Nassouri, E., Sène, A. & Sène, M. (2019), 'Mathematical analysis of fasciola epidemic model with treatment and quarantine', pp. 133–148.

Diaby, M., Diop, O., Nassouri, E., Sène, A. & Sène, M. (2021), 'Mathematical analysis of fasciola epidemic model with treatment and quarantine', *Modelling, Simulation and Applications of Complex Systems: CoSMoS 2019, Penang, Malaysia, April 8-11, 2019* **359**, 133.

Diaz-Quevedo, C., Frias, H., Cahuana, G. M., Tapia-Limonchi, R., Chenet, S. M. & Tejedo, J. R. (2021), 'High prevalence and risk factors of fascioliasis in cattle in Amazonas, Peru', *Parasitology International* **84**, 102428.

Dietz, K. & Heesterbeek, J. (2002), 'Daniel Bernoulli's epidemiological model revisited', *Mathematical Biosciences* **180**(1-2), 1–21.

Diyana, J. N. A., Lokman, I., Fazila, S. N., Latiffah, H., Ibitoye, E., Hazfalinda, H. N., Chandrawathani, P., Juriah, K. & Mahiza, M. N. (2019), 'A retrospective study on bovine fascioliasis in veterinary regional laboratories in Peninsular Malaysia', *Journal of Parasitology Research* **2019**(1), 7903682.

Dube, A., Kalinda, C., Manyangadze, T., Mindu, T. & Chimbari, M. J. (2023), 'Effects of temperature on the life history traits of intermediate host snails of fascioliasis: a systematic review', *PLoS Neglected Tropical Diseases* **17**(12), e0011812.

Engida, H. A., Gathungu, D. K., Ferede, M. M., Belay, M. A., Kawe, P. C. & Mataru, B. (2024), 'Optimal control and cost-effectiveness analysis for the human melioidosis model', *Heliyon* **10**(4).

Feyisa, T. (2021), 'Review on epidemiology, control and public health importance of bovine fasciolosis', *Austin Journal of Veterinary Science and Animal Husbandry* **8**(2), 1082.

Fontenla, S., Langleib, M., de la Torre-Escudero, E., Domínguez, M. F., Robinson, M. W. & Tort, J. (2022), 'Role of Fasciola hepatica Small RNAs in the Interaction with the Mammalian Host', *Frontiers in Cellular and Infection Microbiology* **11**, 812141.

Gaff, H. & Schaefer, E. (2009), 'Optimal control applied to vaccination and treatment strategies for various epidemiological models', *Mathematical Biosciences & Engineering* **6**(3), 469–492.

García-López, X., Jaramillo-Meza, L., Quiroz-Romero, H., Arriaga-Díaz, C., Martínez-Maya, J., Diosdado-Vargas, F. & Díaz-Otero, F. (2018), 'Effect of coinfection by fasciola hepatica and mycobacterium bovis on bovine tuberculosis immunodiagnosis in an enzootic area Hidalgo State, Mexico', *Journal of Veterinary Healthcare* **1**(4), 41.

Goodall, E., McIlroy, S., McCracken, R., McLoughlin, E. & Taylor, S. (1991), 'A mathematical forecasting model for the annual prevalence of fasciolosis', *Agricultural Systems* **36**(2), 231–240.

Gumel, A. B. (2012), 'Causes of backward bifurcations in some epidemiological models', *Journal of Mathematical Analysis and Applications* **395**(1), 355–365.

Gupta, N., Verma, R., Dhiman, R. K., Rajsekhar, K. & Prinja, S. (2020), 'Cost-effectiveness analysis and decision modelling: a tutorial for clinicians', *Journal of Clinical and Experimental Hepatology* **10**(2), 177–184.

Heffernan, J. M., Smith, R. J. & Wahl, L. M. (2005), 'Perspectives on the basic reproductive ratio', *Journal of the Royal Society Interface* **2**(4), 281–293.

Hershkowitz, D. (1992), 'Recent directions in matrix stability', *Linear Algebra and its Applications* **171**, 161–186.

Hethcote, H. W. (2000), 'The mathematics of infectious diseases', *SIAM Review* **42**(4), 599–653.

Howell, A., Baylis, M., Smith, R., Pinchbeck, G. & Williams, D. (2015), 'Epidemiology and impact of fasciola hepatica exposure in high-yielding dairy herds', *Preventive Veterinary Medicine* **121**(2), 41–48.

Kadaleka, S., Abelman, S., Mwamtobe, P. & Tchuenche, J. (2021), 'Optimal control analysis of a human–bovine schistosomiasis model', *Journal of Biological Systems* **29**(01), 1–26.

Kahuru, J., Luboobi, L. S. & Nkansah-Gyekye, Y. (2017), 'Optimal control techniques on a mathematical model for the dynamics of tungiasis in a community', *International Journal of Mathematics and Mathematical Sciences* **2017**(1), 4804897.

Kamaruddin, N. C., Razali, M. A. I., Busayo, I. E., Hamzah, N. H., Idris, L. H. & Md Isa, N. M. (2021), 'The first report of ruminant fascioliasis in Sabah, East Malaysia', *Journal of Parasitology Research* **2021**(1), 6691483.

Kanyi, E., Afolabi, A. S. & Onyango, N. O. (2021), 'Mathematical modeling and analysis of transmission dynamics and control of schistosomiasis', *Journal of Applied Mathematics* **2021**(1), 6653796.

Kaset, C., Eursitthichai, V., Vichasri-Grams, S., Viyanant, V. & Grams, R. (2010), 'Rapid identification of lymnaeid snails and their infection with Fasciola gigantica in Thailand', *Experimental Parasitology* **126**(4), 482–488.

Kelley, J. M., Elliott, T. P., Beddoe, T., Anderson, G., Skuce, P. & Spithill, T. W. (2016), 'Current threat of triclabendazole resistance in fasciola hepatica', *Trends in Parasitology* **32**(6), 458–469.

Khan, M. A., Bonyah, E., Li, Y.-X., Muhammad, T. & Okosun, K. (2021), 'Mathematical modeling and optimal control strategies of Buruli ulcer in possum mammals', *AIMS Mathematics* **6**(9), 9859–9881.

Kirk, D. E. (2004), *Optimal control theory: an introduction*, Courier Corporation.

Knubben-Schweizer, G., Rüegg, S., Torgerson, P. R., Rapsch, C., Grimm, F., Hässig, M., Deplazes, P. & Braun, U. (2010), 'Control of bovine fasciolosis in dairy cattle in Switzerland with emphasis on pasture management', *The Veterinary Journal* **186**(2), 188–191.

Kouidere, A., Balatif, O. & Rachik, M. (2023), 'Cost-effectiveness of a mathematical modeling with optimal control approach of spread of COVID-19 pandemic: A case study in Peru', *Chaos, Solitons & Fractals: X* **10**, 100090.

Koyama, S. (2023), 'Estimating effective reproduction number revisited', *Infectious Disease Modelling* **8**(4), 1063–1078.

Kuddus, M. A. & Rahman, A. (2021), 'Analysis of COVID-19 using a modified SLIR model with nonlinear incidence', *Results in Physics* **27**, 104478.

Lalor, R., Cwiklinski, K., Calvani, N. E. D., Dorey, A., Hamon, S., Corrales, J. L., Dalton, J. P. & De Marco Verissimo, C. (2021), 'Pathogenicity and virulence of the

liver flukes *Fasciola hepatica* and *Fasciola Gigantica* that cause the zoonosis *Fasciolosis*', *Virulence* **12**(1), 2839–2867.

Lan, Z., Zhang, X.-H., Xing, J.-L., Zhang, A.-H., Wang, H.-R., Zhang, X.-C., Gao, J.-F. & Wang, C.-R. (2024), 'Global prevalence of liver disease in human and domestic animals caused by fasciola: A systematic review and meta-analysis', *Journal of Global Health* **14**, 04223.

LaSalle, J. (1976), *The Stability of Dynamical Systems*, Vol. 25, SIAM.

Lenhart, S. & Workman, J. T. ((2007)), *Optimal control applied to biological models*, CRC Press.

Leon, T. M., Porco, T. C., Kim, C. S., Kaewkes, S., Kaewkes, W., Sripa, B. & Spear, R. C. (n.d.), 'Modeling liver fluke transmission in Northeast Thailand: impacts of development, hydrology, and control', *Acta Tropica 188 (2018) 101-107* .

Li, F. & Zhao, X.-Q. (2019), 'A periodic seirs epidemic model with a time-dependent latent period', *Journal of Mathematical Biology* **78**(5), 1553–1579.

Logue, C. M., Barbieri, N. L. & Nielsen, D. W. (2017), 'Pathogens of food animals: Sources, characteristics, human risk, and methods of detection', *Advances in food and Nutrition Research* **82**, 277–365.

Lukes, D. L. (1982), 'Differential equations: classical to controlled', *New York: Academic Press* **162**.

Madubueze, C. E., Gweryina, R. I. & Abokwara, A. (2022), 'Mathematical analysis and optimal control of schistosomiasis transmission model', *Biomath Communications* **9**(1), 2203071.

Mahardika, R., Widowati & Sumanto, Y. (2019), Routh-hurwitz criterion and bifurcation method for stability analysis of tuberculosis transmission model, *in* 'Journal of physics: Conference series', Vol. 1217, IOP Publishing, p. 012056.

Malik, K. & Althobaiti, S. (2025), 'Impact of the infected population and nonlinear incidence rate on the dynamics of the sir model', *Advances in Continuous and Discrete Models* **2025**(1), 21.

Maqbool, I., Wani, Z., Shahardar, R., Allaie, I. & Shah, M. (2017), 'Integrated parasite management with special reference to gastro-intestinal nematodes', *Journal of Parasitic Diseases* **41**(1), 1–8.

Mas-Coma, S. (2005), 'Epidemiology of fascioliasis in human endemic areas', *Journal of Helminthology* **79**, 207–216.

Mas-Coma, S., Agramunt, V. H. & Valero, M. A. (2014), 'Neurological and ocular fascioliasis in humans', *Advances in Parasitology* **84**, 27–149.

McCann, C. (2013), '*Bifurcation Analysis of Non-linear Differential Equations*', *University of LiverPool* pp. 1–47.

Mekuriaw, Z. & Harris-Coble, L. (2021), 'Ethiopia's livestock systems: Overview and areas of inquiry', *USAID: AFeed the Future Innovation Lab for Livestock Systems* .

Mesfin, T., Solomon, T. & Temesgen, A. B. (2024), 'Prevalence of bovine fasciolosis and identify the risk factors in and around Bahir Dar, Ethiopia', *BioRxiv* pp. 2024–08.

Mollinedo, S., Gutierrez, P., Azurduy, R., Valle, F., Salas, A., Mollinedo, Z., Soto, P., Villarroel, C. F., Ransom, J., Lawrence, R. et al. (2019), 'Mass drug administration of Triclabendazole for Fasciola Hepatica in Bolivia', *The American Journal of Tropical Medicine and Hygiene* **100**(6), 1494.

Montgomery, R. M. (2024), 'Understanding the hartman-grobman theorem: A gateway to predicting dynamical system behavior near hyperbolic equilibria', *International Journal of Pure and Applied Mathematics Research* **10**, 20–34.

MSD (2022), 'Life cycle of fasciola hepatica'.
URL: *https://www.msdmanuals.com/home/multimedia/image/life-cycle-of-fasciola-hepatica*

Mwamtobe, P. M., Abelman, S., Tchuenche, J. M. & Kasambara, A. (2014), Optimal (control of) intervention strategies for malaria epidemic in Karonga District, Malawi, Vol. 2014, Wiley Online Library, p. 594256.

Mwasunda, J. A., Irunde, J. I., Kajunguri, D. & Kuznetsov, D. (2022), 'Optimal control analysis of taenia saginata bovine cysticercosis and human taeniasis', *Parasite Epidemiology and Control* **16**, e00236.

Nana-Kyere, S., Boateng, F. A., Jonathan, P., Donkor, A., Hoggar, G. K., Titus, B. D., Kwarteng, D., Adu, I. K. et al. (2022), 'Global Analysis and optimal control model of COVID-19', *Computational and Mathematical Methods in Medicine* **2022**, 1–18.

Nur, W., Suryanto, A., Kusumawinahyu, W. M. et al. (2022), Optimal control problem and cost-effectiveness analysis of schistosomiasis model, *in* 'American Institute of Physics Conference Series', Vol. 2498, p. 020011.

Nur, W., Trisilowati, T., Suryanto, A. & Kusumawinahyu, W. M. (2022), 'Schistosomiasis model with treatment, habitat modification and biological control', *Mathematical Biosciences and Engineering* **19**(12), 13799–13828.

Nyindo, M. & Lukambagire, A.-H. (2015), 'Fascioliasis: an ongoing zoonotic trematode infection', *BioMed Research International* **2015**(1), 786195.

Ogunmiloro, O. M. (2021), 'Mathematical analysis and approximate solution of a fractional order caputo fascioliasis disease model', *Chaos, Solitons & Fractals* **146**, 110851.

Ogunmiloro, O. M. (2022), 'Optimal control analysis of fascioliasis disease transmission dynamics', *Mathematica Applicanda* **50**(2).

Okosun, K. O., Rachid, O. & Marcus, N. (2013), 'Optimal control strategies and cost-effectiveness analysis of a malaria model', *BioSystems* **111**(2), 83–101.

Opio, L. G., Abdelfattah, E. M., Terry, J., Odongo, S. & Okello, E. (2021), 'Prevalence of fascioliasis and associated economic losses in cattle slaughtered at Lira Municipality Abattoir in Northern Uganda', *Animals* **11**(3), 681.

Osterhaus, A. D., Vanlangendonck, C., Barbeschi, M., Bruschke, C. J., Christensen, R., Daszak, P., de Groot, F., Doherty, P., Drury, P., Gmacz, S. et al. (2020), 'Make science evolve into a one health approach to improve health and security: a white paper', *One Health Outlook* **2**, 1–32.

PAHO (2016), 'Plan of action for the elimination of neglected infectious diseases and post-elimination actions, 2016-2022. fascioliasis'.
URL: *https://www.paho.org/en/topics/fascioliasis*

Pal, S., Kundu, K. & Chattopadhyay, J. (2006), 'Role of standard incidence in an eco-epidemiological system: A mathematical study', *Ecological modelling* **199**(3), 229–239.

Pan, M., Bai, S.-Y., Ji, T.-K., Fan, Y.-M., Liu, D.-D., Yang, Y., Tao, J.-P. & Huang, S.-Y. (2022), 'Epidemiology of fasciola spp. in the intermediate host in China: A potential risk for fasciolosis transmission', *Acta Tropica* **230**, 231–240.

Parr, S. & Gray, J. (2000), 'A strategic dosing scheme for the control of fasciolosis in cattle and sheep in Ireland', *Veterinary Parasitology* **88**(3-4), 187–197.

Perko, L. (1991), *Differential Equations and Dynamical Systems*, 2nd edn, Springer, New York.

Pontryagin, L. S. (2018), *Mathematical theory of optimal processes*, Routledge.

Qi, L., Cui, J.-a., Huang, T., Ye, F. & Jiang, L. (2014), Mathematical model of schistosomiasis under flood in Anhui province, *in* 'Abstract and Applied Analysis', Vol. 2014, Wiley Online Library, p. 972189.

Qi, L., Xue, M., Cui, J.-a., Wang, Q. & Wang, T. (2018), 'Schistosomiasis transmission model and its control in Anhui province', *Bulletin of Mathematical Biology* **80**, 2435–2451.

Rahmann, G. & Seip, H. (2006), 'Alternative strategies to prevent and control endoparasite diseases in organic sheep and goat farming systems–a review of cur-

rent scientific knowledge', *Ressortforschung für den Ökologischen Landbau 2006* pp. 49–90.

Rizwan, H. M., Sajid, M. S., Abbas, H., Ghazanfer, S. & Arshad, M. (2022), 'An insight into different strategies for control and prophylaxis of fasciolosis: A review', *Journal of Advances in International Veterinary Research* **4**(1), 5–14.

Rodrigues, H. S., Monteiro, M. T. T. & Torres, D. F. (2014), 'Optimal control and numerical software: an overview', *arXiv preprint arXiv* .

Ross, J. (1970), 'The stormont "wet day" forecasting system for fascioliasis', *British Veterinary Journal* **126**(8), 401–408.

Sabourin, E., Alda, P., Vázquez, A., Hurtrez-Boussès, S. & Vittecoq, M. (2018), 'Impact of human activities on fasciolosis transmission', *Trends in Parasitology* **34**(10), 891–903.

Seid, U. & Melese, M. (2018), 'Review on prevalence, distrbution and economic significance of liver fluke in Ethiopia', *ARC Journal of Animal and Veterinary Sciences* **4**, 38–48.

Shao, P. & Shateyi, S. (2021), 'Stability Analysis of SEIRS Epidemic Model with Nonlinear Incidence Rate Function'.

Sharma, S., Coetzee, E. B., Lowenberg, M. H., Neild, S. A. & Krauskopf, B. (2015), 'Numerical continuation and bifurcation analysis in aircraft design: an industrial perspective', *Philosophical Transactions of the Royal Society A: Mathematical, Physical and Engineering Sciences* **373**(2051), 20140406.

Smith, G. (2011), 'Models of macroparasitic infections in domestic ruminants: a conceptual review and critique', *Rev Sci Tech.* **30**(2), 447.

Solomon, T. & Alemu, B. (2019), 'Economic loss caused by organ condemnation in cattle slaughtered at Hawassa Municipal Abattoir, Southern Ethiopia', *Journal of Global Biosciences* **8**(2), 5966–5977.

Tolan Jr, R. W. (2011), 'Fascioliasis due to Fasciola hepatica and Fasciola gigantica infection: an update on neglected tropical disease', *Laboratory Medicine* **42**, 107–116.

Turner, J., Howell, A., McCann, C., Caminade, C., Bowers, R. G., Williams, D. & Baylis, M. (2016), 'A model to assess the efficacy of vaccines for control of liver fluke infection', *Scientific Reports* **6**, 1–13.

van den Driessche, P. & Watmough, J. (2002), 'Reproduction numbers and subthreshold endemic equilibria for compartmental models of disease transmission', *Mathematical Biosciences* **180**(1-2), 29–48.

Vázquez, A. A., Alda, P., Lounnas, M., Sabourin, E., Alba, A., Pointier, J.-P. & Hurtrez-Boussès, S. (2019), 'Lymnaeid snails hosts of fasciola hepatica and fasciola gigantica (trematoda: Digenea): a worldwide review', *CABI Reviews* (2018), 1–15.

Vladimirov, V. (2004), 'Handbook of mathematical fluid dynamics', *Journal of Fluid Mechanics* **513**, 373–378.

Waikagul, J., Sato, M. & Sato, M. (2015), 'Foodborne trematodes', pp. 221–255.
URL: *https://www.sciencedirect.com/science/article/pii/B9781782423324000102*

Webb, C. M. & Cabada, M. M. (2018), 'Recent developments in the epidemiology, diagnosis, and treatment of fasciola infection', *Current Opinion in Infectious Diseases* **31**(5), 409–414.

Wesolowska, A., Basalaj, K., Norbury, L. J., Sielicka, A., Wedrychowicz, H. & Zawistowska-Deniziak, A. (2018), 'Vaccination against fasciola hepatica using cathepsin L3 and B3 proteases delivered alone or in combination', *Veterinary Parasitology* **250**, 15–21.

WHO (2023), *Global report on neglected tropical diseases:Fascioliasis*, World Health Organization.

Wiggins, S. et al. (1990), 'Introduction to applied nonlinear dynamical systems and chaos'.

Xiao, D. & Ruan, S. (2007), 'Global analysis of an epidemic model with nonmonotone incidence rate', *Mathematical Biosciences* **208**(2), 419–429.

Yadav, R. P. (2015), 'Efficacy of plant origin molluscicides: Control of fascioliasis', *Science International* **3**(3), 103–106.

Yusuf, T. T. & Benyah, F. (2012), 'Optimal control of vaccination and treatment for an SIR epidemiological model', *World Journal of Modelling and Simulation* **8**, 194–204.

Zamir, M., Zaman, G. & Alshomrani, A. S. (2016), 'Sensitivity analysis and optimal control of anthroponotic cutaneous leishmania', *PloS one* **11**(8), e0160513.

Zewde, A., Bayu, Y. & Wondimu, A. (2019), 'Prevalence of bovine fasciolosis and its economic loss due to liver condemnation at Wolaita Sodo Municipal Abattair, Ethiopia', *Veterinary Medicine International* **2019**(1), 9572373.

Zhang, P. (2010), *Advanced Industrial Control Technology*, William Andrew Publishing, Oxford.

Zilberman, D. (1982), 'The use and potential of optimal control models in agricultural economics', *Western Journal of Agricultural Economics* **7**(2), 395–405.

Zwillinger, D. & Dobrushkin, V. (1998), *Handbook of differential equations*, Chapman and Hall/CRC.

Appendices

A Presentation Certificates

1. Debre Berhan University Conference Certificate

Debre Berhan University

Certification of Participation

This Certificate is awarded to Mr. **Dagnaw Tantie** for presenting his/her research paper entitled *"Modelling Human-Cattle Dynamics for Effective Fasciola Hepatica Management"* on the 4th Annual National Research Conference on the theme **"Investing in Science for innovation and Development of Sustainable Technologies"** organized by College of Natural and Computational Sciences held on March 25, 2025, Debre Berhan University.

Mastewal H/Mariam (MSc)
Vice Dean

Minbale Gashu (PhD)
Dean, College of Computational and Natural Science

2. Addis Ababa University Conference Certificate

NAASCO

UPPSALA UNIVERSITET

Certificate of Participation

This is to certify that **Dagnaw Tantie Yihunie** from *Bahir Dar University* has attended a school with a theme *"Classical and New Approaches for Modeling Life Science Problems"* and also participated in the second workshop of the *" Ethio-Italy Colloquium on Applied Mathematics (ETICAM-2)"*, which was held in Addis Ababa-Ethiopia, hosted by the Department of Mathematics at Addis Ababa university from 10th February to 13th February, 2025 with an ***oral*** presentation titled:

"Optimal Control and Cost-Effectiveness Analysis of Fasciola Hepatica Model"

Tadesse Abdi (PhD)
Head, Department of Mathematics
Addis Ababa University

Bruno Buonomo (Professor)
NAASCo Coordinator
University of Naples Federico II

3. Arba Minch University Conference Certificate

Arba Minch University

CERTIFICATE Of APPRECIATION

This certificate is awarded to

Dagnaw Tantie(Mr.)

He has successfully presented his paper at the 11th National Symposium on *"Science for Sustainable Development"* held at Arba Minch University, Ethiopia.

Feb 21, 2025

Tesfaye Habtemariam (PhD)
Executive Research Director

Teklu Wegayehu (PhD)
VP for Research & Cooperation

B Mathematical Preliminaries

B.1 Invariant Sets and Stability Analysis

Invariant sets and stability analysis are some of the most crucial concepts in the study of dynamical systems, providing very important information on the time behavior of such systems. The concepts have widespread use in various fields, including *fasciolasis* disease modeling, to understand and make long-term predictions of complex systems.

Definition B.1 (Invariant sets)**.** Consider an autonomous, time-invariant system

$$\dot{x} = f(x),\ f : \mathbb{R}^n \to \mathbb{R}^n. \tag{B.1}$$

A set $\mathbf{C} \subseteq \mathbb{R}^n$ is invariant with respect to the system if for every trajectory, $x(t) \in \mathbf{C}$ then $x(\tau) \in \mathbf{C}$ for all $\tau \geq t$ (Vladimirov 2004).

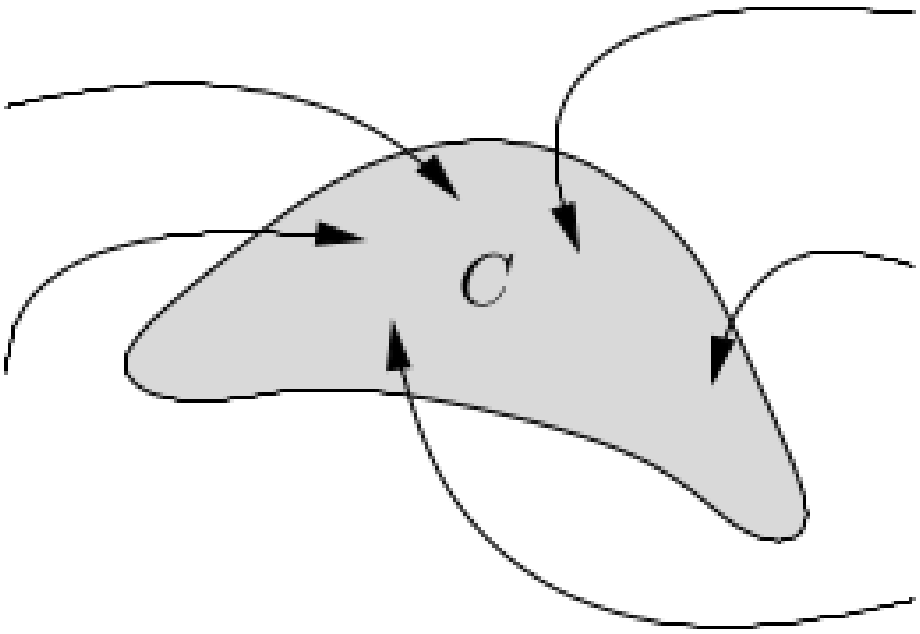

Figure B.1: Invariant sets.

In other words, if a trajectory enters **C**, then it stays in **C**. In addition, trajectories can cross the boundary of **C**, but never outside of **C** as shown in Figure B.1.

Definition B.2 (Equilibrium point)**.** An equilibrium point of a dynamic system is a state in which the system remains constant over time (Perko 1991). That is, the point $\bar{x} = (x_1, x_2, ..., x_n) \in \mathbb{R}^n$ is called the equilibrium point of (B.1) if $f(\bar{x}) = 0$.

Equilibrium points in disease models are critical states in which disease dynamics stabilizes, informing strategies for persistence, control and eradication. Stability analysis determines whether model solutions converge to or diverge from these equilibria, predicting the system's future behavior and its sensitivity to change.

Definition B.3 (Stability of the equilibrium point)**.** The equilibrium point $\bar{x} \in \mathbb{R}^n$ of the system (B.1) said to be:

1) local stable if for every $\epsilon > 0$ there $\delta > 0$ such that for every solution $x(t)$ that satisfies $||x(t_0) - \bar{x}|| < \delta$ implies $||x(t) - \bar{x}|| < \epsilon$ for each $t \geq t_0$. That is, if trajectories staring close to the equilibrium point stay close or converge to it, then the equilibrium is locally stable.

2) local asymptotically stable if the equilibrium point $\bar{x} \in \mathbb{R}^n$ is stable and $\delta > 0$ such that for every solution $x(t)$ that satisfies $||x(t_0) - \bar{x}|| < \delta$ implies $\lim_{x \to \infty} x(t) = \bar{x}$. The equilibrium point is asymptotically stable if the trajectories do not stay close to the equilibrium point but also eventually converge to the equilibrium point over a time.

3) unstable if the equilibrium point $\bar{x} \in \mathbb{R}^n$ does not meet condition (1).

4) globally stable if, regardless of initial conditions, it eventually returns to a stable equilibrium state or follows a predictable bounded trajectory.

Stability analysis is obtained by determining the eigenvalues of the Jacobian matrix around the equilibrium points (Anggreini 2016). Various methods have been developed for the study of stability of invariant sets in dynamical systems:

A) **Linearization**: The Hartman-Grobman theorem, or linearization theorem, describes the behavior of dynamical systems near a hyperbolic equilibrium point. It states that the behavior of a system near this point is similar to its linear

approximation, which is found using the Jacobian matrix. The eigenvalues of the matrix are all-important for stability analysis.

Proposition B.4. *If all eigenvalues of the matrix have negative real parts, the point is asymptotically stable; if any have positive real parts, it is unstable. If any have zero real parts, then further analysis is needed.*

Theorem B.5 (Hartman-Grobman theorem)**.** *Consider a dynamical system (the state of a system evolves over time)* $\frac{dx}{dt} = f(x)$ *with a state* $x(t) \in \mathbb{R}^n$*; where* $f : \mathbb{R}^n \to \mathbb{R}^n$ *is continuously differentiable* (C^1) *near an equilibrium point* x^**. If the equilibrium point* x^* *is hyperbolic, that is the Jacobian matrix* $A = Df(x^*)$ *has no eigenvalues with zero real parts, then there exists a homeomorphism* $h : U \to V$ *between a neighbourhood* $U \subset \mathbb{R}^n$ *of* x^* *and neighborhood* $V \subset \mathbb{R}^n$ *of the origin such that the nonlinear system* $\frac{dx}{dt} = f(x)$ *is topologically conjugated to its linearized system,* $\frac{dy}{dt} = Ay$*, where h preserves the qualitative structure of trajectories (Montgomery 2024).*

Definition B.6. An equilibrium point $\bar{x}$ of the system (B.1) is said to be hyperbolic critical point if all eigenvalues of the Jacobian evaluated at $\bar{x}$ have non zero real parts, otherwise $\bar{x}$ is non-hyperbolic.

B) **Lyapunov Method**: Lyapunov's Theorem offers a powerful method for analyzing the stability of equilibrium points in dynamical systems, without explicitly solving the equations. This method relies on finding a scalar function(Lyapunov function), which is positive definite and decreases along trajectories of the system. The existence of such a function guarantees stability.

Theorem B.7 (Lyapunov Stability)**.** *Consider an autonomous system (Arrowsmith & Place 1992):*

$$\dot{x} = f(x),$$

with an equilibrium at x^**.*
Let $V : D \to \mathbb{R}^n$ *be a continuously differentiable function defined* $D \subset \mathbb{R}^n$ *containing* x^**. Then:*

(i) If $\dot{V}(x^*) = 0$, $\dot{V}(x) > 0$ for all $x \neq x^*$ in some neighborhood of x^* (D) and $\dot{V}(x) \leq 0$ for all $x \in D$, then the equilibrium point $x^*$is stable.

(ii) If $\dot{V}(x^*) = 0$, $\dot{V}(x) > 0$ for all $x \neq x^*$ in D and $\dot{V}(x) < 0$ for all $x \in D$, then the equilibrium point x^* is asymptotically stable.

(iii) The equilibrium point x^* is globally asymptotically stable if it is asymptotically stable and $V(x) \to \infty$ as $|x| \to \infty$ (radially unbounded).

Theorem B.8 (LaSalle's Invariance Principle)**.** *Consider an autonomous system in (B.1) with equilibrium x^*. Let*

- *Ω be a compact (closed and bounded) set that is positively invariant ,*
- *$\Omega \to \mathbb{R}$ be a continuously differentiable function such that $\dot{V}(x) = \nabla V(x).f(x) \leq 0, \quad \forall \in \Omega.$*

Define the set

$$E = \left\{x \in \Omega : \dot{V}(x) = 0\right\},$$

and let M be the largest invariant set in E. Then every solution starting in Ω converges to M as $t \to \infty$.

B.2 Routh-Hurwitz Criterion for Stability Analysis

Routh-Hurwitz stability criterion is a method to show time-invariant continuous systems by constructing a Routh array from the coefficients of the characteristic equation.

Consider the characteristic equation:

$$p(\lambda) = a_0\lambda^n + a_1\lambda^{n-1} + a_2\lambda^{n-2} + ... + a_{n-1}\lambda + a_n \tag{B.2}$$

with a_j is a coefficient in a real number, $j = 1, 2, ..., n$.

Definition B.9. The matrix

$$H_n = \begin{bmatrix} a_1 & a_3 & a_5 & a_7 & a_9 & \cdots & 0 \\ a_0 & a_2 & a_4 & a_6 & a_8 & \cdots & 0 \\ 0 & a_1 & a_3 & a_5 & a_7 & \cdots & 0 \\ 0 & a_0 & a_2 & a_4 & a_6 & \cdots & 0 \\ 0 & 0 & a_1 & a_3 & a_5 & \cdots & 0 \\ 0 & 0 & a_0 & a_2 & a_4 & \ddots & 0 \\ \vdots & \vdots & \vdots & \vdots & \vdots & \vdots & a_n \end{bmatrix} \tag{B.3}$$

is called the Hurwitz matrix, associated with $p(\lambda)$ (Mahardika et al. 2019).

Definition B.10. The polynomial $p(\lambda)$ is called Hurwitz polynomial if all its eigenvalues are positive real parts.

Proposition B.11 (The Routh-Hurwitz stability criterion)**.** *The polynomial given in (B.2) is Hurwitzian if and only if all the principal minors of the Hurwitz matrix H_n must be strictly positive.*

B.3 A General Compartmental Epidemic Model and Next Generation Matrix

Consider a general epidemic model designed for a diverse population, categorizing individuals into n uniform groups based on attributes such as age, behavior, location, or stage of the disease. It uses a vector $x = (x_1, x_2 \ldots, x_n)$, with each $x_i \geq 0$, to represent the number of individuals in each group, with the initial m groups specifically assigned to the infected individuals. The distinction between infected and uninfected groups is based on epidemiological interpretation rather than the model's inherent structure, allowing for various interpretations. Consequently, the basic reproduction number depends on this definition. In addition, the model identifies all possible disease-free states. We define X_s as the set of all disease-free states. That is,

$$X_s = \{x \geq 0 |\ x_i = 0,\ i = 1, ..., m\}.$$

To compute R_0, it is important to distinguish new infections from all other changes in the population. Let $F_i(x)$ be the rate of appearance of new infections in compartment i, $V_i^+(x)$ be the rate of transfer of individuals to compartment i by all other means and $V_i^-(x)$ be the rate of transfer of individuals out of compartment i. It is assumed that each function can be continuously differentiable at least twice in each variable. The disease transmission model consists of non-negative initial conditions together with the following system of equations:

$$\dot{x}_i = f_i(x) = F_i(x) - V_i(x),\ i = 1,...,n \tag{B.4}$$

where $V_i(x) = V_i^-(x) - V_i^+(x)$ and the functions satisfy the assumptions (A1)–(A5) described below (van den Driessche & Watmough 2002). Since each function represents a directed transfer of individuals, they are all non-negative. Thus,

(A1) if $x \geq 0$, then $F_i, V_i^-, V_i^+ \geq 0,\ i = 1,...,n$.

If a compartment is empty, then there can be no transfer of individuals from the compartment by death, infection, or any other means. Thus,

(A2) if $x_i = 0$, then $V_i^- = 0$. In particular, if $x \in X_s$ then $V_i^- = 0,\ i = 1,...,m$.

Consider the disease transmission model given by (B.4) with $f_i(x),\ i = 1,\ldots,n$, satisfying conditions (A1), (A2). If $x_i = 0$, then $f_i(x) \geq 0$, and hence the non-negative term ($x_i \geq 0,\ i = 1,\ldots,n$) is forward invariant. By Theorems 1.1.8 and 1.1.9 of Wiggins et al. (1990) for each non-negative initial condition, there is a unique non-negative solution.

The next condition arises from the simple fact that the incidence of infection in the uninfected compartments is zero.

(A3) $F_i = 0$, if $i > m$.

To ensure that the disease-free subspace is invariant, we assume that if the population is free of disease, then the population will remain free of disease. That is, there is no density-independent infective immigration. This condition is stated as follows:

(A4) if $x \in X_s$, then $F_i(x) = 0$ and $V_i^+(x) = 0$ for $i = 1, \ldots, m$.

The remaining condition is based on the derivatives of f near a DFE. For our purposes, we define a DFE of (B.4) as a (locally asymptotically) stable equilibrium solution of the disease-free model, i.e. (B.4) restricted to X_s. Note that we need not assume that the model has a unique DFE. Consider a population near the DFE x_0. If a small number of infected individuals does not cause an epidemic, the population will return to the DFE according to the linearized system.

$$\dot{x}_i = Df(x_0)(x - x_0) \tag{B.5}$$

where $Df(x_0)$ is the derivative $[\partial f_i/\partial x_j]$ evaluated in DFE, x_0. Here, and in what follows, some derivatives are one-sided, since x_0 is on the domain boundary. We restrict our attention to systems in which the DFE is stable in the absence of new infection. That is,

(A5) if $F(x)$ is set to zero, then all eigenvalues of $Df(x_0)$ have negative real parts.

B.4 The Reproduction Number in Epidemics

In epidemiology, the reproductive number is a useful epidemiologic metric to monitor and control the development of an epidemic (Batista 2021). The basic reproduction number (R_0) and the effective reproduction number (R) offer different perspectives on the dynamics of infectious disease.

- **Basic Reproduction Number**: The average number of secondary infections produced by a single infected individual in a completely susceptible population. Quantifies the potential of an infectious disease to spread within a population, only at the beginning of an outbreak (Hethcote 2000). If $R_0 > 1$, the infection will spread through the population; if $R_0 < 1$, the infection will likely die out.

- **Effective Reproduction Number**: The effective reproduction number is the average number of secondary cases per infectious case at a specific time in a population, accounting for both susceptible and non-susceptible individuals as

well as interventions (Koyama 2023). Unlike the basic reproduction number, it is a dynamic measure that reflects changes in population immunity (from infection, vaccination, or other interventions) throughout an outbreak, making it a more practical indicator of transmission.

The next generation matrix is the common method of computing the basic reproduction number in epidemiological models. The method has the following steps to compute.

(i) Identify all infected states.

(ii) Rewrite the system in the form B.4.

(iii) Linearize at the disease-free equilibrium.

(iv) The basic reproduction number is the spectral radius (dominant eigenvalue) of FV^{-1}.

B.5 Incidence Rates in Epidemiology

In mathematical modeling of infectious diseases, incidence rates are used to describe how individuals in a population interact and how such interactions affect the spread of a disease. There are various incidences, and among them are:

- **Mass Action Incidence**: Mass action assumes that the rate of new infections is proportional to the product of susceptible (S) and infectious (I) individuals, implying that each individual has the same probability of interacting with any other. In a well-mixed population with random and uniform interactions, the rate of new infections is described as linear incidence αSI, where α represents the transmission or contact rate.

- **Standard Incidence**: The standard incidence is a model in which the rate of new infections is proportional to both the number of susceptible individuals and the number of infected individuals, but adjusted for the size of the population (Pal et al. 2006). Specifically, the rate is given by $\alpha S\frac{I}{N}$, where N represents the

total population. This formulation acknowledges that contact rates decrease in larger populations.

- **Saturating Incidence**: As the number of infected individuals increases, the infection rate may saturate due to limitations in contacts or transmission capacity (for example, limited resources or behavioral changes). The saturated incidence rate was first described by Anderson & May (1991) in 1978. It saturates as a result of the concentration of infectious individuals at high levels of infection. This is modeled as $\frac{\alpha SI}{1+\beta I}$; where, α is the transmission rate, and β is a saturation factor that reduces transmission with increasing infection prevalence (Malik & Althobaiti 2025).

B.6 Bifurcation Analysis

Bifurcation analysis studies qualitative changes in the dynamics of a system as the parameters vary. These bifurcations can create or destroy invariant sets, such as fixed points or limit cycles, and affect their stability (Aderyani et al. 2025). A bifurcation arises when parameter changes alter equilibrium point solutions. Transcritical bifurcations, specifically, involve stability exchanges between equilibrium points and occur when an eigenvalue has a zero real part. In nonlinear systems, the centre manifold theory simplifies stability analysis near non-hyperbolic fixed points by enabling dimensional reduction. Recently, the forward bifurcation showed the existence of both local and global stability of equilibrium points obtained from epidemiological models (Cheneke 2023).

The Castillo-Chavez & Song (2004) theorem expands this analysis by providing a framework for understanding systems with non-hyperbolic equilibria. Specifically, it offers insights into bifurcations in, for example, epidemiological models by characterizing the conditions for their occurrence and their impact on system dynamics. We summarize the theorem as follows.

Theorem B.12 (Castillo-Chavez & Song (2004))**.** *Consider the following general system of ordinary differential equations with a parameter ϕ, where 0 is an equilibrium*

point of the system

$$\frac{dy}{dt} = f(y,t), \quad f : \mathbb{R}^n \times \mathbb{R}, \quad and \quad f \in \mathbb{R}^n \tag{B.6}$$

That is, $f(0,\phi) \equiv 0$ *for all* ϕ*, such that:*

(1) $A = D_y(0,0) = \frac{\partial f_i}{\partial y_j}$ *is the linearization matrix of the system around the equilibrium 0 with* ϕ *evaluated at 0.*

(2) Zero is a simple eigenvalue of A, and all other eigenvalues of A have negative real parts.

(3) Matrix A has a right eigenvector w and a left eigenvector v that corresponds to the zero eigenvalue. Let f_k *be the kth - component of f and:*

$$a = \sum_{k,i,j=1}^{n} v_k w_i w_j \frac{\partial^2 f_k}{\partial y_i \partial y_j}(0,0),$$
$$b = \sum_{k,i=1}^{n} v_k w_i \frac{\partial^2 f_k}{\partial y_i \partial \phi}(0,0).$$

Then the local dynamics of the system around the equilibrium point 0 are totally determined by signs of a and b.

(i) if $a > 0$, $b > 0$. *when* $\phi < 0$ *with* $|\phi| << 1$, *0 is locally asymptotically stable and there exists a positive unstable equilibrium; when* $0 < \phi << 1$, *0 is unstable and there exists a negative and locally asymptotically stable equilibrium.*

(ii) $a < 0$, $b < 0$. *When* $\phi < 0$ *with* $|\phi| << 1$, *0 is unstable, when* $0 < \phi << 1$, *0 is locally asymptotically stable and there exists a positive unstable equilibrium.*

(iii) $a > 0$, $b < 0$. *When* $\phi < 0$ *with* $\phi << 1$, *0 is unstable and there exists a locally asymptotically stable negative equilibrium; when* $0 < \phi << 1$, *0 is stable and a positive unstable equilibrium appears.*

(iv) $a < 0$, $b > 0$. *When* ϕ *changes from negative to positive, 0 changes its stability from stable to unstable. Consequently, a negative unstable equilibrium becomes positive and locally asymptotically stable. In particular, if* $a > 0$ *and* $b > 0$, *then a backward bifurcation occurs at* $\phi = 0$.

B.7 Volterra–Lyapunov Stable Matrix

In dynamical systems and control theory, the stability analysis of matrices often relies on Lyapunov stability concepts. Although the Volterra-Lyapunov stability criterion is not a standard term, it combines the Volterra integral equation and the Lyapunov stability principles. Applying the Lyapunov method, the global stability of the endemic equilibrium can be analyzed using a stable Volterra-Lyapunov matrix (Chien & Shateyi 2021). A matrix is considered Volterra–Lyapunov stable if it is diagonally stable, which implies the existence of a positive definite diagonal matrix D such that $DA+A^TD$ is negative definite. This condition stems from Lyapunov stability theory, applied to systems with a diagonal Lyapunov function, which is frequently employed in ecological models, such as the Lotka–Volterra equations.

B.8 Optimal Control Problem

Optimal control is believed to be one of the best tools for studying the dynamics of infectious diseases and their potential control (Khan et al. 2021). Optimal control theory is the science of maximizing returns and minimizing the costs of operating physical, social, and economic processes (Kirk 2004). It is a powerful mathematical tool for making decisions that involve complex dynamical systems (Kahuru et al. 2017). The process of determining the control and state trajectories of a dynamic system over time to optimize a given performance index is known as optimal control (Rodrigues et al. 2014). Optimal control models describe how a system evolves over time and determine the optimal levels of decision variables over time (Zilberman 1982).

An optimal control is a set of differential equations that describe the path of the control variable that minimizes the cost function (i.e., a function of state and control variables). Pontryagin's maximum principle and Bellman's dynamic programming are two powerful tools that are used to solve constrained closed set variation problems, related to the most optimal control problems (Zhang 2010). Pontryagin's maximum principle, which can be seen as an extension of the calculus of variations (COV),

is widely used to obtain the strategy for optimal control of continuous processes (Dhar 2016). The Pontryagin maximum (or minimum) principle can be used to determine the solution to the problem of a two-point boundary value problem (Capó-Lugo & Bainum 2011). This problem refers to the solution of fixed end constraints. The objective of optimal control is to determine the control signals that will cause a process to satisfy the physical constraints and, at the same time, minimize (or maximize) some performance criterion. A performance measure is a mathematical description of the desired behavior we wish the system under study to exhibit.

The control and states of a system can be constrained for various reasons. A common form of control constraint is the saturation constraint, which is due to the limited control authority of the physical system. This constraint is described as

$$u_i^{min} \leq u_i(t) \leq u_i^{max}, \quad i \in \{1,2,...,m\}, \quad t \in [0,t_f] \tag{B.8}$$

The states of a system can be constrained, as well.

In the basic optimal control problem for ordinary differential equations, we use u(t) for the control and x(t) for the state variable. The state variable satisfies a differential equation that depends on the control variable:

$$\dot{x} = f(x(t),u(t),t). \tag{B.9}$$

As the control function is changed, the solution to the differential equation will change. The optimal control problem consists of finding a piecewise continuous control $u(t)$ and the associated state variable $x(t)$ to minimize the given objective functional.

$$J = \min_u \int_{t_0}^{t_f} L(x(t),u(t),t)\,dt, \tag{B.10}$$

subject to $\dot{x} = f(x(t),u(t),t), \qquad x(t_0) = x_0$ and $x(t_f)$ free.

Such a minimizing control is called an optimal control.

Pontryagin Minimum Principle and Optimally Conditions

The Hamiltonian is a function that is used to solve an optimal control problem for a dynamical system. A control Hamiltonian function H can be constructed by

appending the state equation to the integrand f using the Lagrange multipliers, $\lambda(t)$, as follows.

$$H(x(t),u(t),\lambda(t),t) = L(x(t),u(t),t) + \lambda^T(t).f(x(t),u(t),t), \tag{B.11}$$

where $u(t)$ is the optimal control, and $x(t)$ is the corresponding optimal state.

The Pontryagin Minimum Principle (PMP) states that there exists a continuous function λ known as an adjoint function, that is the solution of the adjoint equation

$$\dot{\lambda}(t) = -H_x(x(t),u(t),\lambda(t),t), \tag{B.12}$$

along with the appropriate initial (or final) condition of λ.

The adjoint function is a Lagrange multiplier that brings the information of the state equation constraint to the optimization problem. According to the PMP, the optimal control, $x(t)$, and corresponding optimal state, $u(t)$, and adjoint, $\lambda(t)$, must minimize the Hamiltonian so that

$$H(x(t),u^*(t),\lambda(t),t) \leq H(x(t),u(t),\lambda(t),t), \tag{B.13}$$

for all time and for all admissible (i.e., feasible) trajectory control variables $u^*(t)$, while the adjoint equation Eq. (B.12) is satisfied. Admissible trajectories are defined as a set of variables that are in the neighborhood of the minimal solution and satisfies all of the constraints.

We now define the necessary and sufficient conditions for optimality on the basis of the preceding considerations. For a feasible trajectory that satisfies the minimum principle, condition Eq. (B.13) implies that the Hamiltonian is minimum at the optimal control u(t), such that

$$H_u(x(t),u^*(t),\lambda(t),t) = 0. \tag{B.14}$$

The condition (B.14) is the first order necessary condition for optimally.

The necessary conditions are sufficient to ensure the optimal control variable for purely convex functional objectives with respect to the control variables. In general,

the optimal control variable, as well as the corresponding state and adjoint, can be computed by solving an ODE system.

$$\begin{cases} H_u(x(t),u(t),\lambda(t),t)=0 \quad \text{(control equation)}, \\ \dot{\lambda}(t)=-H_x(x(t),u(t),\lambda(t),t) \quad \text{(co-state equation)}, \\ \dot{x}(t)=H_\lambda(x(t),u(t),\lambda(t),t) \quad \text{(state equation)}, \\ \lambda(t_f)=0 \quad \text{(triviality condition)}. \end{cases}$$

B.9 Cost-Effective Analysis for Optimal Control Model

Cost-Effective Analysis (CEA) is a method used to evaluate the economic efficiency of different strategies or interventions, particularly in fields such as healthcare, public policy, and engineering. It involves comparing the relative costs and results (often in terms of effectiveness or utility) of two or more courses of action (Gupta et al. 2020). In the context of optimal control analysis, CEA can be applied to determine the most efficient way to achieve a desired result while minimizing costs.

These are different cost-effectiveness analysis, among them the infection averted ratio (IAR), the average cost-effectiveness ratio (ACER), and the incremental cost-effectiveness ratio (ICER).

A) Infection Averted Ratio (IAR)

The infection averted ratio (IAR) can be expressed as

$$IAR = \frac{\text{Number of infections averted}}{\text{Number of infected individuals without any control implementation}},$$

where the number of infections averted represents the difference between the total number of infected individuals without any control implementation and the total number of infected individuals with control throughout the simulation, a control strategy with the highest IAR value is considered as the most cost-effective (Agusto & ELmojtaba 2017).

0.5cm

B) Average Cost-Effectiveness Ratio (ACER)

The average cost-effectiveness ratio (ACER) of an optimal control strategy S is given by the formula (Engida et al. 2024):

$$ACER(S) = \frac{\text{Total cost incurred on the implementation of a particular intervention strategy S}}{\text{Total number of infections averted by the intervention strategy S}}.$$

where, the total cost incurred on implementing a particular intervention strategy is estimated from (Asamoah et al. 2022),

$$L(u) = \int_0^T \sum_{i=0}^{n} C_i u_i^2 \, du.$$

C) Incremental Cost-Effectiveness Ratio (ICER)

The incremental cost-effectiveness ratio (ICER) measures the difference in costs and health benefits between two competing intervention strategies for the same limited resources. ICER is defined as the ratio of the difference in cost between strategies p and q, divided by the difference in the number of averted infections between those strategies (Asamoah, Yankson, Okyere, Sun, Jin, Jan et al. 2021, Kouidere et al. 2023). Taking strategies p and q as two competing control intervention strategies, the ICER is stated as

$$ICER = \frac{\text{Change in total costs in strategies p and q}}{\text{Change in control benefits in strategies p and q}},$$

ICER numerator includes differences in disease averted costs, costs of prevented cases, intervention costs, and others. Although the ICER denominator accounts for differences in health outcome, including the total number of infections averted or the total number of susceptibility cases prevented.